

UNIVERSITY OF LJUBLJANA
BIOTECHNICAL FACULTY

Katja KOLOŠA

**OPTIMIZATION OF HUMAN MESENCHYMAL
STEM CELLS PRODUCTION AND THEIR MUTUAL
INTERACTIONS WITH TUMOR CELLS**

DOCTORAL DISSERTATION

Ljubljana, 2016

UNIVERSITY OF LJUBLJANA
BIOTECHNICAL FACULTY

Katja KOLOŠA

**OPTIMIZACIJA PRIDOBIVANJA ČLOVEŠKIH MEZENHIMSKIH
MATIČNIH CELIC IN MEDSEBOJNI VPLIVI S TUMORSKIMI
CELICAMI**

DOKTORSKA DISERTACIJA

**OPTIMIZATION OF HUMAN MESENCHYMAL STEM CELLS
PRODUCTION AND THEIR MUTUAL INTERACTIONS WITH
TUMOR CELLS**

DOCTORAL DISSERTATION

Ljubljana, 2016

On the basis of the Statute of the University of Ljubljana and by decisions of the Senate of the Biotechnical Faculty and the decision of University Senate, dated from January 11th 2012, the continuation to doctoral Postgraduate Study of Biological and Biotechnical Sciences, field: Biology, was approved. Prof. Tamara Lah Turnšek, PhD, as the supervisor, and Prof. Stevens Kastrup Rehen, PhD, as the co-advisor, were confirmed.

Na podlagi Statuta Univerze v Ljubljani ter po sklepu Senata Biotehniške fakultete in sklepa Senata Univerze z dne 11/1/2012 je bilo potrjeno, da kandidatka izpolnjuje pogoje za neposreden prehod na doktorski Podiplomski študij bioloških in biotehniških znanosti ter opravljanje doktorata znanosti s področja biologije. Za mentorico je bila imenovana prof. dr. Tamara Lah Turnšek ter za somentorja prof. dr. Stevens Kastrup Rehen.

Doctoral Dissertation was carried out at the Department of Genetic Toxicology and Cancer Biology, National Institute of Biology in Ljubljana.

Doktorska disertacija je bila opravljena na Oddelku za genetsko tehnologijo in biologijo raka, Nacionalnega inštituta za biologijo v Ljubljani.

Supervisor (mentorica): Prof. Dr. Tamara LAH TURNŠEK
National Institute of Biology, Department of Genetic Toxicology and
Cancer Biology

Co-supervisor (somentor): Prof. Dr. Stevens KASTRUP REHEN
University of Rio de Janeiro, Institute of Biomedical Sciences

Committee for evaluation and the defence (Komisija za oceno in zagovor):

Chairman (predsednik): Prof. Dr. Mojca NARAT
University of Ljubljana, Biotechnical Faculty, Department of Zootechnics

Member (član): Assist. Prof. Dr. Miomir KNEŽEVIĆ
Educell, d.o.o., Trzin

Member (član): Prof. Dr. Marko KREFT
University of Ljubljana, Biotechnical Faculty, Department of Biology

Date of defence (datum zagovora): 11/3/2016

I, the undersigned doctoral candidate declare that this doctoral dissertation is a result of my own research work and that the electronic and printed versions are identical. I am hereby non-paidly, non-exclusively, and spatially and timelessly unlimitedly transferring to University the right to store this authorial work in electronic version and to reproduce it, and the right to enable it publicly accessible on the web pages of Digital Library of Biotechnical faculty.

Katja Kološa

KEY WORDS DOCUMENTATION (KWD)

DN Dd
DC UDC 557.2(043.3)=111
CX mesenchymal stem cells/adipose tissue/harvest site/microcarriers/spinner flasks/umbilical cord-derived mesenchymal stem cells/bone marrow-derived mesenchymal stem cells/paracrine effects/glioma stem-like cells/senescence/differentiation
AU KOLOŠA, Katja, M. Sc. Biochem.
AA LAH TURNŠEK, Tamara (supervisor) / KASTRUP REHEN, Stevens (co-advisor)
PP SI-1000 Ljubljana, Jamnikarjeva 101
PB University of Ljubljana, Biotechnical Faculty, Postgraduate Study of Biological and Biotechnical Sciences, Field: Biology
PY 2016
TI OPTIMIZATION OF HUMAN MESENCHYMAL STEM CELLS PRODUCTION AND THEIR MUTUAL INTERACTIONS WITH TUMOR CELLS
DT Doctoral Dissertation
NO XVI, 130 p., 10 tab., 44 fig., 3 ann., 216 ref.
LA en
AL en/sl
AB Mesenchymal stem cells (MSCs) are used in cell therapies and tissue engineering because of their availability and multipotency, and also due to their homing ability and release of various soluble factors. MSCs have been shown to have antitumor effects in many cancers, including glioblastoma, which is one of at least successfully treated diseases, apparently due to the presence of a highly tumorigenic subpopulation of cells, the glioma stem-like cells (GSLCs). To obtain the large numbers of cells that are necessary for clinical applications, MSCs need to be isolated from the tissue source and expanded *in vitro*. Adipose tissue is the most convenient origin for MSCs, and thus we explored the thighs, hips and abdomen as harvest sites for adipose tissue-derived MSCs (AT-MSCs), and examined the key parameters for AT-MSC expansion on microcarriers in spinner flasks. Furthermore, we studied the paracrine effects of bone marrow-derived MSCs (BM-MSCs) and umbilical cord-derived MSCs (UC-MSCs) on GSLC cultures. We show that the anatomical location of the harvest site has no influence on the AT-MSC proliferation rates, although it affects the onset of replicative senescence of AT-MSCs in cell culture, with the hip-derived AT-MSCs more prone to earlier onset of senescence compared to the thigh and abdomen AT-MSCs. The differentiation of AT-MSCs in terms of the harvest site revealed increased osteogenic and chondrogenic differentiation of thigh-derived AT-MSCs. For the expansion of AT-MSCs in spinner flasks, the adhesion of AT-MSCs onto Cytodex-3 and Cytodex-1 microcarriers was higher with an intermittent agitation regime compared to a static regime, and it was independent of initial pre-coating of the microcarriers with various concentrations of serum. However, our data revealed that higher initial AT-MSC adhesion to microcarriers does not result in higher final AT-MSC yield. For the expansion of AT-MSCs on microcarriers, a 2-day feeding regime was optimal. The addition of fresh microcarriers during AT-MSC cultivation resulted in higher final cell yields, and with Cytodex-3, also in their limited aggregation, thus indicating the superior applicability of Cytodex-3 over Cytodex-1 for AT-MSC expansion in spinner flasks. In the study of the BM-MSC and UC-MSC paracrine effects on GSLC cell lines, soluble factors present in MSC conditioned media impaired proliferation of GSLCs via Cyclin-D1-mediated cell-cycle arrest, which resulted in induction of senescence. This appeared to be mediated via signalling through two powerful tumor-suppressor pathways: p53-p21-pRB and p16-pRB. MSC paracrine signals also increased the sensitivity of GSLCs towards the chemotherapeutic temozolomide, and induced astrocyte-directed differentiation of GSLCs by down-regulation of Sox-2 and Notch-1, and induction of vimentin and GFAP gene expression. To conclude, our data have delineated the influence of harvest site on AT-MSCs characteristics and defined a protocol for expansion of AT-MSCs on microcarriers in spinner flasks. Moreover, our findings indicate the intrinsic MSC induction of senescence and differentiation, and reduction of chemoresistance, in GSLCs.

KLJUČNA DOKUMENTACIJSKA INFORMACIJA (KDI)

- ŠD Dd
DK UDK 557.2(043.3)=111
KG mezenhimske matične celice/maščevje/mesto odvzema/mikronosilci/mešalni bioreaktor/mezenhimske matične celice iz popkavnice/mezenhimske matične celice iz kostnega mozga/parakrino delovanje/gliomske matičnim-podobne celice/senescenca/diferenciacija
AV KOLOŠA, Katja, univ. dipl. biokem.
SA LAH TURNŠEK, Tamara (mentor) / KASTRUP REHEN, Stevens (so-mentor)
KZ SI-1000 Ljubljana, Jamnikarjeva 101
ZA Univerza v Ljubljani, Biotehniška fakulteta, Podiplomski študij bioloških in biotehniških znanosti, področje biologije
LI 2016
IN OPTIMIZACIJA PRIDOBIVANJA ČLOVEŠKIH MEZENHIMSKIH MATIČNIH CELIC IN MEDSEBOJNI VPLIVI S TUMORSKIMI CELICAMI
TD Doktorska disertacija
OP XVI, 130 str., 10 pregl., 44 sl., 3 pril., 216 vir.
IJ en
JI en/sl
AI Mezenhimske matične celice (MMC) so multipotentne celice prisotne v različnih tkivih, ki imajo sposobnost usmerjene migracije in sproščanja topnih faktorjev, zaradi česar so široko uporabne v celični terapiji in regenerativni medicini. Protitumorsko delovanje MMC je bilo dokazano pri različnih oblikah raka, tudi glioblastomu, ki navkljub zdravljenju sodi med bolezni s slabo prognozo, najverjetneje zaradi prisotnosti tumorigene subpopulacije celic, t.i. gliomske matičnim-podobne celice (GMC). Za uporabo MMC v kliničnih aplikacijah moramo MMC izolirati iz tkiva in jih namnožiti *in vitro*. Maščobno tkivo je eden najprimernejših virov MMC (AT-MMC), zato smo preučili anatomske lokacije stegen, bokov in trebuha kot virov MMC in preiskali ključne parametre gojenja AT-MMC na mikronosilcih v mešalnih steklenkah. Nadalje smo raziskali parakrino delovanje MMC iz kostnega mozga (BM-MMC) in popkavnice (UC-MMC) na GMC. Ugotovili smo, da izolacija AT-MMC iz različnih anatomskih lokacij nima vpliva na proliferacijo AT-MMC, vpliva pa na nastop replikativne senescence AT-MMC v celični kulturi, saj je pri AT-MMC izoliranih iz maščevja bokov prišlo do zgodnejšega nastopa senescence kot pri AT-MMC izoliranih iz maščevja stegna in trebuha. Diferenciacija AT-MMC je pokazala, da so AT-MMC izolirane iz maščevja stegna bolj dovzetne za diferenciacijo v kostne in hrustančne celice. Pri namnoževanju AT-MMC na mikronosilcih v mešalnih steklenkah smo opazili boljše pritrjevanje AT-MMC na Cytodex-1 in Cytodex-3 mikronosilce po izmeničnem mešanju kot brez mešanja. Pritrjevanje AT-MMC na mikronosilce je bilo neodvisno od predinkubacije mikronosilcev v mediju z različnimi deleži seruma, kljub temu pa višji delež pritrjenih AT-MMC ni vodil do večjega končnega števila namnoženih AT-MMC. Menjava gojitvenega medija vsaka 2 dni se je izkazala za najustreznejšo. Dodajanje novih mikronosilcev tekom gojenja je vodilo do večjega končnega števila pridobljenih AT-MMC, pri Cytodex-3 pa se je zmanjšala tudi agregacija mikronosilcev. Iz tega sklepamo, da so Cytodex-3 primernejši za gojenje AT-MMC. Študija parakrinega delovanja BM-MMC in UC-MMC na celične linije GMC je pokazala, da topni dejavniki prisotni v kondicioniranem mediju MMC znižajo izražanje ciklina D1, kar vodi v ustavitvev celičnega cikla GMC in posledično v nastop senescence. Slednja je najverjetneje posledica sproženega signaliziranja preko dveh tumors-surpresorskih poti: p53-p21-pRB in p16-pRB. Parakrini signali MMC so zvišali dovzetnost GMC na kemoterapevtik temozolomid in sprožili astrocitno diferenciacijo GMC z znižanjem izražanja Sox-2 in Notch-1, ter povišanjem izražanja genov za vimentin in GFAP. Delo kaže, da mesto odvzema maščevja vpliva na značilnosti izoliranih AT-MMC, ki jih lahko z določenimi parametri gojenja uspešno namnožimo na mikronosilcih v mešalnih steklenkah. Dokazana je tudi sposobnost MMC, da sprožijo senescenco, diferenciacijo in znižanje odpornosti GMC.

TABLE OF CONTENTS

	KEY WORDS DOCUMENTATION (KWD)	III
	KLJUČNA DOKUMENTACIJSKA INFORMACIJA (KDI)	IV
	TABLE OF CONTENTS	V
	INDEX OF TABLES	VIII
	INDEX OF FIGURES	IX
	ABBREVIATIONS AND SYMBOLS	XI
1	INTRODUCTION	1
2	LITERATURE OVERVIEW	4
2.1	MESENCHYMAL STEM CELLS	4
2.1.1	Tissue sources of MSCs	4
2.1.1.1	Bone marrow-derived MSCs	4
2.1.1.2	Umbilical cord Wharton's jelly-derived MSCs	5
2.1.1.3	Adipose tissue-derived MSCs	5
2.1.2	Characteristics of MSCs	6
2.1.2.1	MSC release of bioactive proteins	6
2.1.2.2	Homing potential of MSCs	8
2.1.3	The route to therapeutic application of MSCs	8
2.2	BIOREACTOR CULTURE SYSTEMS USING MICROCARRIER TECHNOLOGY	10
2.2.1	General properties of microcarriers	10
2.2.2	Cultivation of MSCs on microcarriers	11
2.2.2.1	Selection of microcarrier expansion for MSCs	11
2.2.2.2	Expansion of MSCs on microcarriers	12
2.2.3	Differentiation of MSCs upon expansion on microcarriers	13
2.3	GLIOBLASTOMA	15
2.3.1	Hierarchical model of cancer development	16
2.3.2	Glioma stem-like cells	16
2.3.2.1	GSLCs at the apex of the hierarchical model	16
2.3.2.2	Identification of GSLCs	18
2.3.2.3	Resistance of GSLCs	19
2.3.2.4	GSLCs as therapeutic targets	20
2.3.3	MSCs in cancer treatment	20
2.3.3.1	Influence of naïve MSCs on GBM	22
3	MATERIALS AND METHODS	24
3.1	ISOLATION AND CHARACTERIZATION OF ADIPOSE TISSUE-DERIVED MESENCHYMAL STEM CELLS (AT-MSCs)	24

3.1.1	Isolation of AT-MSCs	24
3.1.2	Immunophenotyping of AT-MSCs by fluorescence activated cell sorting (FACS)	25
3.1.3	The evaluation of MSC's differentiation potential	26
3.1.3.1	Adipogenic differentiation	26
3.1.3.2	Osteogenic differentiation	26
3.1.3.3	Chondrogenic differentiation	27
3.1.4	Characterization of AT-MSC life-span	27
3.1.4.1	Cumulative population doubling level (CPDL) determination	27
3.1.4.2	Detection of replicative senescence	27
3.1.5	Statistical analysis	28
3.2	CULTIVATION OF AT-MSCs ON MICROCARRIERS IN SPINNER FLASKS	29
3.2.1	Microcarrier characteristics	29
3.2.2	Determination of AT-MSC seeding efficiency on microcarriers	29
3.2.2.1	AT-MSC seeding efficiency under static conditions	29
3.2.2.2	AT-MSC seeding efficiency in spinner flasks	30
3.2.3	AT-MSC harvest from microcarriers	30
3.2.4	AT-MSC expansion on microcarriers in spinner flasks	30
3.2.4.2	Differentiation potential of AT-MSCs upon cultivation on microcarriers	31
3.2.5	Statistical analyses	31
3.3	THE EFFECT OF UMBILICAL CORD-DERIVED MESENCHYMAL STEM CELLS (UC-MSCs) AND BONE MARROW-DERIVED MESENCHYMAL STEM CELLS (BM-MSCs) ON GLIOMA STEM-LIKE CELLS (GSLCs)	32
3.3.1	Cell isolation and cultivation	32
3.3.1.1	Isolation of UC-MSCs	32
3.3.1.2	Immunophenotyping of UC-MSCs by FACS	33
3.3.1.3	The evaluation of UC-MSCs differentiation potential	33
3.3.1.2	Cultivation of BM-MSCs	33
3.3.1.3	Generation of GBM cell primary culture enriched for GSLCs	34
3.3.1.4	Cultivation of GSLC lines	34
3.3.2	Conditioned media collection	35
3.3.3	FACS analysis of CD133 expression	35
3.3.4	Analysis of cell migration in vitro	36
3.3.5	Cell cycle analysis	36
3.3.6	Apoptosis assays	37
3.3.6.1	Anexin V/PI assay	37
3.3.6.2	Mitochondrial membrane potential detection	37
3.3.7	Cell senescence	38
3.3.8	Gene expression analysis	38
3.3.8.1	Isolation of RNA	38

3.3.8.2	Determination of RNA concentration	39
3.3.8.3	Reverse transcription	39
3.3.8.4	Real-time quantitative PCR	39
3.3.9	Chemotherapeutics cytotoxicity effect on NCH421k and NCH644 cells	40
3.3.10	Statistical analyses	40
3.4	INDIRECT CO-CULTURES OF UC-MSCs AND BM-MSCs WITH NCH421k CELLS	42
3.4.1	Indirect co-cultures set up	42
3.4.2	Proliferation assay using Ki-67 antibody	42
3.4.3	FACS analysis of CD133 expression	43
3.4.4	Gene expression	43
3.4.5	Statistical analyses	43
4	RESULTS	44
4.1	ISOLATION AND CHARACTERIZATION OF ADIPOSE TISSUE DERIVED MESENCHYMAL STEM CELLS (AT-MSCs)	44
4.1.1	Number of isolated cells	44
4.1.2	Analysis of AT-MSC surface markers	45
4.1.3	Differentiation of isolated AT-MSCs	46
4.1.4	Growth properties of AT-MSCs	49
4.1.5	Replicative senescence in AT-MSCs	50
4.2	EXPANSION OF AT-MSCs ON MICROCARRIERS	51
4.2.1	AT-MSC seeding efficiency on microcarriers	51
4.2.1.1	Effect of microcarriers pre-coating on AT-MSC seeding in static and in spinner flasks culture system	51
4.2.1.2	Effect of agitation regime on the AT-MSC seeding efficiency in spinner flasks	52
4.2.2	AT-MSC expansion in spinner flasks	54
4.2.2.1	Effect of pre-coating of microcarriers on AT-MSC expansion	54
4.2.2.2	Effect of agitation regime on AT-MSC expansion	55
4.2.2.3	Effect of the feeding regime on AT-MSC expansion	55
4.2.2.4	Effect of subsequent microcarriers addition on AT-MSC expansion	57
4.2.3	Characterization of AT-MSCs after expansion on microcarriers	60
4.3	PARACRINE EFFECTS OF BM-MSC AND UC-MSC CONDITIONED MEDIA ON GSLCs	63
4.3.1	Isolation and characterization of umbilical cord-derived mesenchymal stem cells (UC-MSCs)	63
4.3.2	Confirmation of GSLCs identity	65
4.3.3	Influence of GSLC conditioned media on migratory capacity of UC-MSCs and BM-MSCs	66
4.3.4	MSC-CM influence on cell cycle of GSLCs	67
4.3.5	MSC-CM impact on induction of apoptosis in GSLCs	69

4.3.6	MSC-CM influence on activation of senescence in GSLCs	70
4.3.7	MSC-CM influence on stemness and differentiation marker expression in GSLC	74
4.3.8	MSC-CM impact on chemoresistance of NCH421k and NCH644 cells	77
4.4	INDIRECT CO-CULTURES OF NCH421k CELLS WITH BM-MSCs AND UC-MSCs	79
4.4.1	MSC influence on proliferation of NCH421k cells	79
4.4.2	MSC influence on activation of senescence in NCH421k cells	79
4.4.3	MSC influence on onset of apoptosis in NCH421k cells	80
4.4.4	Influence of MSCs on stemness and differentiation markers expression in NCH421k cells	81
5	DISCUSSION AND CONCLUSIONS	83
5.1	DISCUSSION	83
5.1.1	Influence of adipose tissue harvesting-site on characteristics of isolated MSCs	83
5.1.2	Expansion of AT-MSCs microcarrier-based spinner system	85
5.1.2.1	Optimization of AT-MSC seeding efficiency on microcarriers	85
5.1.2.2	Optimization of AT-MSC expansion on microcarriers in spinner flasks	86
5.1.2.3	Differentiation of AT-MSCs after expansion on MCs in spinner flasks	87
5.1.3	Paracrine effect of UC-MSCs and BM-MSCs on GSLCs	88
5.1.3.1	Antiproliferative effects of MSC paracrine signaling	88
5.1.3.2	Paracrine effects of UC-MSCs and BM-MSCs change stemness profile of GSLCs	92
5.1.3.3	Decreased resistance of GSLCs in presence of MSCs conditioned media	93
5.2	CONCLUSIONS	96
6	SUMMARY (POVZETEK)	98
6.1	SUMMARY	98
6.2	POVZETEK	100
7	REFERENCES	108
	ACKNOWLEDGEMENT (ZAHVALA)	
	ANNEXES	

INDEX OF TABLES

Table 1: Commonly used microcarriers for expansion of MSCs	11
Table 2: Expansion of human MSCs on microcarriers	14
Table 3: Composition of X-gal staining solution	28
Table 4: Characteristics of Cytodex-1 and Cytodex-3 microcarriers	29
Table 5: Summary of donor, sampling characteristics and cells	44
Table 6: Summary of surface marker expression in isolated AT-MSc lines	46
Table 7: Influence of various tested culture conditions on AT-MSc yield at day 10	58
Table 8: Examination of apoptosis in NCH421k cells by AnnexinV/PI measurements	70
Table 9: List of de-regulated genes in NCH421k cells exposed to either UC-CM or BM-CM relative to NBE exposed NCH421k cells	72
Table 10: KEGG pathway analysis of de-regulated genes in NCH421k cells as detected with Senescence RT ² Profiler PCR Array	73

INDEX OF FIGURES

Figure 1:	Immunomodulatory and trophic effects of MSCs	7
Figure 2:	Schematic representation of the hierarchical model of GBM development	17
Figure 3:	Schematic overview of the CD133 transmembrane protein	18
Figure 4:	Morphology of AT-MSCs as noted at passage 6	25
Figure 5:	Morphology of UC-MSC clone10 (left picture) and clone 13 (right picture)	32
Figure 6:	Morphology of BM-MSC-2 (left picture) and BM-MSC-3 (right picture)	33
Figure 7:	Spheroid morphology of NIB26 (left) and NIB50 (right) GSLCs	34
Figure 8:	Spheroid morphology of NCH421k (left) and NCH644 (right) GSLCs	35
Figure 9:	Schematic representation of indirect MSC and GSLC co-culture in the Boyden chamber set up	42
Figure 10:	MSC surface marker expression in isolated AT-MSCs as detected by FACS	45
Figure 11:	Differentiation of AT-MSCs	47
Figure 12:	Quantification of AT-MSC differentiation	48
Figure 13:	Growth profiling of AT-MSCs	49
Figure 14:	Spontaneous senescence arising in isolated AT-MSCs during prolonged <i>in vitro</i> culture	50
Figure 15:	AT-MSC seeding efficiency on differently pre-coated microcarriers	52
Figure 16:	AT-MSC seeding efficiency on microcarriers pre-coated with GM and grown for 24 h at different agitation regimens	53
Figure 17:	Effect of Cytodex-1 and Cytodex-3 pre-coating with GM and FBS on AT-MSC proliferation	54
Figure 18:	Influence of agitation regime applied during the first 24 h of cultivation on AT-MSC expansion on Cytodex-1 and Cytodex-3 microcarriers	55
Figure 19:	Influence of the feeding regime on AT-MSC growth on Cytodex-1 and Cytodex-3 microcarriers	56
Figure 20:	AT-MSC appearance on Cytodex-1 and Cytodex-3 microcarriers at day 6 of cultivation	57

Figure 21: Influence of microcarrier addition during cultivation process on AT-MSC expansion	58
Figure 22: The influence of microcarriers addition on the AT-MSC-microcarrier aggregation upon expansion in spinner flasks	59
Figure 23: Adipogenic differentiation of the AT-MSCs after cultivation on microcarriers	60
Figure 24: Chondrogenic differentiation of the AT-MSCs after cultivation on microcarriers	61
Figure 25: Osteogenic differentiation of the AT-MSCs after cultivation on microcarriers	61
Figure 26: AT-MSC surface marker expression prior and post culturing on microcarriers	62
Figure 27: Phenotypic characterization of UC-MSCs	63
Figure 28: Analysis of differentiation capacity of UC-MSCs	64
Figure 29: Expression of CD133 surface marker in GSLCs isolated from primary GBM tissue	65
Figure 30: NCH421k CM influence on UC-MSCs and BM-MSCs migration	66
Figure 31: GSLCs cell cycle analysis in presence of UC-CM and BM-CM	67
Figure 32: Morphology of GSLCs cells in presence of UC-CM and BM-CM	68
Figure 33: MSC-CM influence on activation of apoptosis in GSLCs lines	69
Figure 34: Induction of senescence in GSLCs in presence of MSC-CM	70
Figure 35: p21 and p16 gene expression in GSLCs exposed to MSC-CM	73
Figure 36: MSC-CM influence on CD133 expression in GSLCs	74
Figure 37: MSC-CM influence on stemness and glial differentiation markers expression	76
Figure 38: MSC-CM influence on NCH421k and NCH644 resistance upon exposure to TMZ	77
Figure 39: MSC-CM influence on NCH421k and NCH644 resistance upon exposure to 5-FU	78
Figure 40: Proliferation of NCH421k cells co-cultured with MSCs	79
Figure 41: Analysis of genes associated with senescence in NCH421k cells indirectly co-cultured with UC-MSCs and BM-MSCs	80
Figure 42: Apoptosis in NCH421k cells indirectly co-cultured with UC-MSCs and BM-MSCs	80
Figure 43: Analysis of CD133 expression of NCH421k cells indirectly co-cultured with UC-MSCs and BM-MSCs	81

Figure 44: Analysis of stemness markers in NCH421k cells indirectly co-cultured with UC-MSCs and BM-MSCs

82

ABBREVIATIONS AND SYMBOLS

5-FU	5-fluoro-uracil
ATM	ataxia telangiectasia mutated
AT-MSCs	adipose tissue-derived mesenchymal stem cells
BAX	BCL2-associated X protein
BCL-2	B-cell CLL/lymphoma 2
bFGF	basic fibroblast growth factor
BM-CM	BM-MSC conditioned media
BM-MSCs	bone-marrow-derived mesenchymal stem cells
CCND1	cyclin D1
CD105	endoglin
CD11b	integrin, alpha M (complement component 3 receptor 3 subunit)
CD133	prominin-1
CD14	CD14 molecule
CD15	fucosyltransferase 4 (alpha (1,3) fucosyltransferase
CD19	CD19 molecule
CD34	CD34 molecule
CD44	CD44 molecule
CD45	protein tyrosine phosphatase, receptor type, C
CD73	5'-nucleotidase
CD79a	CD79a molecule, immunoglobulin-associated alpha
CD90	Thy-1 cell surface antigen
CDKN1A	p21; cyclin-dependent kinase inhibitor 1A
CDKN2A	p16; cyclin-dependent kinase inhibitor 2A
cDNA	complementary DNA
CITED2	Cbp/p300-interacting transactivator, with Glu/Asp-rich carboxyterminal domain, 2
CM	conditioned media
COL1A1	collagen, type I, alpha 1
CPDL	cumulative population doubling level
CSC	cancer stem cells

CXCL-1	chemokine (C-X-C motif) ligand 1
CXCL-12	chemokine (C-X-C motif) ligand 12
CXCL-2	chemokine (C-X-C motif) ligand 2
CXCL-3	chemokine (C-X-C motif) ligand 3
CXCL-8	chemokine (C-X-C motif) ligand 8
CXCR4	chemokine receptor (C-X-C motif) receptor 4
DEPC	diethylpyrocarbonate
DMEM	Dulbecco's Modified Eagle's Medium
EDTA	ethylenediaminetetraacetic acid
EGF	epidermal growth factor
FACS	fluorescence activated cell sorting
FBS	foetal bovine serum
FN1	fibronectin 1
GAPDH	glyceraldehyde 3-phosphate dehydrogenase
GBM	glioblastoma
GFAP	glial fibrillary acidic protein
GM	growth medium
GSLCs	glioma stem-like cells
HGF	hepatocyte growth factor
HLA-DR	major histocompatibility complex, class II, DR alpha
IBMX	3-isobutyl-1-methyl-xanthine
IGFBP3	insulin-like growth factor binding protein 3
IGFBP5	insulin-like growth factor binding protein 5
IL-1	interleukin 1
IL-3	interleukin 3
IL-6	interleukin 6
IL-8	interleukin 8
JC-1	5,5',6,6'-tetrachloro-1,1',3,3'-tetraethylbenzimidazolylcarbocyanine iodide
L1CAM	L1 cell adhesion molecule
MCP-1	monocyte chemotactic protein 1
MGMT	enzyme O6-methylguanine-DNA- methyltransferase

MMP	mitochondrial membrane potential
MORC-3	MORC family CW-type zinc finger 3
mRNA	messenger RNA
MSCs	mesenchymal stem cells
NBE	neurobasal medium
NBE-CM	NCH421k or NCH644 conditioned media
NOX-4	NADPH oxidase 4
NSCs	neural stem cells
PBS	phosphate-buffered saline
PI	propidium iodide
PRCKD	protein kinase C, delta
qRT-PCR	real-time reverse transcription polymerase chain reaction
RNA	ribonucleic acid
RT	room temperature
SA- β -gal	senescence associated β -gal assay
SDF-1 α	stromal cell-derived factor 1 α
SERPINE1	serpin peptidase inhibitor, clade E
SOX-2	SRY (sex determining region Y)-box 2
STS	staurosporine
TGF β	transforming growth factor- β
TMZ	temozolomide
TNF	tumor necrosis factor receptors I
UCB-MSCs	umbilical cord blood-derived MSCs
UC-CM	UC-MSC conditioned media
UC-MSCs	umbilical cord-derived mesenchymal stem cells
VEGF	vascular endothelial growth factor
X-gal	5-bromo-4-chloro-3-indolyl- β -D-galactopyranoside
XIAP	X-linked inhibitor of apoptosis protein

1. INTRODUCTION

Mesenchymal stem cells (MSCs) have a promising future in the field of regenerative medicine and treatment of many diseases, including autoimmune diseases, neurodegenerative diseases and cancers, with the number of clinical trials gradually increasing and producing encouraging preliminary data (Heathman et al., 2015). Various adult and birth-associated sources of MSCs have been extensively studied, such as bone marrow, adipose tissue, umbilical cord blood and umbilical cord. These stem cells have a major role in the repair of damaged tissue in two different ways: first, by directly differentiating to different resident cell types, and second, by secreting trophic factors that can trigger the tissue repair processes (D'souza et al., 2015). Firm conclusions of MSC efficiency in wound and soft-tissue repair, and also in the repair of bone defects, have been drawn from several preclinical trials (Murphy et al., 2013). It is also widely accepted that MSCs have a role not just in repair mechanisms, but also more prominently in tissue cell turnover, as encouraging data have been provided by studies and clinical research into the treatment of liver, kidney and pancreas disorders (D'souza et al., 2015). At the same time, MSCs can be exploited as immunosuppressive agents in the treatment of autoimmune diseases, through cell-to-cell contact with immune cells or through the soluble factors produced by MSCs (e.g., rheumatoid arthritis and graft-*versus*-host disease (Glenn and Whartenby, 2014).

The MSC homing potential can be effectively exploited for use of MSCs in cancer treatments, where MSCs can act as a delivery platform for therapeutic agents to release the anticancer agents directly at the tumor site. In view of this property, approaches have been developed to genetically modify MSCs to produce high levels of prodrug-activating enzymes to increase the local concentrations of active chemotherapeutic agents, as molecules that induce apoptosis and oncolytic viruses, which has been shown to be efficient in suppression of tumor growth in *in-vivo* animal studies (Duebgen et al., 2014; Stuckey and Shah, 2014). Moreover, through their secretion of soluble factors, MSCs themselves have antitumor properties in various cancer types, including glioma (Hong et al., 2014; Sun et al., 2014; Yang et al., 2014).

The research carried out in this dissertation can be separated into the three parts, as follows.

In the first part of the dissertation we aimed to define the anatomical location of adipose tissue for superior extraction of best quality adipose tissue-derived MSCs (AT-MSCs). Adipose tissue is considered a valuable source of MSCs due to its good accessibility and especially because of the relative abundance and ease of MSC isolation from this tissue (Dubois et al., 2008, Zuk et al., 2001). AT-MSCs have the typical MSC characteristics in terms of their morphology, surface marker expression, differentiation, and secretion of soluble factors (Ong and Suggi, 2014). Here, the role of adipose tissue harvest site on the characteristics of AT-

MSCs will be investigated, in terms of their proliferation, replicative senescence and differentiation.

Hypothesis 1: To determine whether the harvest site and the various anatomical locations for the isolation of AT-MSCs from adipose tissue have any influence on the life-span of AT-MSCs.

To confirm this first hypothesis, the following experiments were performed:

- AT-MSCs were isolated from adipose tissue from thighs, hips and abdomen, and tested to determine whether of these locations produces more viable and proliferative cells.
- AT-MSCs were tested for their ability to differentiate into cells of mesodermal lineage; analysis of characteristic MSC markers was also performed.

In the second part of the dissertation we aimed to optimise the culture conditions for optimal expansion of AT-MSCs in microcarrier-based bioreactor systems, to obtain high quantities of AT-MSCs for therapeutic applications. For treatment of various disorders, MSCs of good quality and sufficient amounts are a prerequisite for effective therapeutic outcome. MSC cell-based therapies have demands for MSC quantities range from $1-2 \times 10^6$ cells/kg patient, or 10^8 total cell numbers (Murphy et al., 2013). To fulfil these needs, a microcarrier-based bioreactor system represents an appealing option. The cultivation of adherent cells in suspension is enabled through the introduction of microcarriers, which are small particles of 150 μm to 200 μm in diameter that thus prove a large surface area for cell growth (Nienow et al., 2006). Consequently, by using microcarrier cultures, high MSC densities can be obtained under more controllable culture conditions (Chen et al., 2015, Goh et al., 2013).

Hypothesis 2: The cultivation process of AT-MSCs on microcarrier-based spinner systems can be optimised for high yields, where the AT-MSCs retain their MSC characteristics.

To confirm the hypothesis experiments were performed:

- Several culture parameters were tested to increase the adhesion of AT-MSCs on Cytodex-1 and Cytodex-3 microcarriers.
- The culture parameters that influence the expansion of AT-MSCs on Cytodex-1 and Cytodex-3 microcarriers were examined.
- Upon cultivation of AT-MSCs on the surface of microcarriers, MSC differentiation and specific markers expression were analysed.

In the third part of the dissertation we aimed to determine the paracrine effects of umbilical cord-derived MSCs (UC-MSCs) and bone marrow-derived MSCs (BM-MSCs) on the phenotype of glioma stem-like cell (GSLC) lines *in vitro*. MSCs have been shown to have

antitumor effects in many cancers, including the most malignant brain tumor, glioblastoma (GBM) (Hong et al., 2014; Sun et al., 2014). Current GBM treatments are still not successful, most probably due to the presence of highly tumorigenic cells within the tumor, the GSLCs, which are responsible for tumor recurrence and poor patient prognosis. The GSLCs within these tumors are not very abundant, and they are mainly characterised by expression of a panel of specific surface markers, one of the most frequently used of which is CD133 (Campos et al., 2011; Jackson et al., 2015). At the same time, the presence of GSLCs within a GBM is associated with high resistance to cytostatic drugs (Signore et al., 2014; Ulasov et al., 2011). Hence, GSLCs are recognized as the most preferential target for improvement of GBM therapies. Here, we aimed to explore how UC-MSCs and BM-MSCs interact with GSLCs in an indirect, paracrine manner.

Hypothesis 3: Conditioned media of UC-MSCs and BM-MSCs as well as UC-MSC and BM-MSC indirect co-cultures affect in a paracrine manner the proliferation, stemness, and resistance to chemotherapeutics of GSLCs.

To confirm this hypothesis we assayed:

- Proliferation of GSLC lines in the presence of UC-MSC and BM-MSC conditioned media and by indirect co-culturing with both of MSC types.
- Expression of GSLC stemness markers upon exposure to UC-MSC and BM-MSC conditioned media and by indirect co-culturing with both MSC types.
- The resistance of GSLCs towards the cytotoxic drugs temozolomide (TMZ) and 5-fluoro-uracil (5-FU) upon separate and joint exposure to UC-MSC and BM-MSC conditioned media.

2. LITERATURE OVERVIEW

2.1. MESENCHYMAL STEM CELLS

The first reports on MSCs can be traced back to the 1970's, when Friedenstein and colleagues described an adherent, non-haematopoietic cell type in mouse bone marrow (Friedenstein et al., 1976). These adherent cells formed colonies and had spindle-shaped fibroblast-like morphology. In the following years, studies focused on similar populations of bone marrow stromal cells, and then in 1991, Caplan showed that these cells can differentiate into all types of cells of mesodermal lineage, and should be termed 'mesenchymal stem cells' (Caplan, 1991). Confusion arising from the identification and characterisation of MSCs led to the proposal of the International Society for Cellular Therapy that human MSCs should fulfill the following criteria and standards:

- (1) Adherence to plastic under standard culture conditions;
- (2) *In-vitro* differentiation into adipocytes, osteoblasts and chondroblasts;
- (3) Specific surface antigen expression in which 95 % of the cells express the antigens recognized by CD105, CD73 and CD90, with the same cells lacking (as a maximum of 2 % positivity) the haematopoietic antigens CD45, CD34, CD14 or CD11b, CD79a or CD19, and HLA-DR (Dominici et al., 2006).

Although numerous studies investigated the presence and absence of MSC surface markers on cells isolated from various tissues, there are no defined special markers for MSCs today (Murphy et al., 2013, D'sousa et al., 2014).

2.1.1. Tissue sources of MSCs

In addition to bone marrow, MSCs have been derived from a broad range of adult tissues, including adipose tissue (Zuk et al., 2001), peripheral blood, dental pulp (Hass et al., 2011), and others. MSCs can also be obtained from neonatal tissues; e.g., umbilical cord Wharton's jelly (Wang et al., 2004), umbilical cord blood (UCB-MSCs), placenta, and amnion (Hass et al., 2011).

2.1.1.1. Bone marrow-derived MSCs

Bone marrow has for many years been the main source of MSCs, although their collection is an invasive and painful procedure for donors. Also, the frequency of MSCs in bone marrow samples is very low (0.001 %-0.01 %), and their numbers decline with the age of donors (Caplan et al., 2007). The most common method for isolation of BM-MSCs is density

gradient centrifugation of bone-marrow aspirate and collection of the fraction of mononuclear cells for seeding in plastic cell culture dishes (Hass et al., 2011).

2.1.1.2. Umbilical cord Wharton's jelly-derived MSCs

The umbilical cord is an abundant and accessible source of MSCs. As the umbilical cord is considered as waste after child delivery, invasive procedures and ethical problems are avoided. To isolate UC-MSCs, enzymatic digestion with collagenase is usually used for extraction of the cells from Wharton's jelly (Wang et al., 2004). In addition, the explant method can be used, in which the Wharton's jelly is minced into small pieces that are left undisturbed in plastic dishes until the UC-MSCs migrate out and form cell colonies (Ding et al., 2015). In general, the enzymatic method results in higher numbers of a homogenous population UC-MSCs at the initial stages of cultivation compared to the explant method, where less consistent cell numbers are obtained. Moreover, Paladino et al. (2015) reported on higher proliferation rates and onset of senescence in later passages in UC-MSCs extracted with enzymatic method compared to UC-MSCs extracted with the explant method.

2.1.1.3. Adipose tissue-derived MSCs

The main advantage of adipose tissue as a source of MSCs is its lifetime availability and removal under minimal invasive procedures. Adipose tissue can be collected as a waste after liposuction or lipoplastic procedures (Dubois et al., 2008). AT-MSCs can be very efficiently obtained from adipose tissue by its digestion with collagenase, followed by several centrifugation and washing steps (Zuk et al., 2001; Buschmann et al., 2013). Isolation of AT-MSCs can be performed from adipose patches from several anatomical locations, and in these locations the amounts and metabolic activities of the AT-MSCs can vary, which might also influence the AT-MSC characteristics (Schipper et al., 2008). However, the anatomical location of the adipose tissue used has been shown to have no influence on AT-MSC yields (Buschman et al., 2008; Schipper et al., 2008), although Jürgens et al. (2008) reported higher frequencies of colony forming units of AT-MSCs obtained from abdomen adipose deposits compared to thigh/hip fat pads. However, the yield of AT-MSCs has been shown to be influenced by the harvesting technique of the adipose tissue, with resection and tumescent manual liposuction being the preferred methods to obtain higher cell yields, in comparison to ultrasound-assisted liposuction (Oedayrajsingh-Varma et al., 2006, Iyyanki et al., 2015). The influence of donor age on AT-MSC proliferation remains a matter of dispute, however, as some reports have shown no influence (Buschman et al., 2013; Jürgens et al., 2008), while some have claimed that AT-MSCs isolated from younger donors proliferate more rapidly (Choudhery et al., 2014; Schipper et al., 2008). Moreover, no effects of the adipose harvest site on proliferation and differentiation of AT-MSCs have been detected (Buschman et al.,

2013; Jürgens et al., 2008; Schipper et al., 2008). Similarly, AT-MSCs obtained from various anatomical locations from the same donor have shown similar proliferation and differentiation characteristics (Choudhery et al., 2015). In AT-MSCs from distinct anatomical locations, no differences in expression of the pluripotent stem-cell-related genes *Sox-2*, *Oct-4* and *nanog* were detected (Sachs et al., 2012).

2.1.2. Characteristics of MSCs

One of the characteristics of MSCs is their limited *in-vitro* life span. Maximal population doublings for AT-MSCs, BM-MSCs and UC-MSCs have been reported to range from 20-60 population doublings (Choudhery et al., 2013; Christodoulou et al., 2012; Hwang et al., 2014), and this is influenced by many variables, including MSC extraction procedure and culture conditions. The limited lifespan of MSCs is due to replicative senescence, which occurs after a certain number of population doublings under *in-vitro* culture conditions (Wagner et al., 2008). Senescent MSCs become enlarged and show irregular morphologies, and they no longer undergo mitotic division, although they remain metabolically active (Wagner et al., 2010). The key mechanism responsible for the process of *in-vitro* replicative senescence was shown to be progressive telomere shortening (Abdallah and Kassem, 2008). In addition, various molecular pathways significantly contribute to the processes of aging and replicative senescence in MSCs, including DNA damage, mitochondrial changes, and oxidative stress (Wagner et al., 2010). Indeed, the onset of senescence impairs the MSC differentiation potential, thus limiting their therapeutic potential and applicability in cell therapies (Lin et al., 2014; Sepúlveda et al., 2014).

2.1.2.1. MSC release of bioactive proteins

MSCs have two distinct functions, as they can serve as a replacement pool for dead cells in mesenchymal tissues, and they can have trophic effects on cells in their vicinity through the release of bioactive factors, such as cytokines, chemokines and growth factors (Caplan et al., 2007). The secretion of various bioactive factors by MSCs can have autocrine effects or paracrine effects, which can result in profound effects on their local microenvironment and can be exploited for therapeutic applications. For example, the trophic paracrine effects of MSCs can promote the formation of new blood vessels or affect the remodelling of existing ones in tissue ischaemia, and even increase the capillary density through the release of numerous cytokines, such as vascular endothelial growth factor (VEGF), basic fibroblast growth factor (bFGF), monocyte chemoattractant protein 1 (MCP-1), and angiopoietin-1 (Boomsma and Geenen, 2012; Kinnaird et al., 2004). Cumulative evidence implies that the ancestors of MSCs were pericytes, as the gene expression profiles of pericytes and MSCs are very similar and pericytes can even give rise to MSCs when cultured (da Silva Meirelles et al., 2015).

MSCs are also involved in wound healing and regeneration of tissue, through their production of a plethora of cytokines that are involved in wound healing, such as interleukin (IL)-8, IL-6, hepatocyte growth factor (HGF), transforming growth factor- β (TGF β), tumor necrosis factor (TNF) receptors I, and VEGF, and also in stimulation of the production of collagen types I and II and fibronectin in damaged tissue (Huang et al., 2015; Li and Fu, 2012). AT-MSCs have been shown to have beneficial roles in preventing tissue fibrosis, due to their secretion of the anti-fibrotic cytokines HGF and prostaglandin E2, while at the same time, MSCs can reduce the presence of profibrotic factors such as TGF β 1 in damaged tissue, thus protecting lung tissue from radiation-induced fibrosis (Dong et al., 2014). Moreover, BM-MSCs engineered to secrete HGF reduced liver fibrosis in a rat model and improved hepatocyte function, which was accompanied by a reduction in the fibrinogenic cytokine TGF β 1 (Kim et al., 2014).

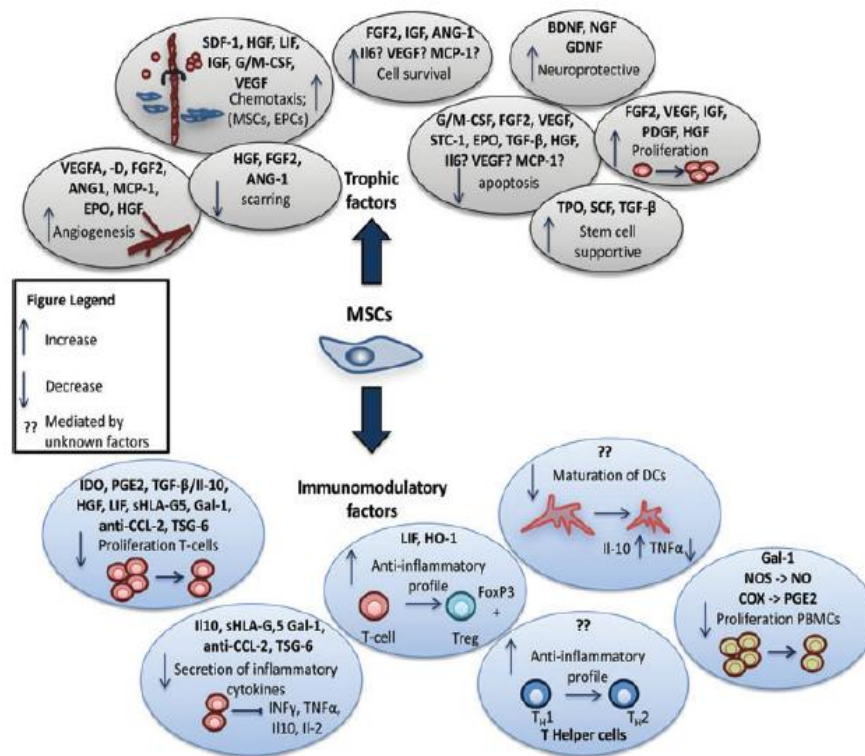


Figure 1: Immunomodulatory and trophic effects of MSCs (Doorn et al., 2011). MSCs mediate their therapeutic efficiency through various mechanisms, such as immunomodulation, anti-apoptosis, angiogenesis, support of growth and differentiation of local stem and progenitor cells, anti-scarring, and chemoattraction.

Through secretion of classic apoptotic inhibitors, such as the anti-apoptotic Akt, MSCs can prevent programmed cell death. In detail, UC-MSCs were reported to reduce apoptosis and necrosis in cardiac myocytes and vascular endothelial cells (Henning et al., 2012). Similarly, BM-MSCs transplanted into a rat model of intracerebral hemorrhage increased the survival of

neural cells by inhibition of apoptosis through activation of Akt and B-cell lymphoma 2 (Bcl-2) (Wang et al., 2012).

Moreover, the MSCs also have immunosuppressive and immunomodulatory functions, by affecting the wide range of immune cells (i.e., T lymphocytes, B lymphocytes, natural killer cells, dendritic cells, macrophages) (Amorin et al., 2014). Indeed, various types of MSCs, such as UC-MSCs, AT-MSCs and BM-MSCs, have already been successfully applied in the treatment of graft-*versus*-host disease (McGuirk et al., 2015).

2.1.2.2. Homing potential of MSCs

In-vitro and *in-vivo* studies have shown that cultured MSCs can migrate and home in on and graft onto sites of injury, and they can colocalise to tumors (Chamberlain et al., 2008; Sousa et al., 2014; Spaeth et al., 2008). The homing efficiency of MSCs has been shown to decrease with their higher passage numbers (Rombouts and Ploemacher, 2003), due to the loss of expression of chemokine receptor CXCR4, which recognises chemokine (C-X-C motif) ligand 12 (CXCL12; stromal cell-derived factor 1 α (SDF-1 α)) during culturing (Wynn et al., 2004). Also, it was shown that hypoxic culture conditions (Schioppa et al., 2003) and availability of cytokines and growth factor supplements such as interleukin (IL)-3, IL-6 and HGF can restore the expression of CXCR4 in MSCs (Shi et al., 2007). An important role in MSC migration has been attributed also to the matrix metallo-proteases, the expression of which is increased at higher cell density, under hypoxic culture conditions, and in the presence of inflammatory cytokines (i.e., TNF α , IL-1 β , TGF-1 β) (Sohni et al., 2013). However, the exact mechanism of MSC migration and homing at injury sites is not fully understood, although the main role was shown to be for chemokine receptor CXCR4 and its binding protein SDF-1 α (Ryu et al., 2010; Wynn et al., 2004).

2.1.3. The route to therapeutic application of MSCs

MSCs are currently being evaluated in clinical and experimental trials for the treatment of many pathological conditions, such as autoimmune diseases (Castro-Manrreza and Montesinos, 2015), acute and chronic inflammation (Murphy et al., 2013), neurodegenerative diseases (Tanna and Sachan, 2014), tissue-repair (Johal et al., 2015), and cancers (Arango Rodriguez et al., 2015). In the field of cell-based therapies, about one third of these use MSCs as therapeutics. With respect to MSC origins, most often bone marrow is used, followed by umbilical cord and adipose tissue (Heatman et al., 2015). For therapies, MSCs should be applied in relatively high amounts, as at least $1-2 \times 10^6$ cells/kg patient, or 10^8 total cell numbers (Murphy et al., 2013). As it is impossible to generate the required numbers of MSCs directly after the isolation process, MSCs need to be expanded under *in-vitro* conditions.

Moreover, successive passaging should eliminate other cell types (e.g., haematopoietic stem cells, endothelial cells) present in cultures after MSC isolation, to ensure the reproducible quality of the cell product (Murphy et al., 2013). However, the preparation of several millions of MSCs in classical laboratory T-flasks would be extremely time-consuming. In addition, long expansion times can increase the biological divergence, or the MSCs might become senescent before the desired cell number can be reached. Thus, new methods that use dedicated bioreactors to provide large surface areas for the cells in the smallest possible volumes are considered as an alternative for the expansion of MSCs in the high numbers that are needed for clinical applications.

2.2. BIOREACTOR CULTURE SYSTEMS USING MICROCARRIER TECHNOLOGY

The definitive need for technologies that can provide the demanded high numbers of MSCs for clinical therapies has led to the implementation of microcarrier-based culturing technologies. The concept of microcarrier culturing systems was developed by van Wezel (1967) and enables the cultivation of anchorage-dependent cells on the surfaces of small particles in suspension in flasks of variable volumes or bioreactors. The main advantage of microcarriers is that they provide a large surface area per unit of volume of bioreactor, which results in greatly increased cell yields compared to conventional two-dimensional culturing. Thus the microcarrier cultivation process is less work intensive and time consuming (Nienow et al., 2006). Moreover, microcarriers also enable scaling-up without passaging of the cells by bead-to-bead transfer, as fresh microcarriers can be added in existing cell cultures, and the cells then begin to colonise the new microcarriers. Using this technique, there is no need for proteolytic enzymes to detach the cells from the microcarriers, which reduces the damage to cell membranes and the risk of contamination. As microcarriers are suspended in stirred medium, the cells are exposed to homogenous environmental conditions throughout the culture, which leads to more reproducible culture conditions. Importantly, microcarrier culture technology can be upscaled from the laboratory set-up in spinner flasks to the larger agitated bioreactors, with flexible modes of operation and monitoring of the culture parameters (Rowley et al., 2012). Bioreactor technology using microcarriers has also been applied to the production of various biopharmaceutical products, such as recombinant proteins, antibodies and viruses (Martin et al., 2004), as also in the field of human embryonic stem cells expansion (Fernandes et al., 2009; Marinho et al., 2013).

2.2.1. General properties of microcarriers

The backbone of microcarriers is composed of several natural or synthetic polymers, and they can also be coated with various chemical compounds to facilitate the attachment of cells, thus enabling further expansion of the cells on microcarriers. The surface of microcarriers is positively charged to attract the negatively charged cells by electrostatic forces. This is achieved by the cross-linking of the microcarrier surface with cationic functional groups, such as primary or tertiary amines, collagen, gelatin, and fibronectin (Schop et al., 2010). The characteristics of the commercially available microcarriers that are most commonly used in protocols for the expansion of MSCs are given in Table 1.

The size of microcarriers should provide enough surface area for several cell doublings during the growth process, with diameters ranging from 100 μm to 230 μm reported to be optimal (Markvicheva and Grandfils, 2004). Although microcarriers are generally spherically shaped, they can be non-porous or macroporous. On non-porous microcarriers, the cells will spread

and grow only on the surface, while macroporous microcarriers provide additional surface area for cell growth and offer protection to the cells from shear stress (Ng et al., 1995).

Table 1: Commonly used microcarriers for expansion of MSCs.

Type	Microcarrier	Matrix composition	Surface feature/coating	Diameter (μm)	Surface area (cm^2/g)	Pore size	Supplier
Positively charged	Cytodex-1	Dextran	DEAE	190 \pm 58	4400	Solid	GE Healthcare
	FACT 102-L	Polystyrene	Cationic	90-150	480	Solid	SoloHill
Collagen coated	Cytodex-3	Dextran	Type I collagen	141-211	2700	Solid	GE Healthcare
	Collagen	Polystyrene	Type I collagen	90-150	480	Solid	SoloHill
Macroporous	Cultispher S	Gelatin	Gelatin	255 \pm 125	7500	Porous	ThermoScientific
	Cultispher G	Gelatin	Gelatin	130-380	N.A.	Porous	ThermoScientific
	Cytopore 1	Cellulose	DEAE	240 \pm 40	11000	Porous	GE Healthcare

N.A., data not available; DEAE, diethylaminoethyl

2.2.2. Cultivation of MSCs on microcarriers

Current MSC production for clinical applications under Good Manufacturing Practice conditions is carried out using classical or multilayer culture flasks, which are limited in terms of cell productivity. Furthermore, they require extensive handling that is accompanied by high contamination risk and multiple cell passages, which consequently leads to decreased MSC quality (Rowley et al., 2012). This cultivation approach can thus support the production of MSCs for low treatment doses or for a limited number of applications (Rowley et al., 2012). As an alternative, several studies have indicated or demonstrated the suitability of microcarrier cultivation systems for the expansion of MSCs (Chen et al., 2015; Goh et al., 2013; Hupfeld et al., 2014; Schop et al., 2010), as discussed in the sections below.

2.2.2.1. Selection of microcarrier expansion for MSCs

Various types of microcarriers have been screened for MSC expansion. Initially, Frauenschuh (2007) examined adhesion of porcine MSCs on Cytodex-1 and Cytodex-3 microcarriers (Table 1). They showed prominent MSC adhesion to Cytodex-1 microcarriers, as approximately 80 % of the inoculated cells adhered, whereas adhesion to Cytodex-3 microcarriers was only about 50 %. The benefits of Cytodex-1 for adhesion of BM-MSCs over several other types of microcarriers (e.g., glass, plastic, FACTIII, pronectin, collagen) has been shown, although it yielded seeding efficiencies of about 60 %, while for other types of microcarriers, the seeding efficiencies were from 30 % to 50 % (Schop et al., 2010).

Further studies of human MSC expansion in bioreactor systems were mainly conducted with Cytodex-1 or Cytodex-3, and the seeding efficiencies ranged from 50 % on Cytodex-1 for UC-MSCs and amniotic membrane MSCs (Hupfeld et al., 2014), to 90 % on Cytodex-1 and Cytodex-3 for placental MSCs (Timmins et al., 2012), and 90 % on Cytodex-3 for foetal MSCs (Goh et al., 2013). In addition, several studies have confirmed the suitability of macroporous Cultispher S microcarriers for MSCs, with reports of about 90 % seeding efficiencies for placental MSCs (Timmins et al., 2012), BM-MSCs and AT-MSCs (Santos et al., 2011). The heterogeneity in the adhesion of MSCs from different sources to Cytodex-1 and Cytodex-3 might result from the variations in cell surface extracellular matrix and integrin expression of MSCs of different origins (Brooke et al., 2008; Maijenburg et al., 2009).

2.2.2.2. Expansion of MSCs on microcarriers

Various types of microcarriers have been screened for the expansion of MSCs of different origins in 100 ml to 250 ml spinner flasks. In these studies, gelatin-based (i.e., Cytodex-3, Cultispher S) and cationic based (i.e., Cytodex-1) microcarriers were reported as the most appropriate for MSC adhesion and expansion, as presented in Table 2. However, in these cultures, wide ranges were reported for the increases in the MSCs populations, which varied from 4-fold to 20-fold increases, with regard to MSC tissue of origin, microcarrier type used, and other culture parameters (Table 2). Thus, the optimal culture parameters should be carefully examined for the selected microcarrier type and source of MSCs.

Above all, microcarrier cultivation systems have been shown to affect the secretion of the MSC paracrine factors and the MSC gene-expression profiles. Hupfeld et al. (2014) cultured UC-MSCs and amniotic membrane MSCs on Cytodex-1 microcarriers, where these secreted higher amounts of VEGF, bFGF-2, SDF-1 and interleukin (IL)-1 receptor antagonist, compared to MSCs cultured in culture flasks. In addition, their gene expression analysis revealed higher expression of the chemokines (chemokine (C-X-C motif) ligand-1 (CXCL-1); -2 (CXCL-2), -3 (CXCL-3) and -8 (CXCL-8)) in MSCs expanded on microcarriers, compared to those expanded in culture flasks. Importantly, Hupfeld et al. (2014) also showed less heterogeneity between MSCs from different donors when the MSCs were cultured on microcarriers. These findings should be further examined to enable successful implementation of MSCs in clinical applications.

2.2.3. Differentiation of MSCs upon expansion on microcarriers

MSCs expanded on microcarriers must retain the capacity to differentiate into cells of mesodermal lineage (adipocytes, osteocytes and chondrocytes). To date, most of the conducted studies confirmed the MSC differentiation efficiency upon culturing on microcarriers, dissociation from microcarriers and further culturing in culture flasks. Interestingly, increased osteogenic differentiation was observed for BM-MSCs and fetal BM-MSCs cultured on Cultispher G and Cytodex-3, respectively (Goh et al., 2013; Sun et al., 2010). The increase of osteogenic differentiation can be attributed to the microcarrier properties, as an increased osteogenic differentiation of amniotic MSCs was reported upon culturing of Cultispher S microcarriers and culture flasks (Chen et al., 2011). Moreover, an increased secretion of paracrine factors such as VEGF, FGF-2 and SDF-1 and differentially expression genes of CXCL family suggesting on increased angiogenic potential of umbilical cord and amniotic membrane MSCs cultured on Cytodex-1 microcarriers compared to those culture in flasks was reported (Hupfeld et al., 2014).

Future investigations are needed to reveal the influence of biochemical properties of microcarriers on differentiation of MSCs to prevent the possible failure of clinical treatment.

Table 2: Expansion of human MSCs on microcarriers

MSC source	Microcarrier type/ concentration	Agitation rate (rpm)	Feeding, medium exchange (days)	MSC expansion (cell density; cells/surface area)	Reference
Bone marrow	Cultispher S 1-2 g/l	30	2	4.2×10^5 cells/ml (8-fold)	Eibes et al. (2010)
Bone marrow	Cytodex-1 (20 cm ² /ml)	30 (18 h); then 40	3	3.4×10^5 cells/ml (4 fold)	Schop et al. (2010)
Bone marrow	Cultispher G 3-5 g/l	25 (30 min); static (10 min); then 25 (2 h)	3	4.5×10^4 cells/cm ² (7-fold)	Sun et al. (2010)
Foetal bone marrow	Cytodex-3 8.3 g/l	30 (24 h): then 50	2	8×10^5 cells/ml (4-fold)	Goh et al. (2013)
Foetal	Cytodex-3 8 g/l	25 (12 h); then 30	2	1.1×10^6 cells/ml N.A.	Chen et al. (2015)
Placenta	Cytodex-3 1 g/l	50	2	3×10^5 cells/ml (20-fold)	Hewitt et al. (2011)
Placenta	Cultispher S N.A.	Static overnight; N.A.	N.A.	1.7×10^6 cells/ml (15-fold)	Timmins et al. (2012)
Umbilical cord Amniotic membrane	Cytodex-1 2500 cm ²	Static overnight; then 40	2	5.2-fold UC- MSCs 4.9-fold AT- MSCs	Hupfeld et al. (2014)
Adipose tissue Bone marrow	Cultispher S 3-5 g/l	25 (15 min); static (2 h); then 40	(25 % daily)	2×10^5 cells/ml (18-fold) 1.4×10^5 cells/ml (14-fold)	Santos et al (2011)

N.A., data not available

2.3. GLIOBLASTOMA

Gliomas are the most frequent and fatal cancers of the central nervous system, and these include astrocytomas, oligodendrogliomas and ependymomas. The World Health Organisation (WHO) assigns four grades to astrocytomas: Grade I, or pilocytic astrocytoma; Grade II, or low-grade astrocytoma (AGII); Grade III, or anaplastic astrocytoma (AGIII); and Grade IV, or GBM. Unfortunately, GBM accounts for 45.6 % of all primary malignant brain tumors (Ostrom et al., 2014). Epidemiological data have shown that 3 to 5 per 100,000 adults each year are diagnosed as GBM cases in Europe and North America (Westermarck et al., 2012). The incidence of GBM also increases with age, with the highest rate observed from 75-84 years, and with 1.6-fold greater incidence in the male population (Ostrom et al., 2014).

GBM can be divided into two clinical forms, as primary and secondary GBM. Primary GBM represents the most common form (about 90 %), which develops *de novo*, primarily in elderly individuals, within 3-6 months. Secondary GBM arises from astrocytomas (WHO-defined Grade II/III) over 5-10 years, and mostly in younger people (mean age, 39 years). These two subtypes of GBM are almost histologically indistinguishable (Ohgaki et al., 2013). Primary GBMs represent highly vascularised tumors with large necrotic areas in the centre (Ohgaki et al., 2013). On other hand, secondary GBMs contain smaller areas of necrosis, and the patients have better prognosis (Li et al., 2015; Ohgaki et al., 2013). Primary and secondary GBM can be distinguished on a molecular basis by an *IDH1* mutation, which has been shown to be a diagnostic molecular marker of secondary GBM (Ohgaki and Kleihues, 2012).

In general, median survival of the patients with GBM is 12 months to 15 months, with <5 % as the 5-year survival rate (Meir et al., 2010; Ostrom et al., 2014). Currently, standard care of GBM patients consists of optimal surgical resection of the tumor, followed by concurrent radiotherapy and chemotherapy, where the most used protocols include temozolomide (TMZ) (Carlsson et al., 2014). Despite treatment, recurrences appear with an average timeframe of 6 months to 12 months (Ohgaki et al., 2013). Also, median survival of patients with GBM was reported to be significantly higher after combined radiotherapy with TMZ (14.2 months), compared to radiotherapy alone (11.2 months) (McNamara et al., 2014). However, this poor therapeutic outcome is due to the highly infiltrating tumor growth into the normal brain tissue, which limits total surgical resection, and inevitably results in tumor recurrence and worsening of patient prognosis (Alifieris et al., 2015).

2.3.1. Hierarchical model of cancer development

The clonal evolution model of cancer development presented nearly 40 years ago postulated that tumors arise from a single cell of origin, as a result of step-wise acquired somatic mutations, with sequential subclonal selection and the capacity to form new tumors. Identification of a small fraction of self-renewal cells in human acute myeloid leukemia with the capacity to reconstitute the clinical state of the disease after xenotransplantation led to the concept of the so-called cancer stem cells (CSCs). The existence of CSCs was subsequently demonstrated in diverse solid tumors, such as breast, GBM, colorectal, pancreatic and lung cancers (Boman et al., 2008, Sandberg et al., 2013). The concept behind the CSC model proposes hierarchical organisation of cells, with a small subset of CSCs at the apex of the tumorigenesis that are capable of self-renewal and can give rise to the variety of phenotypically diverse cells that form the tumor (Visvader and Lindeman, 2008). The key features that define CSC properties are (Gupta et al., 2009):

- (1) Within the tumor population, only CSCs have tumorigenic potential when transplanted to immunodeficient mice;
- (2) CSCs can be distinguished from the rest of the tumor cell population due to the presence of characteristic cell-surface markers;
- (3) CSCs give rise to tumors that consist of tumorigenic and non-tumorigenic cells with features of the original tumor;
- (4) CSCs retain their self-renewal ability through many generations.

Furthermore, the presence of CSCs has a clinical implication, as studies have demonstrated connection between CSCs in a tumor and the response to treatment, and also that CSCs can persist even after chemotherapy and radiotherapy.

2.3.2. Glioma stem-like cells

2.3.2.1. GSLCs at the appex of the hierarchical model

Mounting evidence supports the hypothesis that GBMs arise from the subventricular zone of the brain, which function as a source of neural stem cells (NSCs), and where neurons and glia are produced (Goffart et al., 2013). Following these observations, mutations that occur in NSCs, transit-amplifying progenitors, progenitor cells, or more differentiated types of cells such as astrocytes, oligodendrocytes and neurons, can result in the formation of GSLCs (Fig. 2) (Hadjipanayis and Van Meir, 2009). The GSLC subpopulation within a GBM sustains the entire tumor mass, either by transforming into differentiated tumor cells or by their self-renewal capacity to sustain the GSLC pool. Although a lot of evidence has showed the

intertwining of NSC and GSLC signalling pathways, gene expression and biomarkers, a plethora of examples have also confirmed the involvement of astrocytes in GBM development, which thus favour the astrocyte dedifferentiation theory (Goffart et al., 2013; Sundar et al., 2014). On the other hand, mounting evidence shows that the GSLC phenotype is dynamic rather than a fixed state, and that it is regulated by the surrounding microenvironment, which thus supports the new fluid CSC model (Fessler et al., 2013). In this model, CSCs represent an unstable cell type that is regulated by the surrounding microenvironment, which can even promote the dedifferentiation of differentiated cells to more stem-like cells (Fessler et al., 2013). Recent observations of Fessler et al. (2015) confirm that this high level of plasticity in GBM can mimic the tumor microenvironment stimuli using tumor microvascular endothelial cells, which results in dedifferentiation of GBM cells that have acquired GSLC features. The tumor microenvironment in GBM, with hypoxia, extracellular matrix components, endothelial and stromal cells, has been shown promote GSLC maintenance in the tumor mass (Fessler et al., 2013). Moreover, stromal cells have been identified as a part of the GBM tumor mass (Golebiewska et al., 2013), and they can even express putative GSLC markers (Stieber et al., 2014), which reflects the high plasticity of the cells present in a GBM tumor mass, thus confirming the heterogeneity of GBMs.

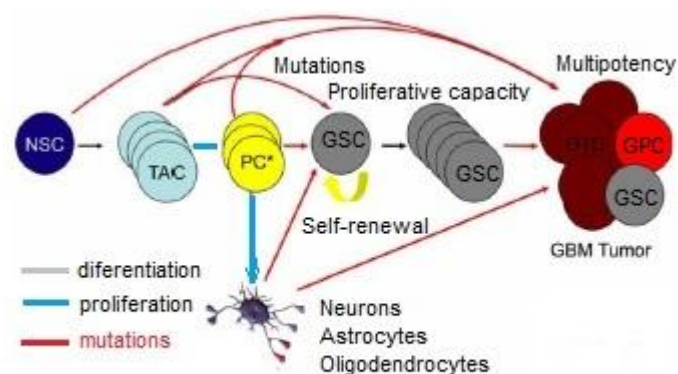


Figure 2: Schematic representation of the hierarchical model of GBM development (Hadjipanayis and Van Meir, 2009). In the central nervous system, NSCs undergo amplification to produce transit-amplifying progenitor cells (TAC), which further differentiate into committed neuronal or glial progenitor cells (PC*). These represent the pool for the development of neurons, astrocytes and oligodendrocytes. Mutations at any of the levels of this central nervous system differentiation can result in the development of GSCs that generate the cell population of the GBM, from GSCs, glioma-progenitor cells (GPC), and more differentiated tumor cells (DTC).

2.3.2.2. Identification of GSLCs

GSLCs were among the first CSCs from solid tumors that were identified as self-renewing and tumor-initiating. Singh et al. (2003) identified CD133-positive sphere-forming cells that represented a minority of the brain tumor cell population, were highly proliferative, and underwent extensive self-renewal and differentiation into cell phenotypes that were identical to the tumor *in situ*. Moreover, these data showed that only CD133-positive cells could reproduce the complexity of the primary tumor in immunodeficient mice, which was also confirmed by others (Bao et al., 2006; Singh et al., 2004). In contrast, several studies have demonstrated the ability of CD133-negative GBM cells to initiate a tumor phenotypically similar to the original tumor (Wang et al., 2008), while others have shown less aggressive behaviour of tumors initiated from CD133-negative cells (Günther et al., 2008).

CD133 (or Prominin 1) is a pentaspan transmembrane glycoprotein with two large extracellular domains that have eight potential N-linked glycosylation sites, as shown in Figure 3 (Osmond et al., 2010). Transcription of CD133 is regulated by five alternative promoters, which results in the formation of several differently spliced mRNA isoforms (Campos et al., 2011). This complexity of the CD133 molecule represents an obstacle for uniform identification of CD133-positive cells, with some CD133-positive cells potentially identified as CD133 negative (Campos et al., 2011).

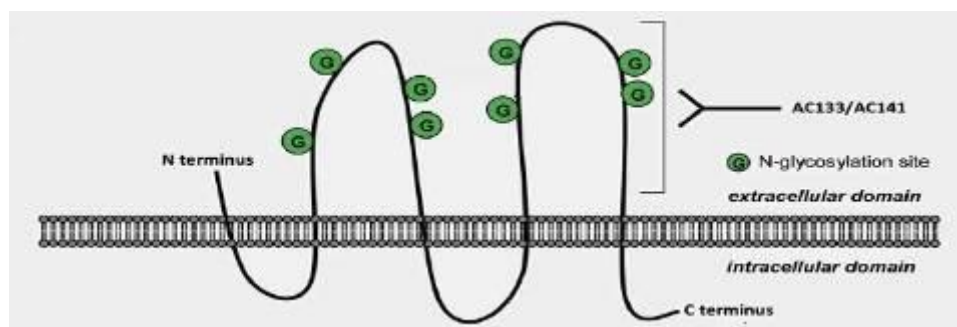


Figure 3: Schematic overview of the CD133 transmembrane protein (Campos et al., 2011). The tetraspan transmembrane glycoprotein CD133 has an extracellular N-terminus, a cytoplasmic C-terminus, two cytoplasmic loops, and two very large extracellular loops, each of which contains four potential sites for N-linked glycosylation. The binding site of AC133/AC141 antibodies was showed to be on the second extracellular loop.

A variety of other GSLC candidate biomarkers have been studied (e.g., CD15, L1CAM [L1 cell adhesion molecule], CD44) but not yet validated, and CD133 remains the most applicable biomarker to date (Jackson et al., 2015; Visvader and Lindeman, 2008). Moreover, GSLCs have been shown to express several other neural stem cell markers (e.g., Nestin, Musashi-1) and to show expression of transcription factors involved in NSC maintenance (Balbous et al.,

2014; Wu et al., 2015). Among these, the SRY (sex determining region Y)-box 2 (SOX-2) is a key transcription factor for NSCs involved in maintenance of the undifferentiated state and self-renewal, and is also highly expressed in GSLCs, supporting the concept that GSLCs originate from NSCs (Alonso et al., 2011; Gangemi et al., 2009). Likewise, the Notch signalling pathway has an essential role in the maintenance of NSCs, and this has also been shown to have an important role in GSLCs maintenance and resistance to therapy (Saito et al., 2013; Sandberg et al., 2013; Wang et al., 2010).

2.3.2.3. Resistance of GSLCs

One of the key features of GSLCs is their cellular properties that enable them to resist radiotherapy and chemotherapy. As a result, GSLCs can remain after the therapy and cause recurrence of the disease (Tamura et al., 2013). Current chemorapeutic treatments of GBM mostly involve TMZ, an alkylating agent, which causes DNA damage by methylating the O6-position of guanine, which results in faulty mismatch repair, thus triggering cell death. Unfortunately, GSLCs have been shown to express high levels of the DNA repair enzyme O6-methylguanine-DNA-methyltransferase (MGMT), which removes the alkyl group and thus limits the effectiveness of TMZ (Bleau et al., 2009). In line with this observation, a study of Liu et al. (2006) demonstrated higher TMZ resistance of CD133-positive cells, which also expressed higher levels of MGMT, compared to CD133-negative cells. Greater resistance of GSLC CD133-positive cells has also been shown by others (Signore et al., 2014; Ulasov et al., 2011). This aspect is in line with the clinical data, as growing evidence relates CD133-positive GSLCs in GBM with treatment failure and poor patient prognosis (Han et al., 2015; Wu et al., 2015). Moreover, an important mechanism for GSLC drug resistance is increased expression of the drug transporters that pump out the chemotherapeutics. Indeed, higher expression of these ABC transporters was shown for GSLC lines, in comparison to GBM cell lines (Martin et al., 2013). These studies revealed higher expression of drug transporters in CD133-positive cells, such as the ATP-binding cassette transporter protein, BCRP1 (Liu et al., 2006) and the P-glycoprotein from the family of ABC transporters (Riganti et al., 2013). In addition, GSLCs are known to show high resistance to apoptosis, as CD133-positive GSLCs were shown to have increased expression of several anti-apoptotic mRNAs, including those for BCL-2, BCL-XL, IAPs and FLIP (Liu et al., 2006). This was further confirmed by the observations that GSLC CD133-positive cells compared to CD133-negative cells are more apoptosis resistant, due to the suppression of caspase-8 expression as a result of promoter methylation of the CASP8 gene (Capper et al., 2009).

In addition to chemoresistance, GSLCs have also been shown to be resistant to radiotherapy. Indeed, a study of Bao et al. (2006) showed that the population of CD133-positive GSLCs increases in tumor xenografts upon radiotherapy, by minimally affecting their tumorigenic

potential. This is likely to be due to the activation of several DNA damage checkpoint proteins, which include ataxia telangiectasia mutated (ATM) and checkpoint kinases Chk1 and Chk2. In line with these observations, increased numbers of CD133-positive cells have been found upon local tumor recurrence after chemotherapy and radiotherapy, which possibly have been responsible for previous treatment failure (Tamura et al., 2013). Moreover, stem-cell maintenance pathways are also involved in the promotion of GSLC radioresistance. Inhibition of the Notch pathway has been shown to sensitise CD133-positive cells to clinically relevant radiation doses, causing extensive cell death (Wang et al., 2010).

2.3.2.4. GSLCs as therapeutic targets

The accumulated knowledge of the properties of GSLCs can be used for the development of new target strategies. In efforts to eradicate GLCSs, or at least to promote their differentiation towards less malignant phenotypes, several investigations have targeted the signalling pathways associated with GSLC stemness maintenance. Among these, targeting the Notch pathway with a γ -secretase inhibitor significantly reduced the presence of CD133-positive cells within GSLC spheroids, and reduced their proliferation in *in-vitro* cultures, while also prolonging the survival of tumor-bearing nude mice (Fan et al., 2010). Similarly, treatment of GSLCs with the γ -secretase inhibitor resulted in their reduced self-renewal and proliferation, induced neuronal and astrocyte differentiation, and improved survival in an intracranial mouse model (Saito et al., 2013). An additional option might represent differentiation therapy, as all-*trans*-retinoic acid has shown antitumorigenic effects on GSLCs *in vitro* and *in vivo*, through exerting antimigratory and growth-inhibiting effects (Campos et al., 2010). Experimental evidence has linked GSLC function to activated epidermal growth factor (EGF) receptor signaling, and at the moment several different anti-EGF-receptor agents, such as erlotinib, gefitinib and cetuximabare, are already under investigation in phase I and II trials, although the results are not promising (Thiessen et al., 2010). A large number of therapies that target GSLC signalling pathways, such as the phosphatidylinositol-3-kinase–Akt pathway and the Sonic hedgehog (SHH) signalling pathway, are under clinical investigation and might provide the foundation for improved GBM treatments (Stopschinski et al., 2013).

2.3.3. MSCs in cancer treatment

MSC homing is activated by tumors and their microenvironment, through the release of various inflammatory cytokines, chemokines and growth factors from endogenous tissue niches or via the blood circulation from bone marrow or adipose tissue (Tajnsšek et al., 2013). At tumor sites, MSCs become part of the tumor microenvironment and have tumor-promoting or tumor-suppressing effects (discussed further below). However, MSCs recruited to tumors can exist in three different forms (Sun et al., 2014):

- (1) Those that have similar features to normal tissue-derived MSCs;
- (2) Those that can differentiate to tumor-associated myofibroblasts;
- (3) Those that can differentiate into vascular endothelial cells.

In GBM, GBM-associated stromal cells have been shown to have tumor-promoting functions, and to facilitate angiogenesis and a hostile microenvironment for the spreading of tumor-initiating cells (Clavreul et al., 2014). Therefore, the role of MSCs in the GBM microenvironment should be carefully examined, to prevent unwanted effects and risks when using MSCs for therapeutic purposes.

Stem cells are considered as an excellent delivery vehicle for drugs or nucleic acids in the first place because of their tumor-homing potential (Nakashima et al., 2010). Indeed, MSCs and NSCs are at the forefront of drug delivery to brain tumors, as they can cross the blood–brain barrier, which represents the major limitation for successful drug delivery (Aleynik et al., 2014). Although NSCs have already been applied in clinical trials to deliver drugs to GBM with promising results, the major obstacle is the limited availability of NSCs in the body, despite the use of advanced techniques for the preparation of NSCs from embryonic or induced-pluripotent stem cells (Mariotti et al., 2014).

In contrast, MSCs from various sources can be harvested and expanded without any ethical or practical burdens (Hass et al., 2011). The homing potential of MSCs has been shown for various tumors (Chamberlain et al., 2008), including glioma (Nakamizo et al., 2005; Bexell et al., 2009). Tumors are thought to mimic chronic wounds, through the release of inflammatory mediators (e.g., cytokines, chemokines, other potential chemo-attractant molecules) (Dvorak et al., 1986), and thus to become targets for MSCs. The recruitment of MSCs to tumors was shown to be dependent on the secretion of various factors, including tumor-derived platelet-derived growth factor (PDGF), EGF, SDF-1 α , VEGF, and IL-6 (Ramdasi et al., 2015). Also, the tropism of MSCs to glioma was shown to be influenced by PDGF, EGF, SDF-1 α , IL-8, neutrophin-3 (NT3) and transforming growth factor beta-1 (TGF- β 1), but not by VEGF and bFGF (Birnbaum et al., 2007; Hata et al., 2010; Nakamizo et al., 2005). Upon engraftment in tumors, MSCs become a part of the tumor stroma and act as precursors of stromal cells (Studený et al., 2004; Nakamizo et al., 2005). However, the ultimate fate of the MSCs engrafted at tumor sites remains elusive, as they might be incorporated into tumors, or differentiate, or communicate with cancer cells and cancer stem cells (Droujinine et al., 2013). As a result of this communication, the MSCs have been shown to have pro-tumorigenic or anti-tumorigenic effects (Hall et al., 2007). Tumor growth promotion was observed in a breast cancer model, where co-injection of MSCs and breast cancer cells resulted in increased cell proliferation, angiogenesis and formation of metastatic lesions (Karnoub et al., 2007). Similarly for a gastric cancer model, were MSCs injected into immunocompromised mice

promoted growth and metastasis of relatively slow growing gastric cancer cells (Song et al., 2014). Moreover, in *in-vitro* experiments, AT-MSCs supported the cell proliferation, suppression of apoptosis, and increased resistance to cytotoxic drugs of melanoma cells, but not of glioma cells, which responded with decreased proliferation upon co-culture with AT-MSCs (Kucerova et al., 2010). This is in line with several other *in vivo* and *in vitro* studies that have shown the MSC repressive potential on glioma cells (Kleinsmidt et al., 2011; Motaln et al., 2012; Yang et al., 2014).

2.3.3.1. Influence of naïve MSCs on GBM

MSCs are known to produce a plethora of cytokines, chemokines, and other soluble factors that can potentially modulate tumor behaviour. Solely by addition of MSC conditioned medium and lysates of cells derived from umbilical cord Wharton's jelly (UC-MSCs), the growth of breast adenocarcinoma (MDA-MB-231), ovarian carcinoma (TOV-112D), and osteosarcoma (MG-63) cell lines was inhibited (Gauthaman et al., 2012). Similarly, conditioned medium derived from UC-MSCs and AT-MSCs caused growth inhibition and G0/G1 cell cycle arrest of U251 glioma cells, and also induced apoptosis mediated by the overexpression of pro-apoptotic proteins such as Bad, Bax, Bim and Bid, and significant down-regulation of anti-apoptotic proteins such as Bcl-2, Survivin and X-linked inhibitor of apoptosis protein (XIAP) (Yang et al., 2014). Down-regulation of XIAP was also identified as a key mediator for the induction of apoptosis through activation of caspase-3 and caspase-9 in two glioma cell lines and two glioma xenograft cell lines co-cultured with UCB-MSCs (Dasari et al., 2010). Similarly, increased expression of Bax, caspase-3 and caspase-8 was detected in C6 tumors upon intra-tumoral administration of amniotic MSCs in mice (Jiao et al., 2011). Moreover, the ability of UCB-MSCs to induce apoptosis was also found in *in-vitro* co-cultured U87 cells (Gondi et al., 2010). The experiments performed in our laboratory showed that BM-MSCs indirectly co-cultured with glioma (U87MG, U251, U373) cell lines inhibited their proliferation and invasion (Motaln et al., 2010), and induced senescence in U87 cells (Motaln et al., 2012). By performing cytokine analysis, high expression of the CCL2/MCP-1 chemokine in BM-MSCs co-cultured with U87MG was seen, as one of the key players for reduced cell invasion (Motaln et al., 2012). Also, several other chemokines, such as chemokine (C-X-C motif) ligand 2 (CXCL2), IL-8, CCL2/MCP-1, VEGF-A, HGF and insulin-like growth factor-binding protein 1 (IGFBP-1), were identified in U87 cells co-cultured with BM-MSCs, which were possibly responsible for the observed impaired cell proliferation and invasion in U87 cells (Motaln et al., 2012). Similarly, reduced growth potential of glioma cells upon co-culture with MSCs has been observed by Kucerova et al. (2010).

The MSC potential to suppress the growth of glioma tumors was also shown in the *in vivo* experiments. Systemic AT-MSC co-administration with 8MGA glioma cells decreased tumor incidence in mice by 63 %, compared to the control mice injected with 8MGA cells only (Kucerova et al., 2010). Interestingly, upon successive implantation of U87 cells and UCB-MSCs into mice, no formation of tumors was observed, whereas implantation of U87 cells alone resulted in the formation of intracranial tumors (Gondi et al., 2010). The potential of MSC to suppress tumor growth was also confirmed in a study of Jiao et al. (2011a), where a 36 % reduction in C6 tumor volume in mice was observed after intra-tumoral injection of UCB-MSCs. This is in agreement with results of Gondi et al. (2010), who reported a 33 % reduction in glioma tumor size in mice upon implantation of UCB-MSCs, as also with a study of Kleinschmidt et al. (2011), who observed a two-fold reduction in tumor size in glioma-bearing rats. Moreover, as well as the decreases in tumor volume in 9L-bearing rats upon administration of MSCs, these animals also has prolonged survival compared to control rats who were excluded from MSCs treatment (Nakamura et al., 2004).

As GSLC persistence to treatment represents the main issue for GBM treatments and MSC suppressive effects on GBM have been shown, the question remains what effects do the MSCs have on GSLCs in GBM tumors? To date, only a few studies have addressed this question. For example, the study of Bago et al. (2013) showed that tumor-implanted MSCs co-localise in high numbers with CD133-positive glioma cells. Also, Jiao et al. (2011a) reported the cytotoxic effects of UCB-MSCs on rat C6 glioma cells that resulted in up to 73 % reduction in the CD133-positive GSLCs subpopulation within C6 cell culture.

It is thus of major importance to obtain more information about the influence of MSCs on GSLCs within the tumor microenvironment to fully understand the impact of MSCs in GBM treatment.

3. MATERIALS AND METHODS

3.1. ISOLATION AND CHARACTERIZATION OF ADIPOSE TISSUE-DERIVED MESENCHYMAL STEM CELLS (AT-MSCs)

3.1.1. Isolation of AT-MSCs

Adipose tissue samples were collected from patients undergoing surgical removal of subcutaneous adipose tissue and the study was approved by the National Ethics Committee of the Republic of Slovenia (Doc. No.: 134/01/11). All donors were females of average age 42.7 years (range 12-71 years). Adipose biopsies were taken from the thighs (n=3), hips (n=3) and abdomen (n=2) from different donors.

Isolation of AT-MSCs was performed according to the standard procedures (Mahmoudifar et al., 2010) with minor modification. Briefly, adipose tissue samples were washed with phosphate-buffered saline (PBS), cut into small pieces, and dissociated with 0.1 % collagenase I at 37°C with vigorous shaking. After 1 h, the collagenase was inactivated by adding heat-inactivated foetal bovine serum (FBS), and the samples were centrifuged at 300× g for 10 min. The pelleted cells were washed with erythrocyte lysis buffer (0.15 M NH₄Cl; 0.1mM EDTA; 0.01M NaHCO₃; pH 7.3) and centrifuged at 300× g for 5 min. The pelleted AT-MSCs were resuspended in MSCs growth medium consisted of Dulbecco's medium (DMEM) with 20 % FBS, supplemented with 100 IU/ml penicillin, 0.1 mg/ml streptomycin, 2 mM L-glutamine, and plated at a density of 3 – 10 x 10⁴/cm². This AT-MSC culture was denoted as passage 0. AT-MSCs were medium changed twice a week and re-plated after reaching 80 % confluence at a density of 6,000 cells/cm².

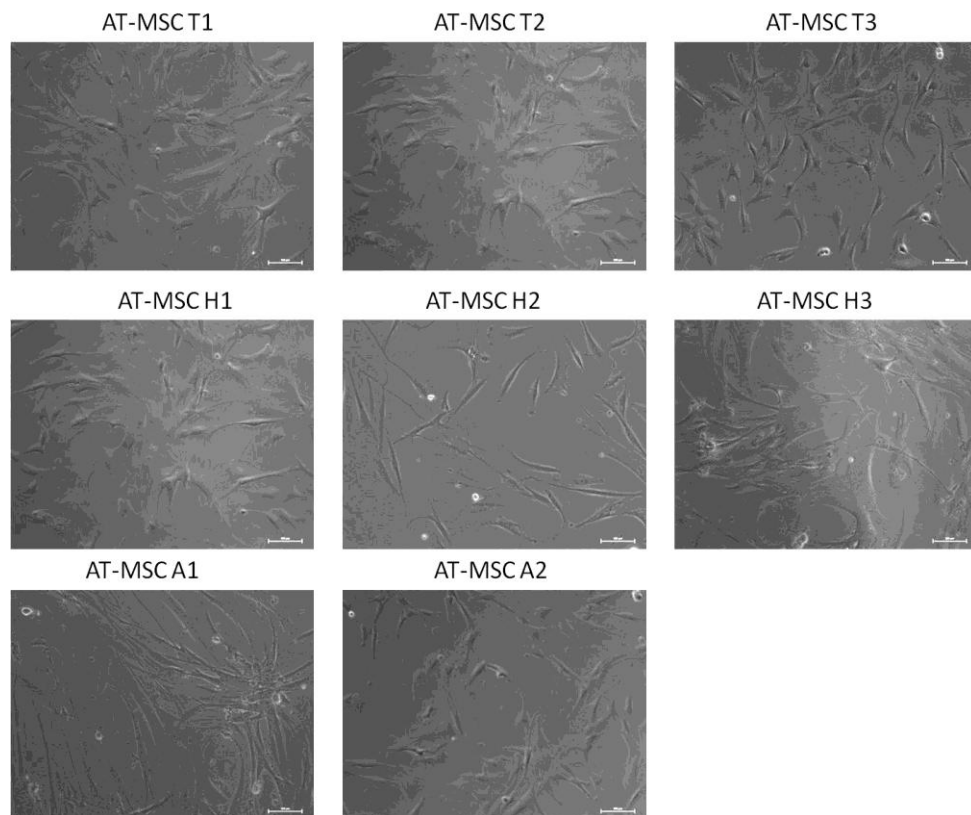


Figure 4: Morphology of AT-MSCs as noted at passage 6. All AT-MSC lines cells displayed a spindle-shaped fibroblast-like morphology that is characteristic for MSCs. Scale bar represents 100 μm .

3.1.2. Immunophenotyping of AT-MSCs by fluorescence activated cell sorting (FACS)

FACS enables the detection of various cell antigens using fluorescently labelled antibodies. When individually labelled cells, flowing in a stream of fluid are passed by a light source, the fluorescent molecules are excited to a higher energy state. Upon returning to their resting states, the fluorochromes emit light energy at higher wavelengths and light signals are detected by photomultiplier tubes and digitized for computer analysis.

One million AT-MSCs were harvested, washed with PBS and labelled with antibodies against CD13, CD29, CD44, CD73, CD90, CD14, CD34, CD45, HLA-DR, CD105 or with the appropriate isotype controls of FITC-IgG1, FITC-IgG2a, PE-IgG1, PE-IgG2b, APC-IgG1, as instructed by the manufacturer (BD Biosciences, USA). To exclude dead cells from the analysis, the cells were also stained with propidium iodide (PI), washed with PBS. The cells were analyzed by flow cytometry using a BD FACSCaliburTM and the CellQuest Software (both BD Biosciences).

3.1.3. The evaluation of MSC's differentiation potential

The AT-MSCs were analysed for their potential to differentiate into adipose, bone and cartilage-like cells at passage 6, respectively. The AT-MSCs were seeded into 48-well plates (Corning-Costar, USA) as six replicates per control and differentiation-induction condition, and left to reach ca. 70 % confluence before the exposure to differentiation induction, as described below.

3.1.3.1. Adipogenic differentiation

For induction of adipogenic differentiation, the medium composed of DMEM supplemented with 10 % FBS, 1 μ M dexamethasone, 0.5 mM 3-isobutyl-1-methyl-xanthine (IBMX), 10 μ g/ml insulin and 100 μ M indomethacin was added to AT-MSCs. After 72 h, the medium was changed to adipogenic maintenance medium composed of DMEM supplemented with 10 % FBS and 10 μ g/ml insulin, for 24 h, and this media change cycle was repeated three times, followed by cell cultivation for 1 week in the maintenance medium (Russell et al., 2010). After 21 days, the cells were fixed in 4 % paraformaldehyde for 10 min, and the accumulated lipid rich vacuoles were stained with 0.3 % oil red O in 0.6 % isopropanol, for 1 h. After washing twice with distilled water, the cells were photographed under a microscope (TE300 Nikon Eclipse). For quantification of the extent of AT-MSCs adipogenic differentiation, the oil red O was extracted from the cells with isopropanol (10 min wash), and measured using spectrophotometer (Synergy™ MX Microplate Reader, Bio-Tec Instruments, USA) at 490 nm (Russell et al., 2010).

3.1.3.2. Osteogenic differentiation

For induction of osteogenic differentiation, the medium composed of DMEM with 10 % FBS, 1 μ M dexamethasone, 50 μ g/ml L-ascorbic acid and 10 mM glycerophosphate was used. The AT-MSCs were exposed to this medium for 21 days, with the medium being changed twice per week. Then the cells were fixed in 4 % paraformaldehyde for 10 min and stained with 1 % Alizarin Red S for 30 min, to reveal the foci of calcified extracellular matrix (Russell et al., 2010). The images were recorded on a microscope (TE300 Nikon Eclipse). For quantification of the extent of osteogenic differentiation of AT-MSCs, the alizarin red S was extracted with 10 % cetylpyridinium chloride and the absorbance was measured at 540 nm using a spectrophotometer (Synergy™ MX Microplate Reader).

3.1.3.3. Chondrogenic differentiation

For induction of chondrogenic differentiation, AT-MSCs were exposed to medium composed of DMEM, 10 % FBS, 10 ng/ml TGF β 3 and 50 μ g/ml L-ascorbic acid for 21 days, with media changes twice per week (Wang et al., 2004). To detect matrix deposition of sulphated glycosaminoglycans, the cells were fixed in 4 % paraformaldehyde for 10 min, and stained with 1 % alcian blue 8-GX in 3 % acetic acid. Upon visual inspection and imaging on a microscope (TE300 Nikon Eclipse), the extent of chondrogenic differentiation in the AT-MSCs was determined by extraction of alcian blue 8-GX in 1 % sodium dodecyl sulphate, and the absorbance measured at 630 nm (Russell et al., 2010) using a spectrophotometer (Synergy™ MX Microplate Reader).

3.1.4. Characterization of AT-MSC life-span

3.1.4.1. Cumulative population doubling level (CPDL) determination

To follow the lifespan of AT-MSCs in the *in vitro* culture, AT-MSCs were passaged till their proliferation stop. The cells were counted at seeding and harvesting, to calculate doubling levels, according to the Equation (1):

$$x = \{\log_{10}(\text{NH}) - \log_{10}(\text{NI})\} \log_{10}^2 \quad \dots \quad (1)$$

where NI stands for the initial number of seeded AT-MSCs and NH stands for the number of AT-MSCs counted at harvesting (Cristofalo et al., 1998). AT-MSCs were always passaged when they reached 80 % confluence. The CPDL of the evaluated AT-MSC clone was obtained by adding the calculated value of its doubling level at each passage to that of the previous passage. All AT-MSC clones were continuously cultivated from passage 1 until the cells ceased to proliferate (to at least passage 18).

3.1.4.2. Detection of replicative senescence

The identification of cellular senescence is based on the detection of the increased level of lysosomal β -galactosidase activity (by senescence associated β -gal assay, SA- β -gal) in the cells. In senescent cells, the lysosomal mass and the amount of β -galactosidase is increased which enables the detection of the β -galactosidase enzymatic activity at sub-optimal pH conditions (at acidic pH 6.0). The method is based on cleavage of 5-bromo-4-chloro-3-indolyl- β -D-galactopyranoside (X-gal substrate) by β -galactosidase, yielding an insoluble blue precipitate, which can be detected within the cells under the light microscope.

The cellular senescence *in vitro* was evaluated in AT-MSCs cultivated under normal growth conditions at passages 6, 12 and 18. Briefly, AT-MSCs were plated on poly-lysine coated round cover slips at a density of 15,000 cells/cover slip in 24-well plates, and left to adhere overnight. Then AT-MSCs were washed with PBS and fixed in 0.5 % glutaraldehyde solution for 20 min at room temperature (RT). Then, AT-MSCs were washed again with PBS and the staining solution (Table 3) containing 1 mg/ml X-gal was added. After 16 h, the AT-MSCs were washed in distilled water and stained with Hoechst 33342 (1:1000) for nuclei detection. The percentage of senescent AT-MSCs was determined by counting senescent cells and nuclei per visual field under light and fluorescent microscope, respectively and expressing those as ratio of AT-MSCs positive for SA-beta-gal staining per number of nuclei detected.

Table 3: Composition of X-gal staining solution

Ingredients (concentration)	Volume
X-gal (1 mg/ml)	60 μ l
Citric acid/sodium phosphate solution (40 mM)	240 μ l
$K_4[Fe(CN)_6] \cdot 3H_2O$ (100 mM)	60 μ l
$K_3[Fe(CN)_6]$ (100 mM)	60 μ l
NaCl (5 M)	36 μ l
MgCl (1 M)	2,4 μ l
dH ₂ O	741,6 μ l

3.1.5. Statistical analysis

To test the correlation between adipose tissue anatomic location and AT-MSCs differentiation, CPDL and onset of senescence we used ANOVA with the Tukey's *post-hoc* tests, using GraphPad Prism version 6 for Windows (GraphPad Software, La Jolla, CA, USA). To test the significance of AT-MSC differentiation as determined by spectrophotometric measurements, the Student's t-tests were applied. The data are expressed as means \pm standard deviation (SD) and the value of $p < 0.05$ is considered significant.

3.2. CULTIVATION OF AT-MSCs ON MICROCARRIERS IN SPINNER FLASKS

3.2.1. Microcarrier characteristics

Microcarriers are typical 125 - 250 μm spheres prepared from a number of different materials including DEAE-dextran, glass, etc. enabling a successful growth of the anchorage-dependent cells. A high density suspension of microcarriers can be prepared, providing a large surface area for the cell growth in monolayer under homogenously stirred conditions. In our experiments, Cytodex-1 and Cytodex-3 (both from GE Healthcare, UK) were used and the characteristics of both are given below (Table 4).

Table 4: Characteristics of Cytodex-1 and Cytodex-3 microcarriers (GEHealthcare, 2013)

	Cytodex-1	Cytodex-3
Density (g/ml)	1.03	1.04
Size d_{50} (μm)*	190	175
Average area (cm^2/g dry weight)	4,400	2,700
Matrix	Cross linked dextran positively charged N,N- diethylaminoethyl groups	Cross linked dextran a thin layer of denatured collagen chemically coupled to a matrix

Preparation of microcarriers

The amount of microcarriers providing the required surface for cell growth was weighted and transferred to PBS for 1.5 h at RT to swell and rehydrate. After that, the microcarriers were sterilized by autoclaving (121°C 20 min) and stored at 4°C until further usage.

3.2.2. Determination of AT-MSC seeding efficiency on microcarriers

3.2.2.1. AT-MSC seeding efficiency under static conditions

Cytodex-1 and Cytodex-3 microcarriers were resuspended in either MSC growth medium (GM, 20 % FBS -described in section 3.1.1.) or 100 % FBS for 2 h to define optimal conditions for cell adhesion. For this, the microcarriers (3.2 cm^2/mL) were washed in MSC growth medium and transferred to 6 well plates (low attachment, Corning, USA) and AT-MSCs (6,000 cells/ cm^2) were added. The surface area on microcarriers and on a 6 well plate was equivalent, 9.6 cm^2 . In paralel, the control AT-MSCs (6,000 cells/ cm^2) were plated in

standard culture conditions on 6 well plates (9.6 cm²). Cells were incubated at 37°C in humid atmosphere with 5 % CO₂. After 24 h, cells were detached from microcarriers or culture plate surface using 0.25 % Trypsin-EDTA solution and the viable cells counted using Trypan Blue exclusion method. AT-MSc seeding efficiency on microcarriers preincubated with GM and 100 % FBS was calculated as percentage of cells removed from microcarriers compared to the number of cells on control culture plate.

3.2.2.2. AT-MSc seeding efficiency in spinner flasks

Both types of microcarriers were pre-incubated in GM and FBS for 2 h, respectively. After that, Cytodex-1 (2 mg/ml) and Cytodex-3 (3 mg/ml) were washed in MSC growth medium and transferred into 250 ml siliconized spinner flasks (Techne, UK). The seeding volume of culture medium was 30 ml with an AT-MSc concentration of 50,000 cells/ml and intermittent agitation regimen was set (5 min at 40 rpm followed by 30 min nonagitated) on magnetic stirrer (Techne, USA). After 24 h, the number of adhered AT-MScs was determined as number of attached cells compared to number of seeded cells. To evaluate the effect of microcarriers pre-coating with GM or FBS on AT-MSc expansion, the cell cultivation was prolonged until day 10. Half the volume of culture medium was changed every two days after day 3 until experiment was completed on day 10. The number of adhered AT-MScs was determined by viable cell counts using the Trypan Blue exclusion method.

3.2.3. AT-MSc harvest from microcarriers

To count the AT-MScs attached on Cytodex-1 and Cytodex-3 microcarriers a 1 mL aliquot of the culture was removed in duplicate from each spinner flask. Microcarriers were allowed to settle. After washing with PBS, microcarriers were incubated in 0.1 % Trypsin at 37°C for 3 min, mixed for 30 sec at 1500 g/min and again incubated at 37°C for 3 min. Then, trypsin was inactivated and number of adhered AT-MScs determined by viable cell counts using the Trypan Blue exclusion method.

3.2.4. AT-MSc expansion on microcarriers in spinner flasks

After 2 h incubation in GM, Cytodex-1 (2 mg/ml) and Cytodex-3 (3 mg/ml) were washed in MSC growth medium and transferred to spinner flasks. AT-MScs (AT-MSc T3 clone, AT-MSc A2 clone) from passage 6 and 7 were cultured to 80 % confluence and seeded into spinner flasks with microcarriers at a density of 50,000 cells/ml and cultured in 30 ml of MSC growth media for the first 24 h. The culturing proceeded on magnetic stirrers in the incubator (37°C, 5 % CO₂). During the first 24 h, an intermittent agitation regimen was set (5 min at 40 rpm followed by 30 min nonagitated phase). Then, 30 ml of fresh culture medium was added

and agitation was set continuous at 50 rpm. Half the volume of culture medium was changed every two days after day 3 until experiment was completed on day 10.

3.2.4.1. AT-MSCs phenotyping upon spinner flask cultivation

AT-MSCs were analyzed for their MSC surface marker expression before and after cultivation on MCs as described section in 3.1.2.

3.2.4.2. Differentiation potential of AT-MSCs upon cultivation on microcarriers

The AT-MSCs were analyzed for their adipogenic and chondrogenic potential before and after the growth on MCs as described in section 3.1.3. The detection of osteogenic differentiation was examined as described below.

Osteogenic differentiation

The osteogenic differentiation medium was prepared with DMEM containing 10 % FBS, 1 μ M dexamethasone, 50 μ g/ml L-ascorbic acid and 10 mM glycerophosphate. AT-MSCs were exposed to it for 21 days. After, the cells were fixed in 4 % paraformaldehyde for 10 min and stained with 5 % silver nitrate in dark for 10 min. After washing with distilled water, the fixed cells were incubated for 10 min with 1 % pyrogallol, washed again and finally exposed to 5 % sodium thiosulphate for 5 min to detect the foci of calcified extracellular matrix.

3.2.5. Statistical analyses

Using GraphPad Prism version 6 for Windows (GraphPad Software, La Jolla, CA, USA) the Student's t-tests were used to test for the differences of AT-MSCs adhesion and proliferation on microcarriers under different growth conditions, and a value of $p < 0.05$ was considered significant. Experiments were repeated three times and results were expressed as the mean \pm standard deviation (SD).

3.3. THE EFFECT OF UMBILICAL CORD-DERIVED MESENCHYMAL STEM CELLS (UC-MSCs) AND BONE MARROW-DERIVED MESENCHYMAL STEM CELLS (BM-MSCs) ON GLIOMA STEM-LIKE CELLS (GSLCs)

3.3.1. Cell isolation and cultivation

3.3.1.1. Isolation of UC-MSCs

Umbilical cords were collected from pregnant women undergoing cesarean section at gestational age of 37-41 weeks upon informed consent. The study was approved by the National Ethics Committee of the Republic of Slovenia (Document No. 119/02/10). Isolation of MSCs from umbilical cord Wharton's jelly was performed according to standard procedures (Wang et al., 2004) with minor modifications. The fresh umbilical cords (5-10 cm) were collected into PBS and processed within the period of 6 h. After removal of blood vessels, Wharton's jelly was scratched from the umbilical cord in PBS and centrifuged at 250 g for 5 minutes. The pellet was resuspended in DMEM with added 1 mg/ml collagenase I and incubated for 16-18 hours in 5 % CO₂ incubator at 37°C. After collagenase inactivation using FBS, the cells were washed with PBS and plated at a density of 10-30 x 10⁴ cells/cm² in the DMEM, with 10 % FBS, supplemented with 100 IU/ml penicillin, 0.1 mg/ml streptomycin, and 2 mM L-glutamine. The resulting UC-MSC culture was denoted as passage 0. UC-MSCs were medium was changed twice a week and replated after reaching 80 % confluence at a density of 6,000 cells/cm².

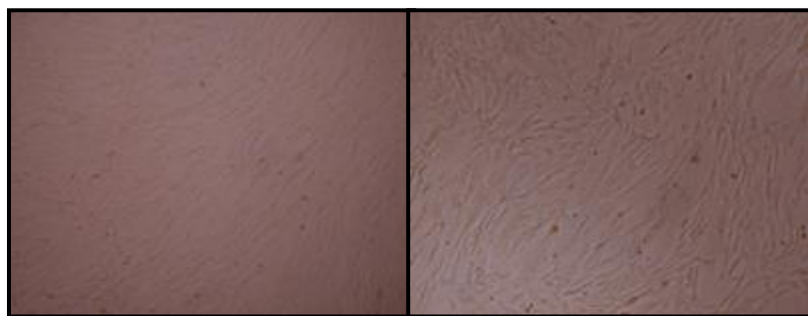


Figure 5: Morphology of UC-MSC clone 10 (left picture) and clone 13 (right picture). Both images were taken at passage 6, using 40× magnification.

3.3.1.2. Immunophenotyping of UC-MSCs by FACS

UC-MSCs were analyzed for their MSC surface marker expression at passage 7 as described section in 3.1.2.

3.3.1.3. The evaluation of UC-MSCs differentiation potential

The UC-MSCs were analysed for their potential to differentiate into adipose, bone and cartilage-like cells at passage 4. The UC-MSCs were seeded into 6-well plates (Corning-Costar, USA) as three replicates per control and differentiation-induction condition, and left to reach ca. 70 % confluence before the exposure to differentiation induction. The analysis of UC-MSC adipogenic and chondrogenic differentiation was conducted as described in section 3.1.3.1 and 3.1.3.2, and the induction of osteogenic differentiation was conducted as described in section 3.2.4.2.

3.3.1.2. Cultivation of BM-MSCs

The human BM-MSCs were purchased from Lonza Bioscience (Walkersville, MD, USA; BM-MSC2: male, age 19, 6F4393; BM-MSC3: female, 22, 7F3677) and cultured in DMEM, with 10 % FBS, supplemented with 100 IU/ml penicillin, 0.1 mg/ml streptomycin, and 2 mM L-glutamine. They were passaged after reaching 80 % confluence at the density of 6,000 cells/cm².



Figure 6: Morphology of BM-MSC-2 (left picture) and BM-MSC-3 (right picture). Both images were taken at passage 6, using 40× magnification

3.3.1.3. Generation of GBM cell primary culture enriched for GSLCs

NIB26 (female, age 75 years) and NIB50 (male, age 81 years) cells were isolated from fresh GBM samples, obtained from the University Medical Centre of Ljubljana (the study approved by the National Ethics Committee of the Republic of Slovenia, Document No. 96/02/12). Tumor samples were mechanically and enzymatically dissociated, and the isolated GBM cells were grown as spheroids to enrich for GSLCs fraction, in neurobasal (NBE) medium supplemented with 1 x B-27, 100 IU/ml penicillin, 0.1 mg/ml streptomycin, 2 mM L-glutamine, 1 U/ml heparin, 20 ng/ml EGF, and 20 ng/ml β FGF. Spheroids were mechanically dissociated after reaching average size of 200 μ m and seeded further at 1×10^5 cells/ml.

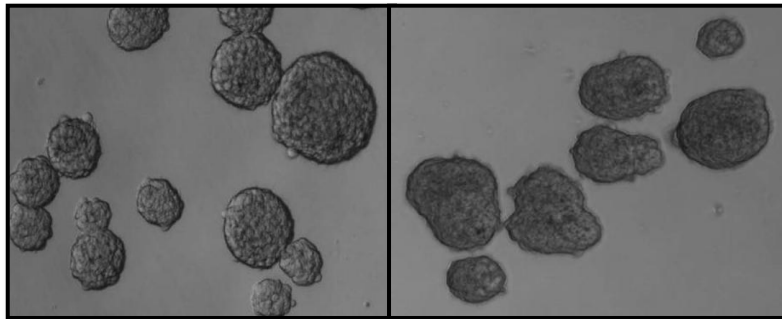


Figure 7: Spheroid morphology of NIB26 (left) and NIB50 (right) GSLCs. Images were taken at 40 \times magnification.

3.3.1.4. Cultivation of GSLC lines

The GSLC lines, NCH421k and NCH644, were kindly provided by Christel Herold-Mende from the University of Heidelberg. Those cells were isolated from GBM resection, sorted for CD133 surface marker and checked for stemness potential (Campos et al., 2010, Capper et al., 2009). GSLCs were grown as spheroids in NBE medium supplemented with 1 x B-27, 100 IU/ml penicillin, 0.1 mg/ml streptomycin, 2 mM L-glutamine, 1 U/ml heparin, 20 ng/ml EGF, and 20 ng/ml β FGF. Spheroids were mechanically dissociated after reaching average size of 200 μ m and seeded further at 1×10^5 cells/ml.

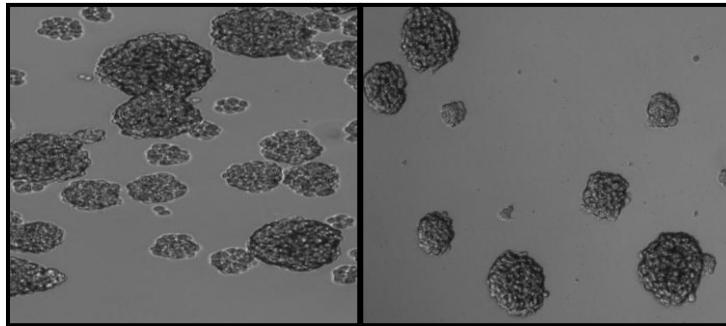


Figure 8: Spheroid morphology of NCH421k (left) and NCH644 (right) GSLCs. Images were taken at 40× magnification.

3.3.2. Conditioned media collection

The MSCs are known to produce a plethora of chemokines/cytokines, which may affect the GLSCs. We prepared the UC-MSC and BM-MSC conditioned media (CM) to investigate their antitumor properties. Briefly, two different clones of UC-MSCs (UC-MSC-10, female and UC-MSC-13, male) and the two clones of BM-MSCs (BM-MSC2: male, age 19; BM-MSC3: female, 22) were plated into T75 flask (Corning-Costar, USA) in a MSC growth medium and a day before the cells would have reached a 90 % confluence they were medium changed with 12.5 ml of fresh neurobasal (NBE) medium (used for GSLCs culturing). After 24 h of conditioning, this medium was removed from the cells, pooled, centrifuged for 10 min at 300× g at 4°C and aliquoted for storage at -80°C before use. Prior the experiment those CMs were mixed in 1:1 ratio with fresh NBE medium and designated as BM-CM and UC-CM, respectively.

The conditioned medium was also collected from cultured NCH421k and NCH644 spheroids in T75 flasks. Similarly, the NBE conditioned media were collected after 24 h from cultured spheroids and diluted at 1:1 ratio with fresh NBE medium and when used designated as NCH421k or NCH644 NBE-CM.

3.3.3. FACS analysis of CD133 expression

The NCH421k cells were harvested upon 3 and 7 days exposure to NBE-CM, UC-CM and BM-CM, and NCH644 cells were harvested upon 3 days exposure to NBE-CM, UC-CM and BM-CM, respectively. The spheroids were washed with PBS, mechanically dissociated to single cells suspension, and 10^6 cells were incubated with 10 µL CD133-PE antibody (clone 293C3; Miltenyi Biotec GmbH, USA) recognising epitope 2 of the human CD133 antigen (CD133/2) and 20 µL isotype control (PE-IgG2b, BD Biosciences, USA), respectively. For

accurate live cell analysis PI was added to all cell samples. After 20 min of incubation at 4°C in dark, the cells were washed with PBS and subjected to FACS analysis using a BD FACSCalibur™ and the CellQuest Software (both BD Biosciences, USA).

3.3.4. Analysis of cell migration in vitro

The wound-healing assay is based on the observation that, upon creation of a new artificial gap, so called scratch, on a confluent cell monolayer, the cells on the edge of the newly created gap will move toward the opening to close the gap. After creation of a scratch on monolayer cells, micrographs images are captured at the beginning and after a certain time point. To determine the rate of cell migration, images taken at different time points are evaluated and the gap length compared.

UC-MSCs and BM-MSCs were seeded on 24 well culture plates in triplicates and grown to confluent monolayer. Using 200 µl pipet tips a straight line scratch was created and the monolayer surface was washed twice with PBS to remove cell debris. For the next 16 h UC-MSCs and BM-MSCs were exposed to NBE and NBE-CM, respectively. Immediately after media change micrographs of scratches were taken to record for the initial scratch width. To obtain the same field during the image acquisitions, xyz coordinates of images were saved in program NIS-Elements (Nikon, Japan). After 16 h, the cells were fixed with 4 % paraformaldehyde, washed with PBS and stained with 0.5 % crystal violet for 15 min at RT. Again the micrographs were taken using saved xyz coordinates and the width of the scratch determined. The cell migration index was calculated by dividing the end scratch width with the initial one.

3.3.5. Cell cycle analysis

Flow cytometry analysis enables to distinguish cells in different phase of cell cycle by measuring of DNA content in individual cells and this way showing the distribution of cell population across the phases of the cell cycle. Cell proliferation is characterized by four distinct phases: G1 phase (metabolic changes to prepare a cell for division, RNA and protein synthesis), S phase (DNA synthesis), G2 phase (growth and preparation for cell division) and M phase (mitosis). Non-proliferative or quiescent cells are not taking part in cell division and are referred to as being in G0 phase. Using FACS, the cell cycle is divided into three identifiable stages G0/G1, S and G2/M based on DNA content detected upon binding of DNA dye, most often PI. Cells in G0/G1 phase have 2n DNA (diploid, normal amount of DNA), during S phase DNA content is increasing, whereas in G2/M phase the 4n DNA content is detected. The fluorescence intensity of the stained cells correlates with their amount of DNA. Prior analysis, the cells have to be fixed or permeabilised with chemicals to ensure the DNA dye enters the cells.

NCH421k spheroids were exposed to NBE, UC-CM and BM-CM for 72 h. Then the spheroids were trypsinized, washed with PBS and left in 75 % ethanol for overnight at 4°C. The fixed cells were washed again with PBS, resuspended in 0.5 ml PI/RNase staining buffer and incubated for 15 min at RT. Cell cycle analysis was performed with BD FACSCalibur™ and the CellQuest Software. The WinMDI and Cyclored were used to analyze the distribution of cell populations in different phases of the cell cycle.

3.3.6. Apoptosis assays

3.3.6.1. Annexin V/PI assay

During the early stages of apoptosis the asymmetry of cell membrane is disrupted as phosphatidylserine (PS) of the plasma membrane flips from the inner surface to the outer surface of the cell. As Annexin V binds specifically to PS, the fluorochrome-conjugated Annexin V can be used to detect apoptotic cells. To distinguish between early and late stages of apoptosis or necrosis, the DNA dye propidium iodide is used, as during the early apoptosis the cell plasma membrane is still functional for viability dyes exclusion, whereas late stages of apoptosis it is not. Therefore, the viable cells should be both Annexin V and PI negative, while the early apoptotic cells are Annexin V positive and PI negative. Cells positive for both Annexin V and PI are in late apoptosis or already necrotic.

Apoptotic cells were detected by staining with Annexin V-FITC and PI. After exposure of NCH421k spheroids to NBE, UC-CM and BM-CM for 72 h, those were harvested, washed with PBS, trypsinized to single cell suspension, resuspended in 100 µl binding buffer, and stained with 5 µl Annexin V-FITC (BD Pharmingen, USA) and 10 µl PI (50 µg/ml). The cells were incubated for 15 min at RT in the dark. After incubation, 400 µl of binding buffer was added to each cell sample. Staurosporine treated (2 µM, 6 h) NCH421k cells were used as a positive control for apoptosis. Annexin V and PI stained cell samples were analyzed with FACSCalibur and CellQuest Software (both BD Biosciences, USA).

3.3.6.2. Mitochondrial membrane potential detection

During apoptosis, the mitochondrial membrane potential (MMP) decreases due to collapse of the electrochemical gradient in mitochondrial membrane. The change in the MMP can be detected by a fluorescent cationic dye JC-1 (5,5',6,6'-tetrachloro-1,1',3,3'-tetraethylbenzimidazolylcarbocyanine iodide). This dye selectively enters the mitochondria and reversibly changes colour from green to red as a result of increase in membrane potential. In healthy cells with high MMP, JC-1 spontaneously forms complexes (J-aggregates) with

intense red fluorescence. Yet, in apoptotic cells with low MMP, JC-1 remains in the monomeric form, which shows only green fluorescence.

To measure MMP changes in NCH421k cells, the Mitochondrial Permeability Transition Detection Kit JC-1 (ImmunoChemistry Technologies, USA) was used according to the manufacturer's instructions. STS (2 μ M, 6 h) and carbonylcyanide-chlorophenyl-hydrazone (25 μ M, 30 min) treated NCH421k spheroids were used as a positive control for apoptosis induction and depolarization of mitochondria. Briefly, the NCH421k spheroids were grown in NBE-CM, UC-CM and BM-CM for 72 h. Spheroids were mechanically dissociated to obtain single cell suspension, resuspended in Mito PT™ JC-1 solution and incubated for 15 min at 37°C. Then the cells were washed in assay buffer to remove the excess JC-1 and resuspended at a density of 10⁶ cells/ml. For each tested condition 100 μ l of cell suspension was dispensed into 5 replicate wells of a black 96-well microtiter plate. JC-1 staining was analyzed using a Synergy™ HT Microplate Reader (Bio-Tec Instruments Inc., USA) at 527 nm (green) and 590 nm (red). The change of mitochondrial potential was assessed by the ratio of red vs green fluorescence readings.

3.3.7. Cell senescence

NCH421k, NCH644, NIB26 and NIB50 spheroids were grown in NBE, UC-CM and BM-CM for 72 h. Then they were mechanically dissociated and single cells were fixed in 0.5 % glutaraldehyde for 20 min at RT. Cells were stained for β -galactosidase activity (SA- β -gal) at pH 6.0 for 6 h, as described previously in section 3.2.3.2. The percentage of senescent cells was obtained by counting the number of blue-stained cells against all cells on the slide in multiple visual fields.

3.3.8. Gene expression analysis

3.3.8.1. Isolation of RNA

NCH421k, NCH644, NIB26 and NIB50 spheroids were grown for 72 h in NBE, UC-CM and BM-CM, respectively. After that, the cells were washed with PBS, centrifuged for 3 min at 1000 rpm and isolation of RNA was conducted using Trizol™ reagent. The reagent is composed of phenol and guanidine isothiocyanate, and maintains the integrity of RNA by inhibition of RNase activity, while disrupting cells and dissolving cell components. Next, the addition of chloroform resulted in a separation of aqueous phase and organic phase, whereat RNA remained exclusively in the aqueous phase. Upon RNA precipitation with isopropyl alcohol, 75 % ethanol was used to remove impurities and RNA precipitate was dissolved in DEPC water at -80°C until further usage (Chomczynski in Sacchi, 1987).

3.3.8.2. Determination of RNA concentration

The total RNA amounts in samples were assessed using Spectrofotometer NanoDrop NT-1000 (Thermo Fisher Scientific, USA). The RNA samples were spectroscopically measured at 260 nm and 280 nm, and purity of the RNA samples was assessed from ratio of 260/280 nm measurements.

3.3.8.3. Reverse transcription

The High-Capacity cDNA Archive Kit (Applied Biosystems, USA) was used for reverse transcription of 1 µg of the total RNA to single-stranded cDNA and conducted on Gene AMP PCR System 9700 (Applied Biosystems, ZDA). The following sequence in the programme was used: in the first step random primers bind to template RNA (25°C 10 min) and in the next step reverse transcriptase produced its complementary cDNA (2 h 37°C). All samples were stored at -20°C until further usage.

3.3.8.4. Real-time quantitative PCR

The real-time quantitative PCR enables the detection of amplified DNA as the reaction progresses, in "real time". We have used the TaqMan® method that relies on the 5'-3' nuclease activity of the enzyme Taq-polymerase and fluorophore-based detection. If the target sequence is present, the fluorogenic probe anneals downstream from one of the primer sites and is cleaved by the 5' nuclease activity of the Taq polymerase enzyme during the extension phase of the PCR. Whilst the probe is intact the fluorescence emission of the reporter dye is absorbed by the quenching dye. Cleavage of the probe by Taq polymerase during PCR separates the reporter and quencher dyes and the fluorescent signal is emitted. Additional reporter dye molecules are cleaved from their respective probes with each cycle, leading to an increase in fluorescence intensity proportional to the amount of amplicon produced. The fractional PCR cycle number at which the reporter fluorescence is greater than the minimal detection level is called ΔC_t and correlates with the quantity of target cDNA. To quantify gene expression in the sample, the housekeeping gene is simultaneously amplified with the target, which serves as an internal reference against which other RNA values can be normalized.

For analysis of gene expression by real-time PCR, 10 µl reactions were prepared using 1:10 dilution (2 µl/well) of each cDNA, PCR reagent solution (TaqMan Universal PCR Master Mix), DEPC-water and primer probes for CDKN2A (p16; cyclin-dependent kinase inhibitor 2A), CDKN1A (p21; cyclin-dependent kinase inhibitor 1A), CCND1 (cyclin D1), BAX (BCL2-associated X protein), BCL-2 (B-cell CLL/lymphoma 2), PROM1 (CD133; prominin

1), SOX2 (SRY (sex determining region Y)-box 2), NES (nestin), NOTCH1 (notch 1), TUBB3 (tubulin, beta 3 class III) VIM (vimentin), P53 (p53; cellular tumor antigen p53) and GFAP (glial fibrillary acidic protein) (all TaqMan Gene Expression Assays; all Applied Biosystems, USA). For normalization of gene expression human glyceraldehyde 3-phosphate dehydrogenase (GAPDH) was used as internal reference. The following programme was used for quantitative PCR on ABI 7900 HT Sequence Detection System (Applied Biosystems, USA):

	<u>50 °C 2 min</u>
	<u>95 °C 10 min</u>
45 cycles	95 °C 15 s
	60 °C 1 min

Upon exposure of NCH421k cells to UC-CM and BM-CM the expression of 84 senescence-related genes was determined by Cellular Senescence RT-Prolifer PCR Array (Qiagen-SABiosciences). On the Array, the average of 3 different housekeeping genes: ACTB (actin beta), GAPDH and RPL13A (ribosomal protein L13a) was used in calculations as an internal control. Fold increase in mRNA levels was calculated with the $\Delta\Delta C_t$ method by online program at <http://pcrdataanalysis.sabiosciences.com/pcr/arrayanalysis.php>. Results were expressed as means of three independent experiments performed in parallel.

3.3.9. Chemotherapeutics cytotoxicity effect on NCH421k and NCH644 cells

GSLCs are well known for their increased resistance to chemotherapeutics. Therefore, we investigated the effect of MSC-CM on NCH421k and NCH644 resistance to temozolomide (TMZ) and 5-fluoro-uracil (5-FU).

The GSLCs were plated in 96-well micro-titer plates at the density of 10^4 cells/well and left to grow for 24 h. Then NBE, UC-CM, BM-MSC, and TMZ (2.5, 250, 500, 1000 μ M) or 5-FU (0.01, 1, 50, 150 μ M) were added. After 48 h and 72 h, 32 μ l of MTS (3-(4,5-dimethylthiazol-2-yl)-5-(3-carboxymethoxyphenyl)-2-(4-sulfophenyl)-2H-tetrazolium) dissolved in phenazine methosulphate (PMS) solution was added to each well to make 333 μ g/ml final concentration and incubated at 37°C. Three hours later, the absorbance at 490 nm (reference 690 nm) was measured with the Synergy™ MX Microplate Reader (Bio-Tec Instruments).

3.3.10. Statistical analyses

All above experiments were independently repeated at least three times and performed in duplicates, except for cytotoxicity testing with MTS assay, which was performed in quadruplicate. The ANOVA test with *post-hoc* Dunnett's tests were used to test the effect of

MSC conditioned media in GSLCs (NCH421k, NCH644, NIB26, NIB50) against the control medium and a value of $p < 0.05$ was considered significant. The differences in GSLCs CM to control media (NBE) effect on UC-MSCs and BM-MSCs migration were tested with Student's t-test. Data were expressed as the means \pm standard deviation (SD).

3.4. INDIRECT CO-CULTURES OF UC-MSCs AND BM-MSCs WITH NCH421k CELLS

3.4.1. Indirect co-cultures set up

To investigate the paracrine effect of UC-MSCs and BM-MSCs on NCH421k cells in the indirect co-culture, we used the Boyden chambers set up with inserts having a 0.4 μm pore size, that allow for the small molecule and culture medium exchange between the two cell types, but not for physical contact between them.

Co-cultures of NCH421k spheroids with UC-MSC-10 and BM-MSC-2 were performed using 6 well plates and corresponding inserts with 0.4 μm pore size (both BD Biosciences, USA). Briefly, 3.2×10^5 of UC-MSCs and BM-MSCs were washed in PBS and plated on the bottom of the wells in the NBE medium. Upon 4 h, the inserts with 0.4 μm pore size were put into those same wells and 3×10^5 of NCH421k cells were plated in these upper compartments. The controls were set, with only NCH421k cells plated in upper compartment of the insert. The controls and co-cultured NCH421k cells with both types of MSCs were left to grow in NBE medium for 72 h.

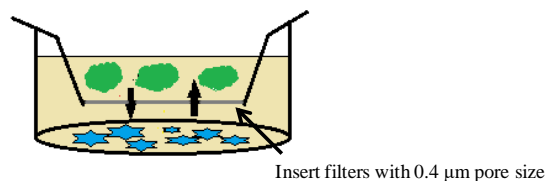


Figure 9: Schematic representation of indirect MSC and GSLC co-culture in the Boyden chamber set up.

3.4.2. Proliferation assay using Ki-67 antibody

Immunocytochemistry is a technique for the visualization of proteins in cells using an antibody which is directly linked to a fluorophore. Alternatively, primary antibody can be unconjugated and a fluorophore-conjugated secondary antibody directed against the primary antibody is used for detection.

Upon 72 h of NCH421k co-culturing with UC-MSCs and BM-MSCs, the NCH421k cells were washed in PBS, mechanically dissociated to single cells and fixed in 0.5 % glutaraldehyde for 20 min at RT. After washing in miliQ H_2O , 5 μl of cell suspension were put on poly-lysine coated round cover slips and left to dry for 20 min on a hot plate (60°C). The cover slips with attached cells were washed in PBS and exposed to 0.1 % Triton X-100/1 % BSA/PBS solution for 15 min for cell membrane permeabilization. After PBS wash, the

cells were incubated for 15 min with 4 % BSA in PBS to block nonspecific binding of primary Ki67 antibody (1 µg/ml; Abcam, UK), which was incubated with the cells, for 1 h. Afterwards, NCH421k cells were intensively washed with PBS and incubated with fluorochrome-conjugated secondary antibodies (goat-anti-rabbit Alexa Fluor 488), washed again and the nuclei of cells were stained with Hoechst 33342 (1:1000). After final wash, poly-lysine cover slides with cells were mounted with Anti-Fade Prolong Gold (Molecular Probes, USA) to microscope slides.

3.4.3. FACS analysis of CD133 expression

NCH421k spheroids co-cultured with UC-MSCs and BM-MSCs or grown alone in NBE medium for 72 h were analysed for CD133 expression as described in section 3.3.3.

3.4.4. Gene expression

For NCH421k cells grown alone or in the indirect co-culture with UC-MSCs and BM-MSCs for 72 h, RNA isolation, reverse transcription and qRT-PCR analysis of CDKN2A, CDKN1A, CCND1, BAX, BCL-2, PROM1, SOX2, NESTIN, NOTCH 1, TUBULIN β3, VIMENTIN and GAPDH gene expression was performed as described in section 3.3.8.

3.4.5. Statistical analyses

All indirect co-culture experiments were performed in duplicates and independently repeated three times. The ANOVA test with *post-hoc* Dunnett's tests were used to test the effect of UC-MSCs and BM-MSCs on NCH421k cells in the indirect co-culture against the mono-culture and vice versa. A value of $p < 0.05$ was considered significant.

4. RESULTS

4.1. ISOLATION AND CHARACTERIZATION OF ADIPOSE TISSUE DERIVED MESENCHYMAL STEM CELLS (AT-MSCs)

In our work we have focused on isolation of AT-MSCs from small pieces of adipose biopsies in order to define an anatomical location harboring good quality AT-MSCs. Adipose tissue samples were collected from healthy donors who were undergoing surgery for aesthetic reasons. All of the donors were female, with a mean age of 42.7 years (range, 12-71 years). Subcutaneous adipose tissue was taken from the thighs (n = 3), hips (n = 3), and abdomen (n = 2), of a total of seven donors.

4.1.1. Number of isolated cells

The efficiency of AT-MSC isolation was compared among the adipose deposits sites, for the thighs, hips and abdomen. The number of isolated cells per ml adipose tissue was highest for the harvest sites from the thighs (23×10^4 cells/ml) compared to the hips (7×10^4 cells/ml) and abdomen (4×10^4 cells/ml) (Table 5).

Table 5: Summary of donor, sampling characteristics and cells. Highest number of cells was isolated from the thigh region compared to hips and abdomen anatomical site (* $p < 0.05$).

Anatomical location	AT-MSC	Donor age (years)	Fat tissue volume (ml)	Fat tissue cells (n/ml)	Isolated cells (mean; n/ml)
Thighs	T1	71	2.0	243,750	239,469**
	T2	71	2.0	300,000	
	T3	70	3.7	174,658	
Hips	H1	35	1.5	91,666	74,305
	H2	35	1.0	37,500	
	H3	12	1.6	93,750	
Abdomen	A1	35	1.0	75,000	41,667
	A2	41	1.5	8,333	

4.1.2. Analysis of AT-MSC surface markers

To confirm the MSCs identity, immunophenotype of generated AT-MSC lines was analyzed according to the standard MSC surface marker expression using FACS (Dominici et al., 2006). All of our AT-MSC lines were shown to express the characteristic MSC markers CD13, CD29, CD44, CD73, CD90, CD105 in more than 95 % of the cells and to lack the hematopoietic stem cells (HSC) markers CD14, CD34, CD45, HLA-DR as these were detected in less than 2 % of the cells. No differences in immunophenotype among the analyzed AT-MSC lines were noticed.

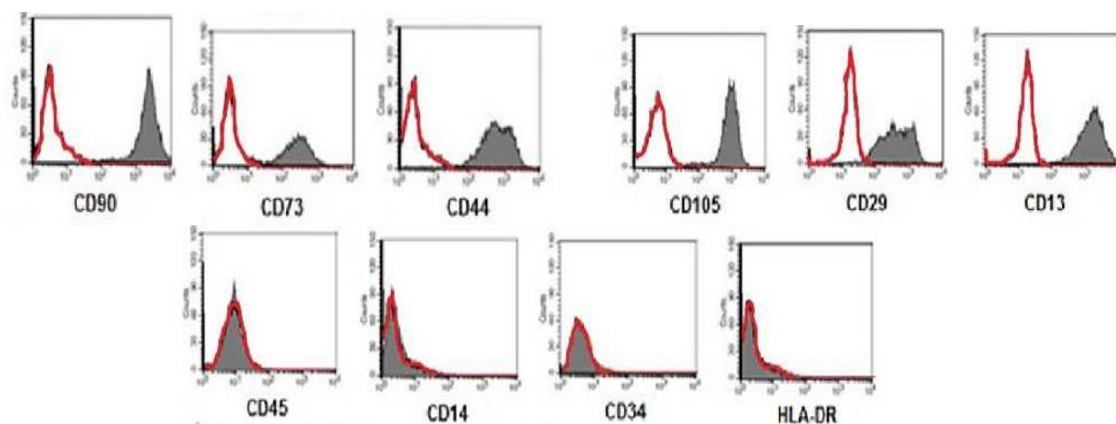


Figure 10: MSC surface marker expression in isolated AT-MSCs as detected by FACS. Representative histograms of AT-MSC immunophenotype profile of AT-MSC T3 line expressing CD90, CD73, CD44, CD105, CD29 and CD13; and lacking expression of CD45, CD14, CD34 and HLA-DR. The red lines represent isotype control for background fluorescence and the shaded areas represent the corresponding marker antibody signal.

Table 6: Summary of the surface marker expression in isolated AT-MSC lines. The percentages of cells expressing each analysed marker are given for isolated AT-MSC lines from thighs, hips and abdomen. The extent of surface marker expression is in accordance with suggested criteria for MSCs.

Specificity	Marker	Marker expression according to AT-MSC source (%)							
		Thighs			Hips			Abdomen	
		T1	T2	T3	H1	H2	H3	A1	A2
HSC markers	CD45	1.8	1.9	0.4	1.2	1.0	1.3	1.4	0.8
	CD14	0.9	0.7	0.4	1.6	1.8	1.8	1.9	1.9
	CD34	0.2	1.4	0.6	1.8	1.4	1.9	1.2	1.6
	HLA-DR	0.9	0.5	1.1	1.4	0.7	0.9	1.6	0.7
MSC markers	CD73	98.4	99.3	98.6	95.3	98.9	97.2	99.9	97.6
	CD44	99.8	99.1	99.3	98.8	95.2	95.9	98.7	96.1
	CD105	99.5	95.6	99.9	99.2	95.9	95.6	96.8	99.4
	CD29	99.5	98.6	98.7	96.9	99.2	98.9	97.1	95.7
	CD13	99.4	99.4	98.7	98.9	96.3	96.8	97.0	99.0

4.1.3. Differentiation of isolated AT-MSCs

To confirm the MSC identity of isolated AT-MSC lines and to examine influence of tissue harvest-site on differentiation capacity of AT-MSCs, their ability to differentiate to adipocytes, osteocytes and chondrocytes was evaluated. Adipogenic differentiation of these AT-MSC lines was confirmed by staining of lipid droplets with oil red O (Fig. 11). The three cell lines (AT-MSC-T3, AT-MSC-H2 and AT-MSC-A2) showed greater accumulation of lipid droplets compared to other AT-MSC lines (Fig. 11). The absorbance readings of extracted oil red O from differentiated AT-MSCs confirmed these observations (Fig. 12A). Yet, the AT-MSC tissue-harvesting site was not significantly related to adipogenic differentiation.

Osteogenic differentiation of AT-MSC lines was assessed by staining of calcified depositions with alizarin red S (Fig. 11) and the subsequent spectrophotometric measurements of the dye extracts (Fig. 12B). By this we demonstrated the greatest level of osteogenic differentiation in three thigh-derived AT-MSCs (i.e. AT-MSC-T1, AT-MSC-T2, AT-MSC-T3).

The chondrogenic differentiation of all AT-MSC lines was also confirmed. Also here, the thigh-derived AT-MSCs showed the greatest chondrogenic differentiation, as indicated by

staining of sulfated glycosaminoglycans with alcian blue (Fig. 11), which was further confirmed by absorbance readings of extracted alcian blue dye (Fig. 12C).

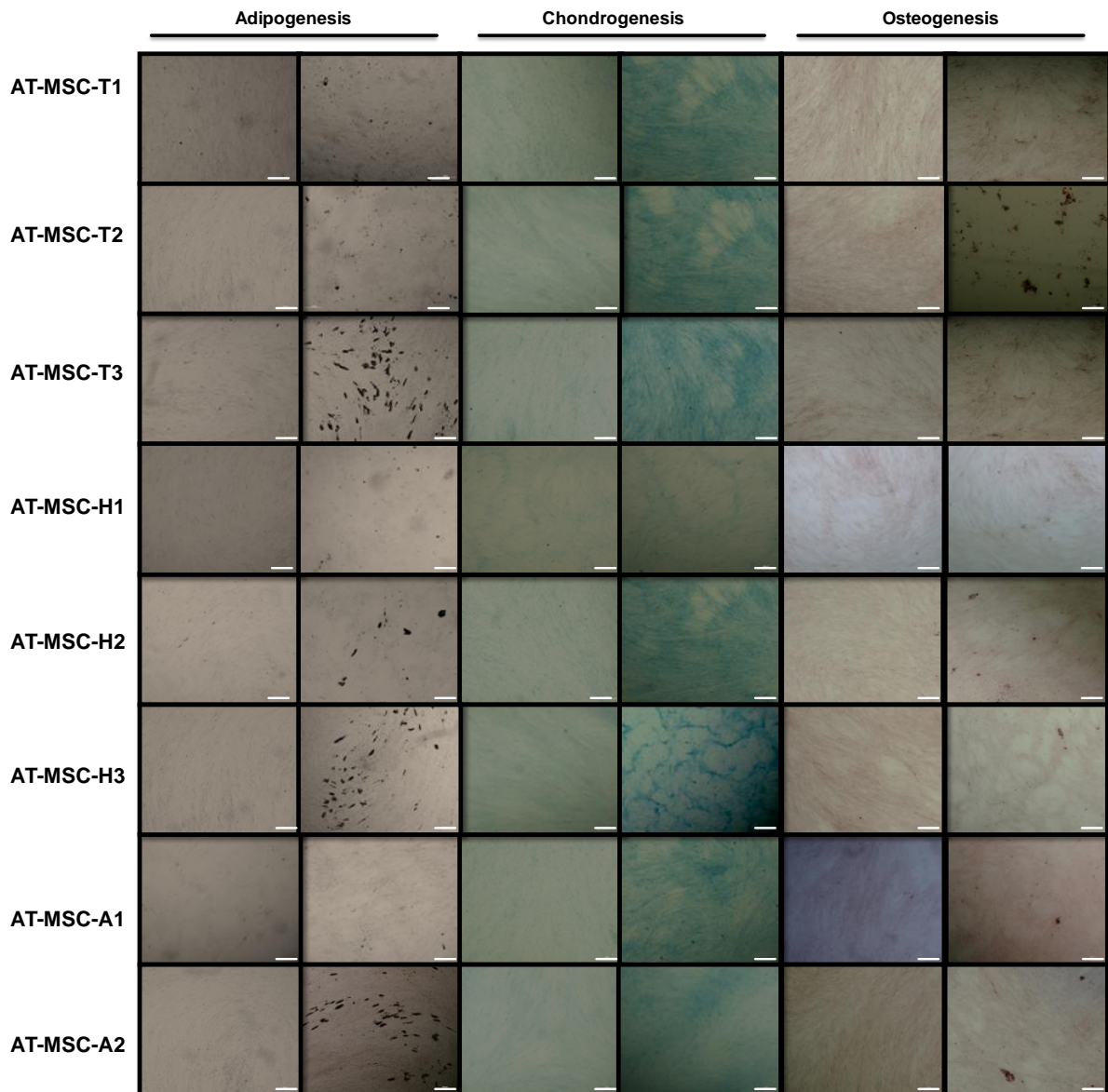


Figure 11: Differentiation of AT-MSCs. AT-MSCs isolated from thighs, hips and abdomen adipose tissue differentiated to adipocytes, chondrocytes and osteocytes after culturing in defined media for 21 days. Representative micrographs of the undifferentiated control cells (left) and the differentiated cells (right). Developed lipid vacuoles were detected by staining with oil red O, mineralization was detected by staining with alizarin red S, and glycosaminoglycan deposition was detected by staining with alcian blue. Scale bars: 100 μ m.

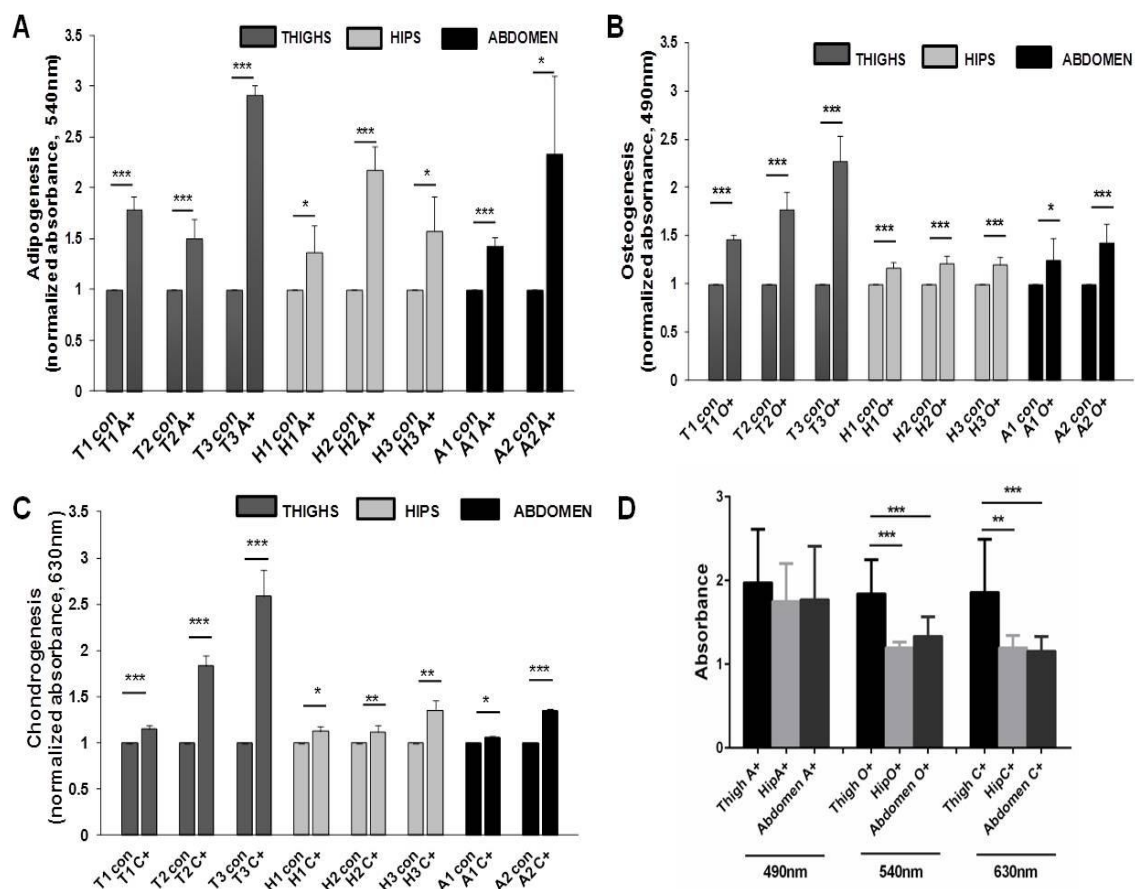


Figure 12: Quantification of AT-MSC differentiation. AT-MSCs were cultured in control (con), adipogenic (A+), osteogenic (O+) or chondrogenic (C+) differentiation media for 21 days. The AT-MSCs were stained for adipo-, osteo- and chondrogenesis and stains were extracted for spectrophotometric analyses, as described in Methods. Differentiation of AT-MSCs was quantified with absorbance measurements conducted at 540 nm for oil Red O (A), 490 nm for alizarin Red S (B) and 630 nm for alcian blue (C). (D) Comparison of adipogenesis, osteogenesis and chondrogenesis levels in AT-MSCs derived from thigh, hip and abdomen harvesting sites. The mean \pm SD of normalised absorbance from three independent experiments are provided. * $p < 0.05$; ** $p < 0.01$; *** $p < 0.001$.

4.1.4. Growth properties of AT-MSCs

To examine the influence of AT-MSC tissue-harvesting site on proliferation of the isolated AT-MSC, these were passaged until they no longer proliferated. Growth profiling of these AT-MSCs from different anatomic sites was determined in terms of their cumulative population doubling levels (CPDLs). Long-term growth curves differed considerably between all the AT-MSC lines, regardless of their tissue-harvesting site (Fig. 13A). AT-MSC-T3, AT-MSC-H2 and AT-MSC-A2 exhibited highest proliferation rates, compared to other AT-MSC lines. AT-MSC-T1, AT-MSC-T2, AT-MSC-H1, AT-MSC-H3 and AT-MSC-A1 formed a cluster, which showed nearly identical CPDLs after 100 days of cultivation (Fig. 13A). After 200 days of culturing, the proliferation rates of all AT-MSC lines started to decrease and halting their growth (Fig. 13A).

Comparison of proliferation rates of AT-MSC lines derived from different anatomical sites revealed these cell lines to exhibit the identical proliferation rate until the passage 6. The CPDLs of these same AT-MSCs at passages 12 and 18 varied more, though not significantly (Fig. 13B).

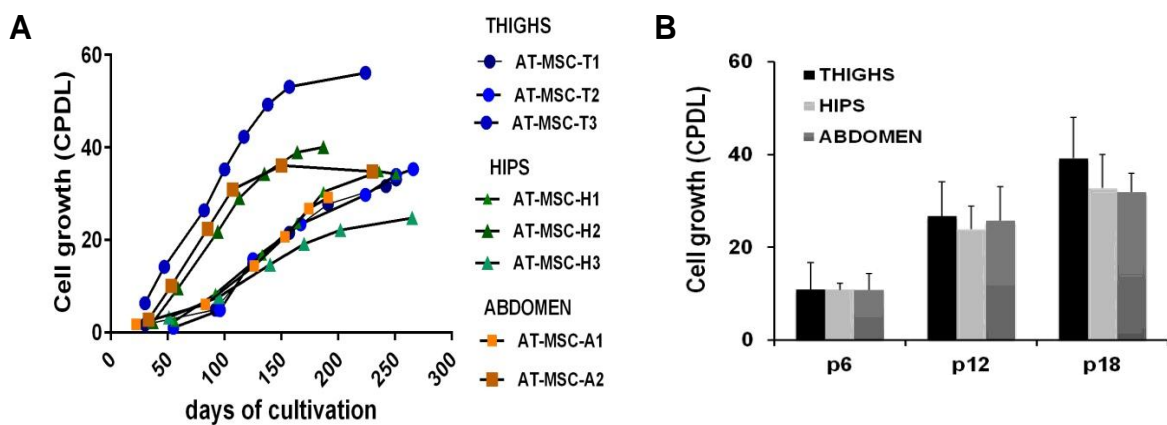


Figure 13: Growth profiling of AT-MSCs. (A) Long-term growth curves of AT-MSCs derived from thigh, hips and abdomen adipose tissue obtained by cumulative population doubling levels (CPDLs) calculation. (B) CPDLs of AT-MSCs derived from thigh, hips and abdomen harvest site were averaged at increasing passages (p6, p12 and p18). The mean \pm SD of three independent experiments are provided.

4.1.5. Replicative senescence in AT-MSCs

The extent of spontaneous senescence was determined in all isolated AT-MSC lines using SA- β -gal staining during their prolonged cultivation *in vitro* at passages 6, 12 and 18 (Fig. 14A). At the early passage 6, the hip derived AT-MSCs contained higher percentage of SA- β -gal positive cells (10.6 %) compared to thigh (4.3 %) and abdomen (3.7 %) derived AT-MSC (Fig. 14B). Similarly, at passage 12 highest percentages of senescent cells was detected in hip derived AT-MSCs (26.7 %) compared to thigh and abdomen derived AT-MSCs, where 11.0 % and 13.2 % of senescent cells were detected, respectively (Fig. 14B). In contrast, at passage 18, higher proportion of senescent cells were detected in the hip (55.5 %) and abdomen (62.1 %) derived AT-MSC lines, compared to the thigh derived AT-MSC lines (28.1 %) (Fig. 14B).

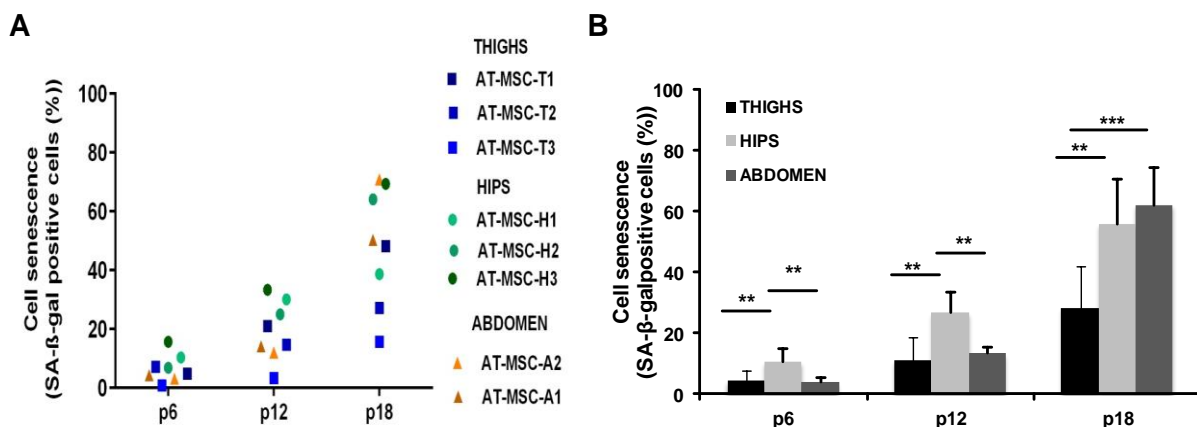


Figure 14: Spontaneous senescence arising in isolated AT-MSCs during prolonged *in vitro* culture. (A) The percentage of senescent cells in AT-MSC lines at passage 6, 12 and 18 was evaluated by counting SA- β -gal stained cells against all cells in a visual field. (B) Percentages of SA- β -gal positive cells in AT-MSC lines averaged regarding the tissue–harvesting site are shown for their early passage 6, middle passage 12 and late passage 18. The mean \pm SD of three independent experiments are provided. ** $p < 0.01$; *** $p < 0.001$.

4.2. EXPANSION OF AT-MSCs ON MICROCARRIERS

The aim of this part of the dissertation was to optimize the parameters for successful expansion of AT-MSCs on Cytodex-1 and Cytodex-3 microcarriers. Thus we investigated the parameters influencing the adhesion of AT-MSCs to selected microcarriers, followed by the investigation of parameters influencing the expansion of AT-MSCs on both types of microcarriers. Finally, the differentiation ability and MSC surface markers expression were analysed in the AT-MSCs before and post expansion on the microcarriers.

4.2.1. AT-MSC seeding efficiency on microcarriers

4.2.1.1. Effect of microcarriers pre-coating on AT-MSC seeding in static and in spinner flasks culture system

The effect of Cytodex-1 and Cytodex-3 microcarriers pre-coating with either growth media (GM) or FBS on the AT-MSC seeding efficiency was investigated in both, 6-well plates and spinner flasks. The ability of the AT-MSCs to attach to either GM or FBS pre-coated Cytodex-1 and Cytodex-3 microcarriers after 24 h of culturing under static conditions in 6 well plates was comparable among tested conditions. The seeding efficiencies were 56.1 % (GM) and 50.4 % (FBS) on Cytodex-1, and 47.7 % (GM) and 42.9 % (FBS) on Cytodex-3 (Fig. 15A) compared to cells attached to the culture plates. Similar results were observed for AT-MSCs cultured in spinner flasks for 24 h, where the seeding efficiencies were 50.0 % (GM) and 52.1 % (FBS) on Cytodex-3, and 53.1 % (GM) and 49.1 % (FBS) on Cytodex-1 (Fig. 15B) compared to initial number of the seeded cells. Thus the pre-coating of microcarriers with GM or FBS did not have any effect on the AT-MSC seeding efficiency. However, the seeding efficiency of AT-MSCs on microcarriers is lower than on culture plates.

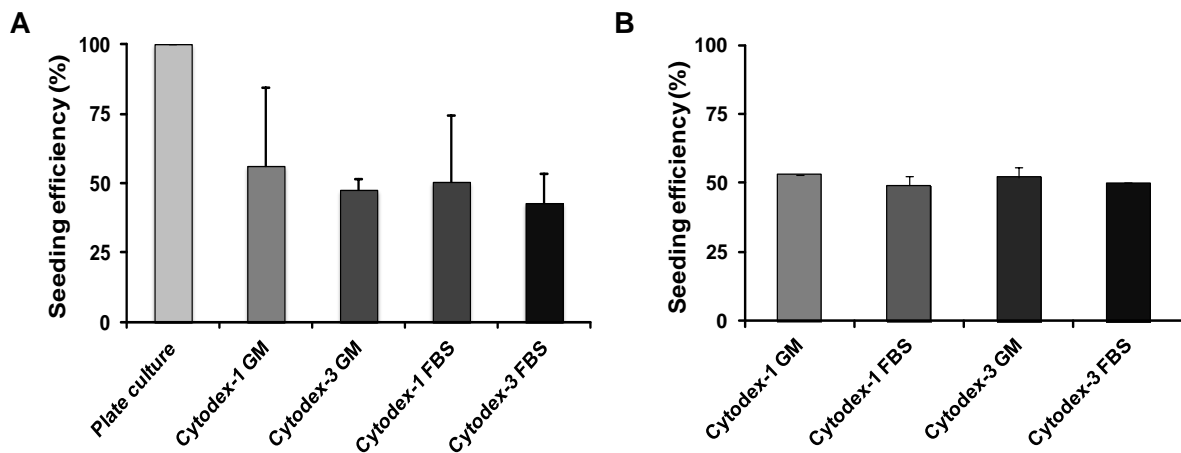


Figure 15: AT-MSC seeding efficiency on differently pre-coated microcarriers. The AT-MSCs were left to attach for 24 h under static conditions in 6 well culture plates (A) and in spinner flasks (B) to both types of microcarriers pre-coated with FBS and growth media (GM), and their seeding efficiency was analyzed after harvesting from microcarriers and counting the AT-MSCs. The number of attached cells was normalized to the number of initially seeded cells. No significant differences of AT-MSC seeding efficiency on both types of microcarriers pre-coated with GM or FBS were noticed. The mean \pm SD of three independent experiments are provided.

4.2.1.2. Effect of agitation regime on the AT-MSC seeding efficiency in spinner flasks

The influence of agitation regime applied during first 24 h of cultivation on AT-MSC seeding efficiency was evaluated. The effects of two agitation regimes were compared: one completely static (static) and the other composed of 5 min agitation at 40 rpm followed by 30 min no agitation periods (mix). After 24 h of culturing AT-MSCs on the microcarriers, the intermittent agitation (mix) resulted in higher AT-MSC seeding efficiency compared to the static conditions. This applied to the use of both, Cytodex-1 (53.2 % -mix vs. 41.3 % -static) and Cytodex-3 (53.1 % -mix vs. 44.2 % -static) microcarriers (Fig. 16).

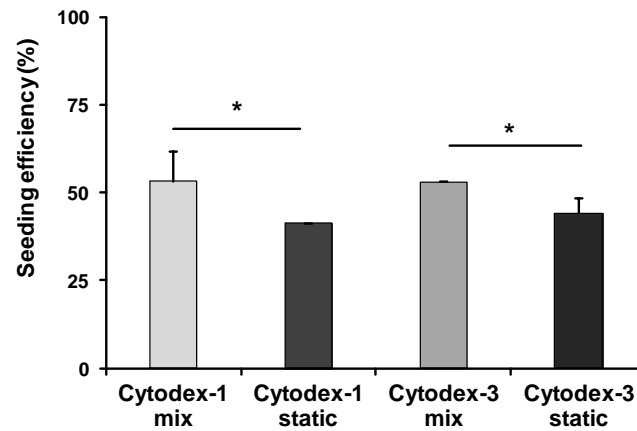


Figure 16: AT-MSC seeding efficiency on microcarriers pre-coated with GM and grown for 24 h at different agitation regimens. After 24 h in spinner flaks with no agitation (static) and under intermittent agitation (mix), the adhered AT-MSCs were dissociated from microcarriers and counted. The number of attached cells was compared to the number of initially seeded cells. Higher seeding efficiencies of AT-MSCs were noticed on both Cytodex-1 and Cytodex-3 microcarries exposed to intermittent agitation. The mean \pm SD of three independent experiments are provided. * $p < 0.05$.

4.2.2. AT-MSC expansion in spinner flasks

4.2.2.1. Effect of pre-coating of microcarriers on AT-MSC expansion

Although the initial AT-MSC attachment efficiency to microcarriers revealed not to be affected by the tested pre-coating conditions, the finally achieved AT-MSC numbers revealed to be affected by pre-coating conditions. The pre-coating of both types of microcarriers with GM resulted in higher AT-MSC density determined at day 10 of culturing compared to the density determined on FBS pre-coated microcarriers. In detail, 20.9 % increase in AT-MSC density was determined on Cytodex-1 pre-coated with GM ($6.2 \times 10^5 \pm 0.4$ cells/ml) compared to FBS pre-coated ones ($4.9 \times 10^5 \pm 0.4$ cells/ml) (Fig. 17A). Likewise, pre-coating of Cytodex-3 microcarriers with GM resulted in 19.6 % increase of AT-MSC density ($6.1 \times 10^5 \pm 0.4$ cells/ml) at day 10 as compared to FBS pre-coated microcarriers ($4.9 \times 10^5 \pm 0.7$ cells/ml) (Fig. 17B). Overall, similar AT-MSC densities were observed across Cytodex-1 and Cytodex-3 microcarriers when pre-coated with GM or with FBS, respectively.

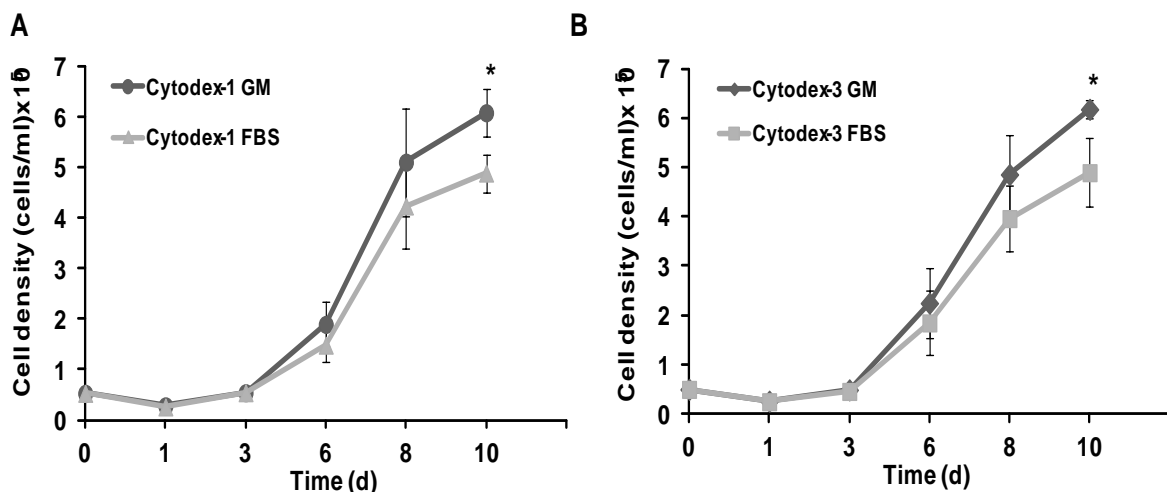


Figure 17: Effect of Cytodex-1 and Cytodex-3 pre-coating with GM and FBS on AT-MSC proliferation. AT-MSC growth on microcarriers was determined as a number of cells/ml of culture media in each spinner flask over 10 days culture period. (A) Pre-coating of Cytodex-1 microcarriers with GM resulted in higher AT-MSC density compared to those pre-coated with FBS. (B) Higher AT-MSC density was detected after Cytodex-3 pre-coating with GM compared to pre-coating with FBS. The mean \pm SD of three independent experiments are provided. * $p < 0.05$.

Henceforth, in all experiments Cytodex-1 and Cytodex-3 microcarriers were pre-coated with GM.

4.2.2.2. Effect of agitation regime on AT-MSC expansion

To ensure optimal conditions for initial AT-MSC adhesion and growth on Cytodex-1 and Cytodex-3 microcarriers, we tested two agitation regimes applied during the first 24 h of culturing; one completely static, and the other with continuous cycles of agitation for 5 min at 40 rpm followed by 30 min of no agitation. Although both tested agitation regimes, applied during the first 24 h had an effect on the AT-MSC seeding efficiency (Fig. 16), the further growth of AT-MSCs on microcarriers was not influenced by those initial agitation regimes, as comparable cell densities on both Cytodex-1 (Fig. 18A) and Cytodex-3 (Fig. 18B) microcarriers were observed during culturing.

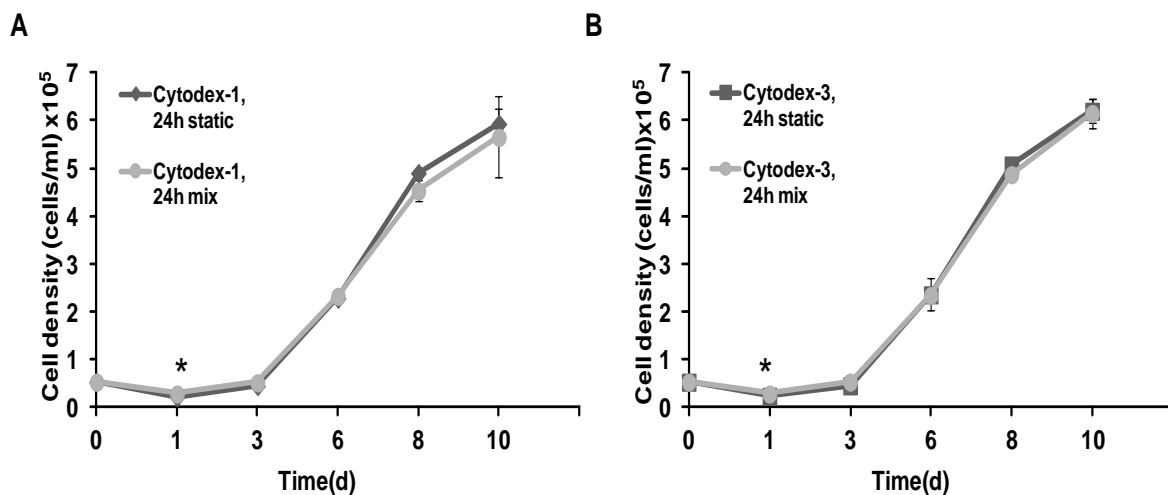


Figure 18: Influence of agitation regime applied during the first 24 h of cultivation on AT-MSC expansion on Cytodex-1 and Cytodex-3 microcarriers. AT-MSC growth on microcarriers was determined as number of cells/ml of culture media in each spinner flask over 10 days culture period. No differences in AT-MSC density on microcarriers were noted when (A) static conditions and (B) intermittent agitation was applied during the first 24 h of culturing. Higher number of attached cells was observed only after 24 h with intermittent agitation. The mean \pm SD of three independent experiments are provided. * $p < 0.05$.

4.2.2.3. Effect of the feeding regime on AT-MSC expansion

To ensure the optimal nutrient supply for AT-MSC growth in spinner flasks, after day 1 of culturing, we tested the effect of two feeding regimes; replacing half of the culture medium either every 2 or 3 days, with the final cell count on day 10. Refreshment of the culture media every 2 days resulted in higher AT-MSC growth compared to growth of AT-MSCs with media change every 3 days. Cultivation of AT-MSCs on Cytodex-1 under condition of media change every 2 days resulted in 27.2 % increase of cell density ($6.1 \times 10^5 \pm 0.5$ cells/ml) observed on day 10 compared to cell density observed under conditions of media change every 3 days ($4.4 \times 10^5 \pm 0.4$ cells/ml) (Fig. 19A). Similarly, when culturing AT-MSCs on

Cytodex-3 20.1 % (day 8) and 26.0 % (day 10) increase in cell densities were observed in favour of media refreshment every 2 days (Fig. 19B). On day 8 and day 10 the AT-MSC densities on Cytodex-3 in conditions of media change every 2 days were $4.9 \times 10^5 \pm 0.8$ cells/ml and $6.2 \times 10^5 \pm 0.2$ cells/ml, whereas in conditions of media change every 3 days those were $3.6 \times 10^5 \pm 0.3$ cells/ml and $4.9 \times 10^5 \pm 0.4$ cells/ml, respectively (Fig. 19B).

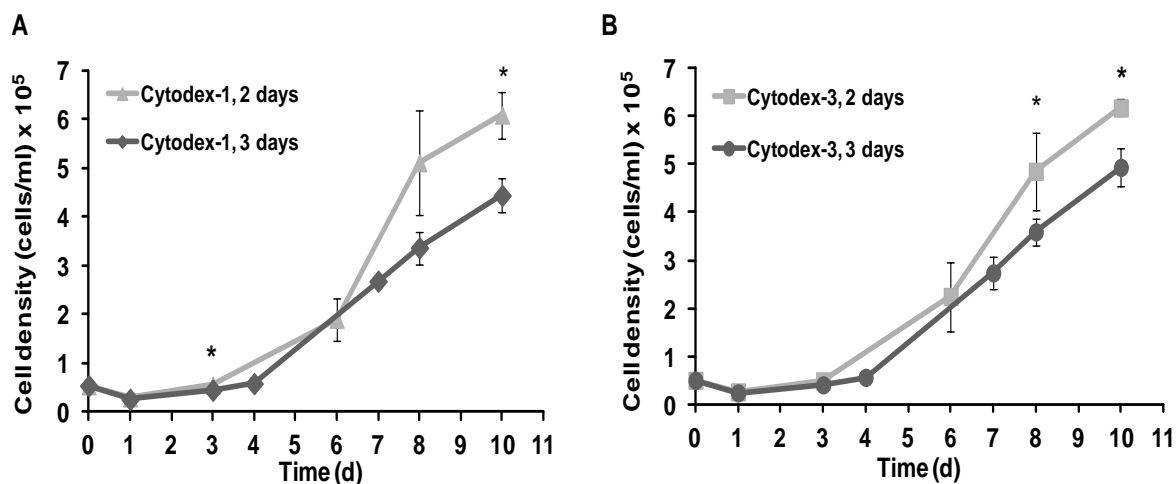


Figure 19: Influence of the feeding regime on AT-MSC growth on Cytodex-1 and Cytodex-3 microcarriers. Medium change in spinner flasks was performed every 2 or 3 days from day 1 until day 10. AT-MSC growth on microcarriers was determined as a number of cells/ml of culture media in each spinner flask on day 10 of culturing. Regardless the microcarrier type used (A, B) medium change every 2 days resulted in higher AT-MSC density compared to media change every 3 days. The mean \pm SD of three independent experiments are provided. * $p < 0.05$.

Simultaneously, observations under a microscope revealed, the occurrence of AT-MSC aggregation on both types of microcarriers, starting at day 6, irrespectively of the applied feeding regime (Fig. 20).

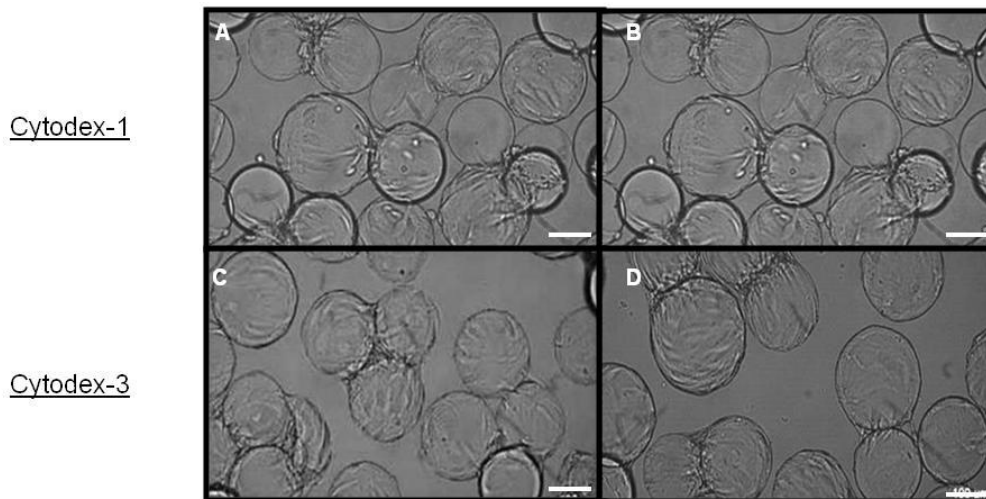


Figure 20: AT-MSC appearance on Cytodex-1 and Cytodex-3 microcarriers at day 6 of cultivation. AT-MSCs cultured on Cytodex-1 or Cytodex-3 under the conditions of media change every 2 days (A, C) or every 3 days (B, D), caused microcarrier/cell aggregation. Scale bar represents 100 μm .

4.2.2.4. Effect of subsequent microcarriers addition on AT-MSC expansion

To limit AT-MSC-microcarrier aggregation during expansion of AT-MSCs in spinner flasks, ensure homogeneous culture conditions and to improve final AT-MSC yields, we increased the cell growth area by the subsequent addition of fresh microcarriers at day 3 of cultivation. As a result, we obtained a higher total number of AT-MSC on day 10 of cultivation compared to all previously tested conditions (Table 7). The AT-MSC densities attained at day 10 upon growth on Cytodex-1 and Cytodex-3 microcarriers and their subsequent addition were $8.5 \times 10^5 \pm 0.3$ cells/ml and $8.3 \times 10^5 \pm 1.0$ cells/ml, respectively (Fig. 21). Furthermore, the addition of fresh Cytodex-3 microcarriers during AT-MSC expansion in spinner flasks resulted in limited aggregates formation (Fig. 22). On contrary, addition of the fresh Cytodex-1 failed to prevent AT-MSC aggregation, as evidenced by formation of the aggregates at day 8 (Fig. 22).

Table 7: Influence of various culture conditions on AT-MSC yield at day 10. Data on total cell counts are given for culturing conditions of microcarriers pre-coating, agitation and feeding regime, and microcarrier additions. The highest numbers of AT-MSCs were obtained after the addition of fresh microcarriers during the cultivation process. The mean \pm SD of three independent experiments are provided. * $p < 0.05$.

Micro-carriers	Pre-coating of microcarriers		Agitation regime		Medium change		Microcarriers addition
	FBS	GM	24h static	intermittant agitation	2 day	3 day	
Cytodex-1	2,94E+07	3,65E+07*	3,56E+07	3,39E+07	3,65E+07*	2,66E+07	5,09E+07
Cytodex-3	2,94E+07	3,71E+07*	3,72E+07	3,69E+07	3,71E+07*	2,96E+07	4,75E+07

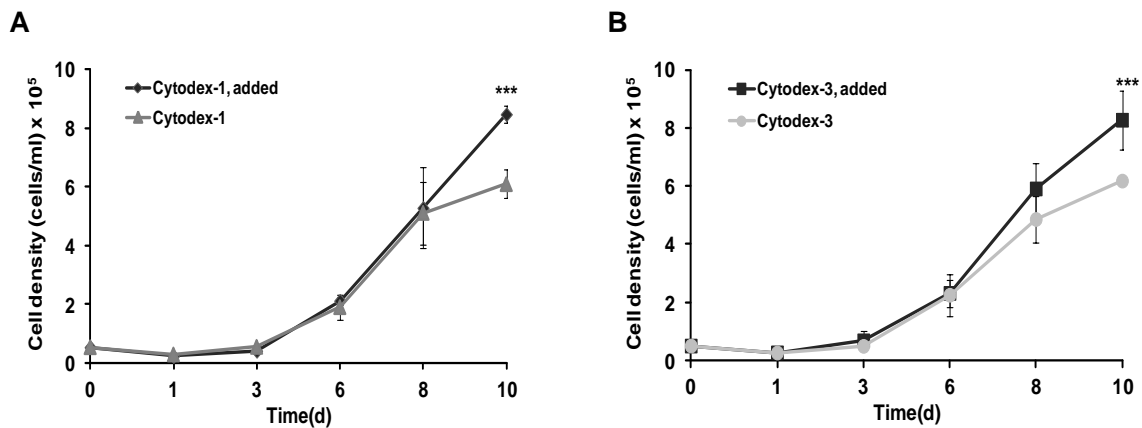


Figure 21: Influence of microcarriers addition during cultivation process on AT-MSC expansion. Fresh Cytodex-1 (A) and Cytodex-3 (B) microcarriers were added at day 3. AT-MSC growth on microcarriers was determined as number of cells/ml of culture media in each spinner flask over 10 days culture period. Higher cell density was observed under condition of fresh microcarrier addition. The mean \pm SD of three independent experiments are provided. *** $p < 0.001$.

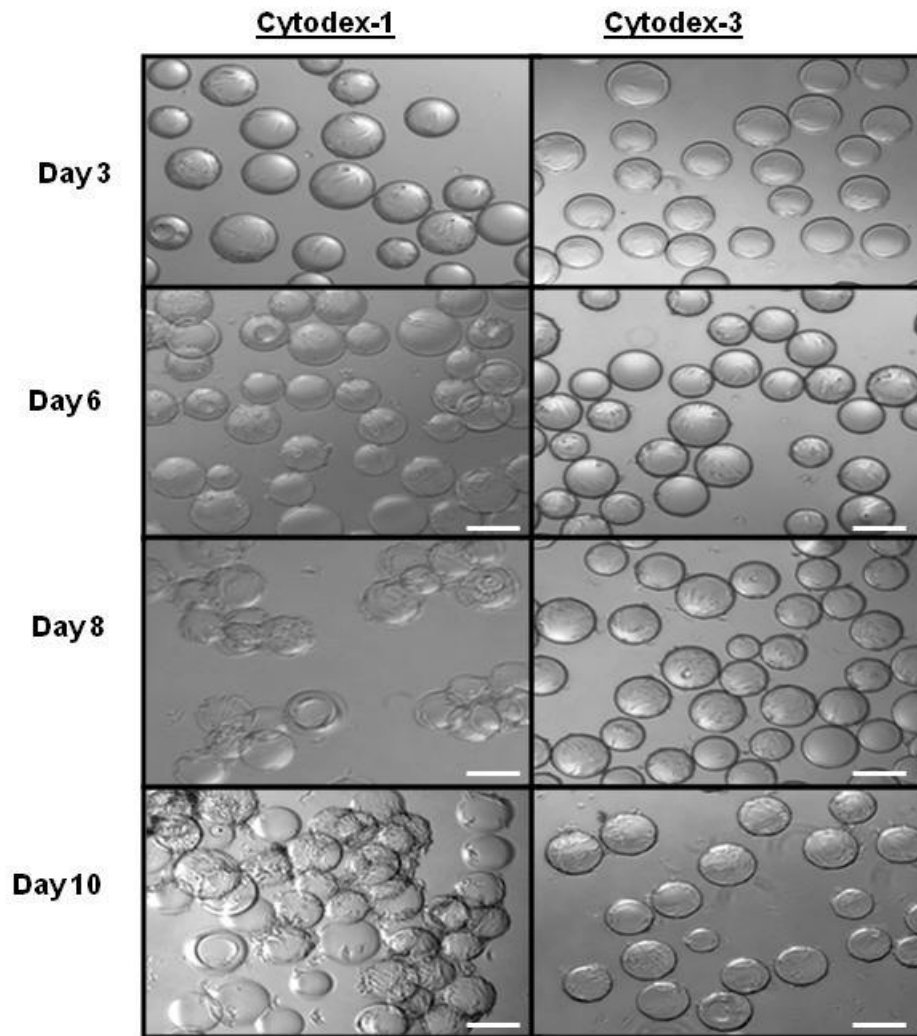


Figure 22: The influence of microcarriers addition on the AT-MSC-microcarrier aggregation upon expansion in spinner flasks. Fresh microcarriers were added at day 3 of AT-MSC cultivation process. The AT-MSCs cultivation on Cytodex-1 started to form aggregates at day 8 despite the fresh microcarriers addition. Oppositely, no aggregation of microcarriers was observed after addition of fresh Cytodex-3 microcarriers during AT-MSC cultivation process. Scale bar represent 100 μm .

4.2.3. Characterization of AT-MSCs after expansion on microcarriers

To verify whether AT-MSCs expanded on microcarriers retain their stemness, their ability to differentiate and immunophenotypic properties were analyzed.

The differentiation of AT-MSCs into adipo-, chondro- and osteo- progenitors was investigated at a passage before cultivation on microcarriers and immediately post-harvesting them from the microcarriers. The capacity of AT-MSCs to differentiate into adipocytes (Fig. 23) and chondrocytes (Fig. 24) was not influenced by culturing the cells in the spinner flasks. Visual inspection of lipid vacuoles detected with oil red O and proteoglycans staining with alcian blue in the AT-MSCs prior and post culturing on microcarriers revealed no differences. Yet, an increased osteogenic capacity was observed for AT-MSC expanded on microcarriers as higher amount of calcium deposits detected by Von Kossa staining (Fig. 25).

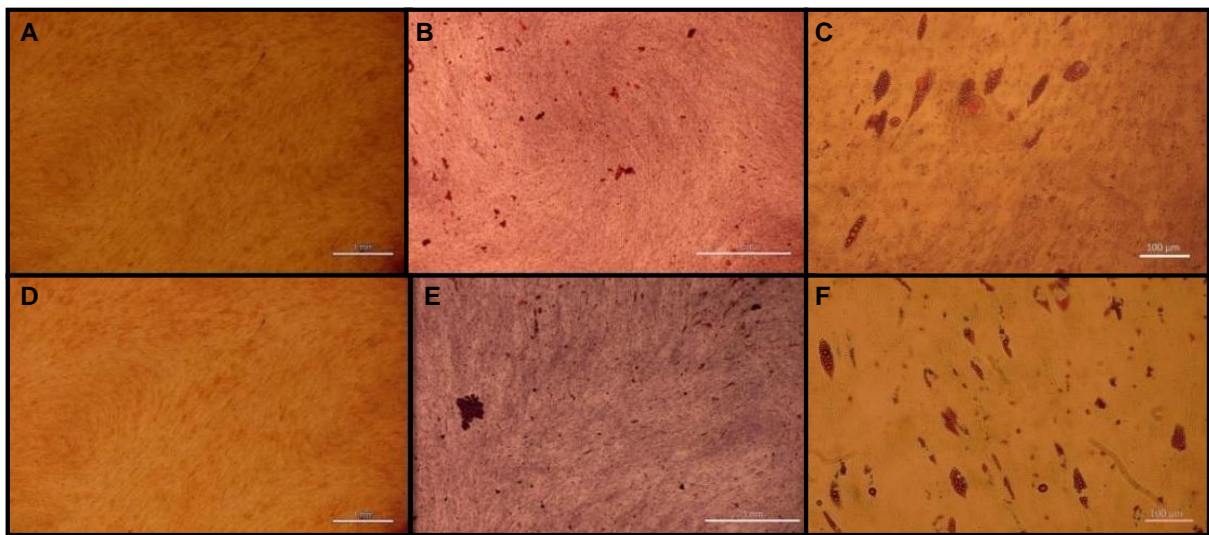


Figure 23: Adipogenic differentiation of the AT-MSCs after cultivation on microcarriers. AT-MSCs before (A-C) and after cultivation on microcarriers (D-F) were used as controls (A, D) and grown in normal culture media or where exposed to adipogenic differentiation medium for 21 days. The developed lipid vacuoles were detected with oil red O staining. Magnification (A, D) 2 \times , (B, E) 4 \times and (C, F) 10 \times .

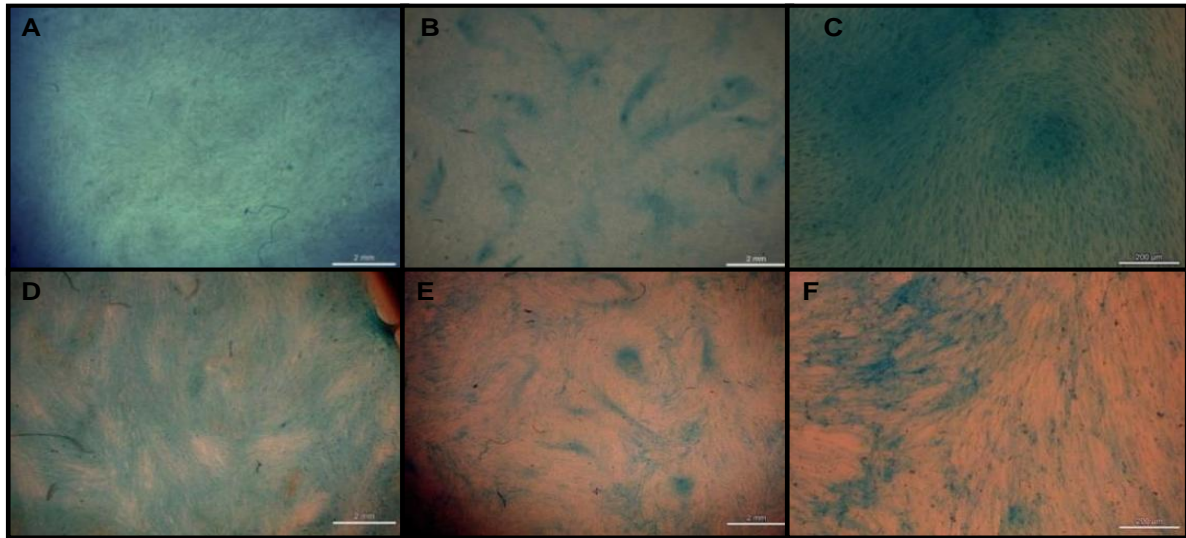


Figure 24: Chondrogenic differentiation of the AT-MSCs after cultivation on microcarriers. AT-MSCs before (A-C) and after cultivation on microcarriers (D-F) were grown in normal culture media (A,D) or exposed to chondrogenic differentiation media for 21 days. Then, the developed proteoglycans were stained with alcian blue. Magnification (A, D) 1×, (B, E) 2× and (C, F) 8×.

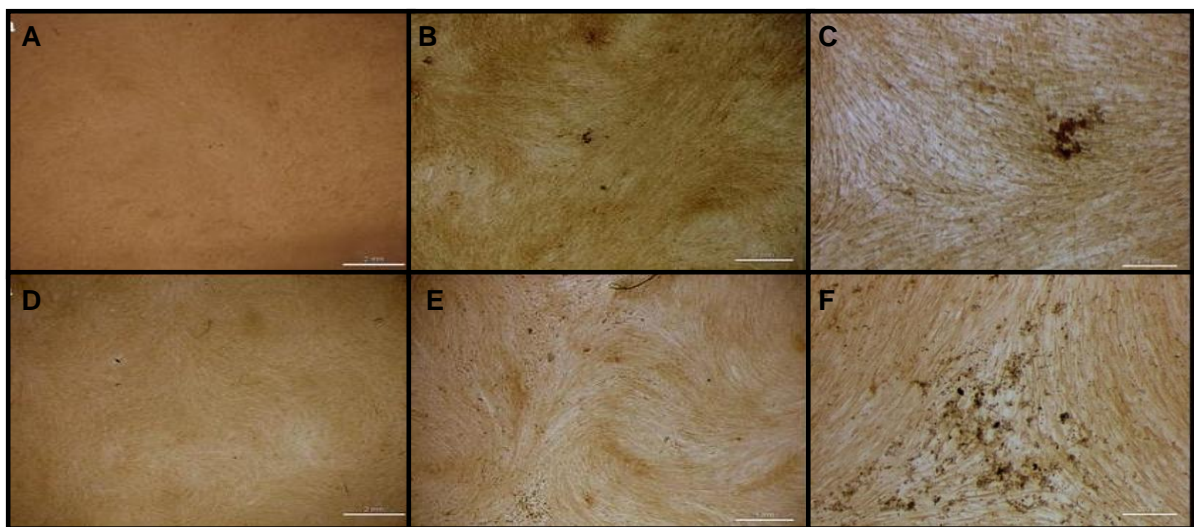


Figure 25: Osteogenic differentiation of the AT-MSCs after cultivation on microcarriers. AT-MSCs before (A-C) and after cultivation on microcarriers (D-F) were grown in normal culture media (A, D) or exposed to osteogenic differentiation media for 21 days. Van Kossa staining was used to detect the developed calcium deposits. Magnification (A, B, D, E) 1× and (C, F) 8×.

Similarly, the expression of MSC specific surface markers did not change in AT-MSC upon their cultivation on Cytodex-3 microcarriers (Fig. 26). Flow cytometry analysis confirmed the expression of characteristic MSC surface antigens CD13, CD29, CD44, CD73, CD90, CD105 and absence of HSC markers CD14, CD34, CD45 and HLA-DR.

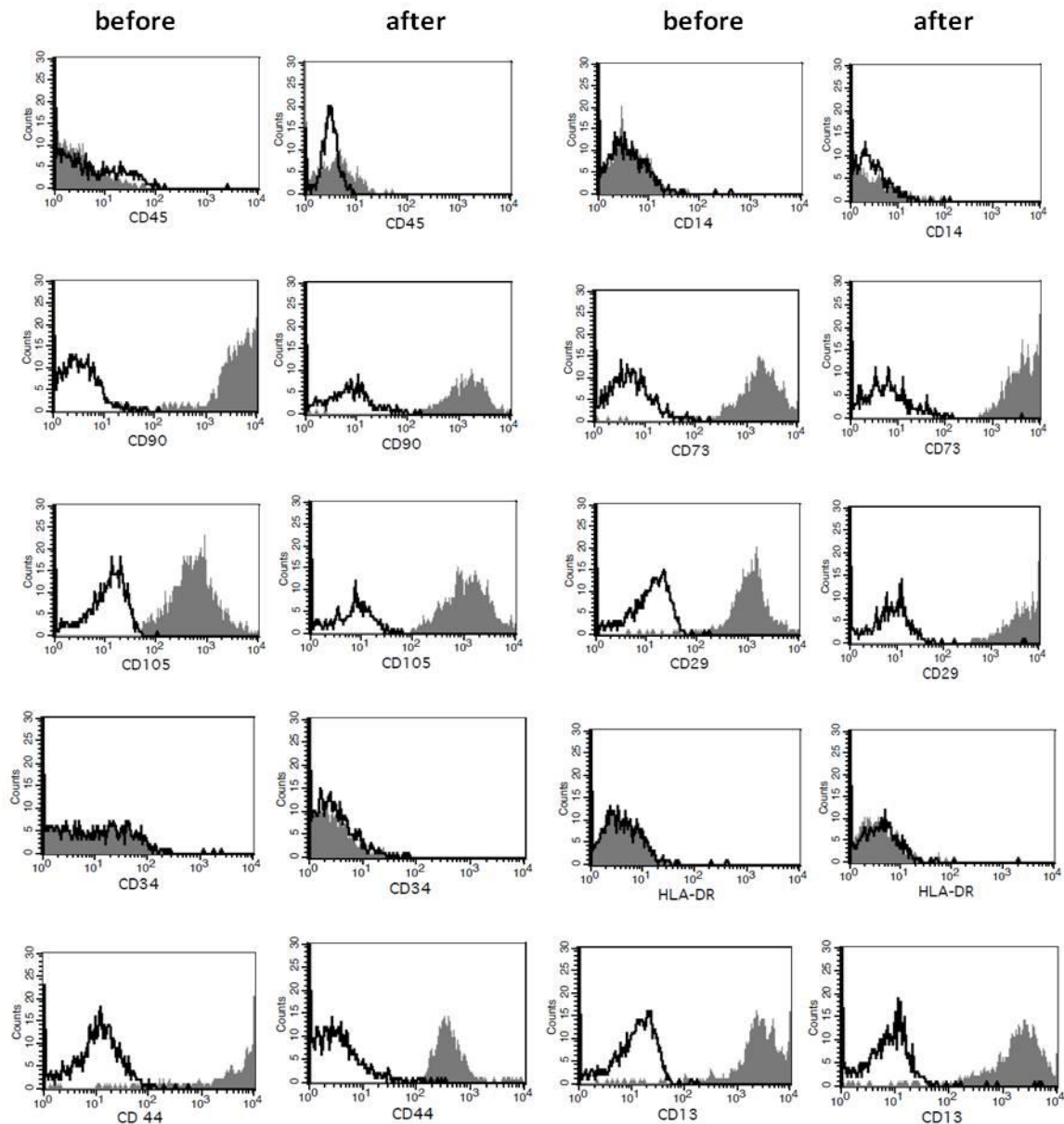


Figure 26: AT-MSC surface marker expression prior and post culturing on microcarriers. Representative histograms of AT-MSC immunophenotype analysis using FACS showed no change in the pattern of the MSC specific surface marker expression. Unfilled histograms with the black line represent isotype control for the background fluorescence and a shaded area show signal from MSC surface marker antibodies.

4.3. PARACRINE EFFECTS OF BM-MSC AND UC-MSC CONDITIONED MEDIA ON GSLCs

4.3.1. Isolation and characterization of umbilical cord-derived mesenchymal stem cells (UC-MSCs)

The isolated UC-MSCs exhibited typical spindle shaped morphology. Using FACS, the presence of CD13, CD29, CD44, CD73, CD90, CD105 and the absence of CD14, CD34, CD45 and HLA-DR surface antigens was confirmed (Fig. 27). The UC-MSCs differentiated into adipocytes, osteoblasts, chondroblasts (Fig. 28).

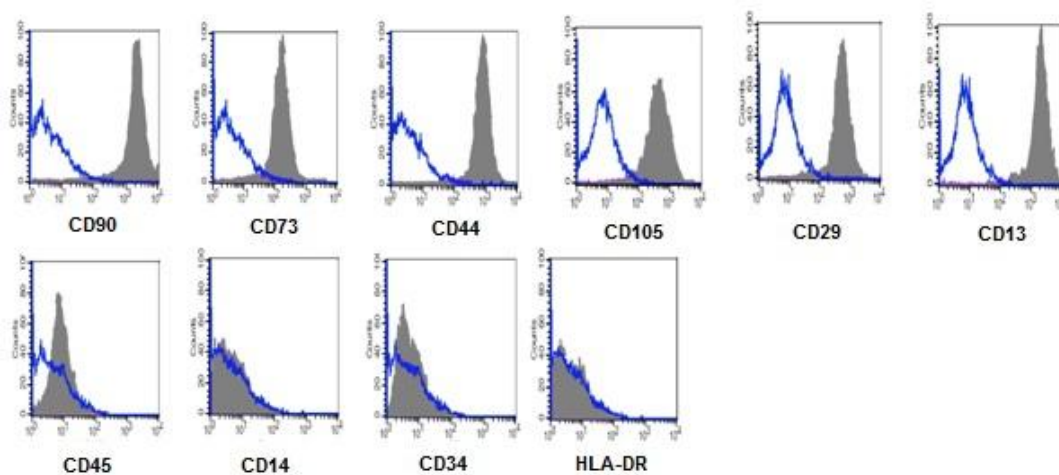


Figure 27: Phenotypic characterization of UC-MSCs. Flow cytometry analysis of UC-MSC surface markers was conducted at passage 7 and representative histograms of their immunophenotype are given. Unfilled histograms with blue lines represent isotype control for background fluorescence and a shaded grey area show signal from MSC surface marker antibodies. More than 95 % of cells were positive for mesenchymal markers (CD13, CD29, CD44, CD73, CD90, CD105), whereas the expression of hematopoietic markers (CD13, CD34, CD45, HLA-DR) was below 2 %.

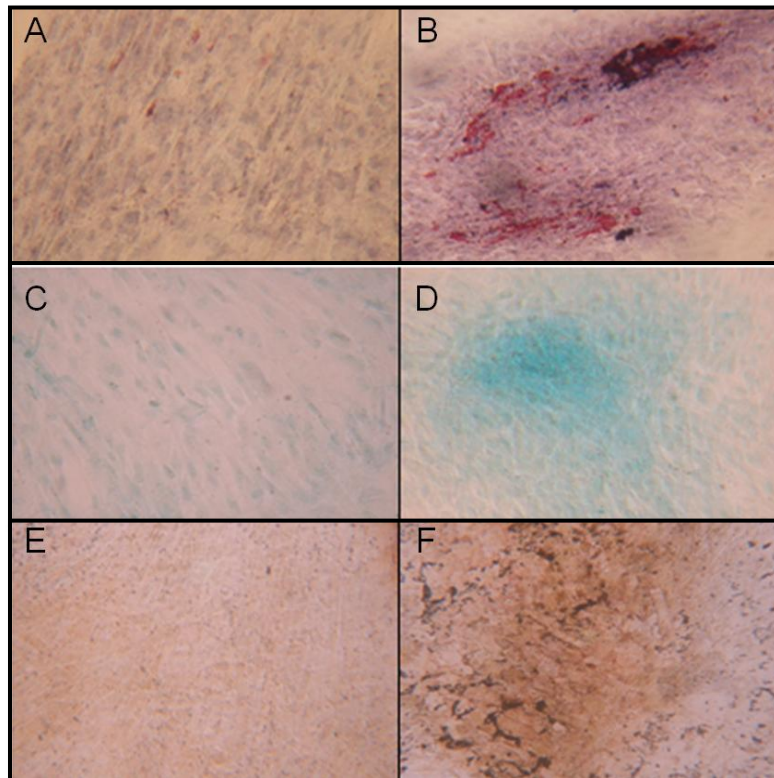


Figure 28: Analysis of differentiation capacity of UC-MSCs. (A) Control cells, not exposed to adipogenic differentiation media. (B) Cells after the induction of adipogenic differentiation, the developed lipid droplets were detected with oil red O staining. (C) Control cells, not exposed to chondrogenic differentiation media. (D) The extent of UC-MSC chondrogenic differentiation visualized with alcian blue staining. (E) Control cells not exposed to osteogenic differentiation media. (F) Calcium deposits after osteogenic differentiation detected with von Kossa staining in differentiated UC-MSC. Magnification 40 \times .

4.3.2. Confirmation of GSLCs identity

NCH421k and NCH644 GSLC lines were established previously by Campos (2011), sorted for CD133 expression and confirmed by DNA copy-number profiling and CGH-array to show typical GBM chromosome aberrations (Campos et al., 2011; Wan et al., 2010). FACS analysis was used to confirm the expression of CD133 in NIB26 (79.9 % CD133 positive cells) and NIB50 (71.4 % CD133 positive cells) that were isolated from primary GBM tissue and grown in spheroids to enrich for their GSLCs fraction (Fig. 29A, Fig. 29B). Analysis of p53 status in NCH421k, NCH644, NIB26 and NIB50 cells was determined by qRT-PCR, with U87 cell line (wild type p53) serving as reference (Fig. 29C).

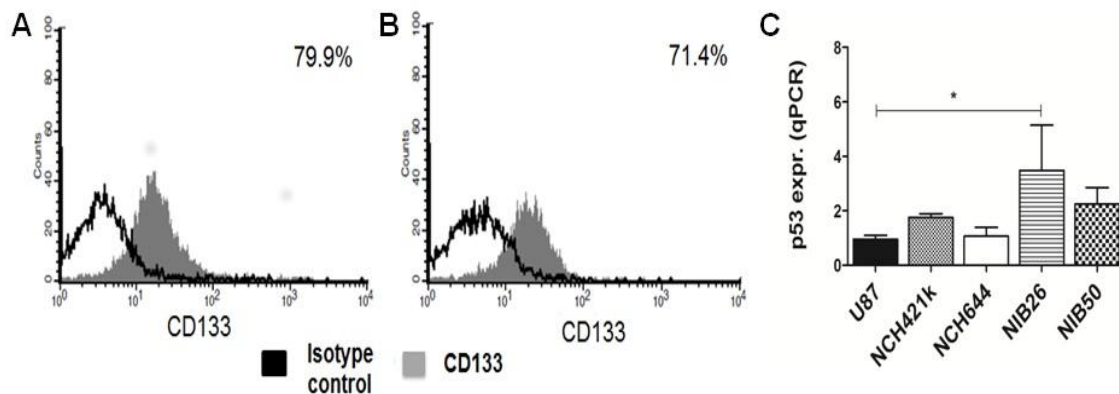


Figure 29: Expression of CD133 surface marker in GSLCs isolated from primary GBM tissue. NIB26 and NIB50 cells were isolated from primary GBM tissue and grown in spheroids to enrich the GSLCs fraction. FACS analysis showed high expression of CD133 in NIB26 (A) and NIB50 (B) cell culture. (C) Analysis of *p53* gene expression in U87, NCH421k, NCH644, NIB26 and NIB50 cells by qRT-PCR. The mean \pm SD of three independent experiments are provided. * $p < 0.05$.

4.3.3. Influence of GSLC conditioned media on migratory capacity of UC-MSCs and BM-MSCs

The potential of UC-MSCs and BM-MSCs to migrate towards GSLCs was assed using a wound-healing assay. Both types of MSCs grown for 16 h in presence of NCH421k conditioned media (CM) displayed increased migration compared to control MSCs grown in NBE medium (Fig. 30).

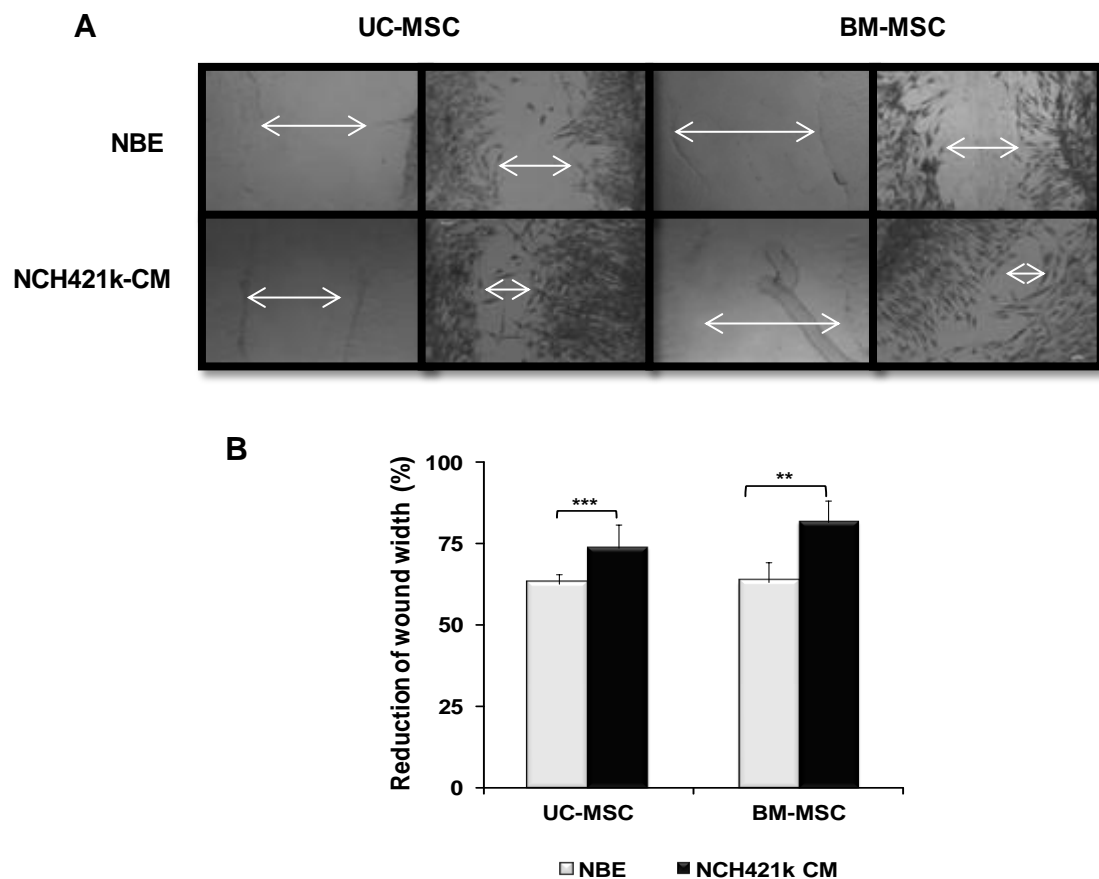


Figure 30: NCH421k CM influence on UC-MSC and BM-MSC migration. The UC-MSCs and BM-MSCs were grown in control medium (NBE) and NCH421k CM for 16 h. (A) Representative microphotographs of scratch wound-healing assay. Magnification 40 \times . (B) Migration of both UC-MSCs and BM-MSCs was increased in the presence of NCH421k CM. The mean \pm SD of three independent experiments are provided. ** $p < 0.01$, *** $p < 0.001$

4.3.4. MSC-CM influence on cell cycle of GSLCs

NCH421k cells were grown with NBE or either type of MSC-CM for 72 h and the cell cycle analysis was performed with FACS. An increased number of NCH421k cells halted in G0/G1 phase in the presence of UC-CM, compared to NBE was detected (Fig. 31A). Additionally, the G0/G1 cell cycle arrest of NCH421k cells grown in MSC-CM of either type was confirmed by analysis of *cyclin D1* (*CCND1*) gene expression, as a 4.2 fold and 2.9 fold decrease of *CCND1* gene expression was observed upon UC-CM and BM-CM exposure, respectively (Fig. 31B). Similarly, the *CCND1* gene expression was found downregulated in NCH644 (1.7-fold, 1.9-fold), NIB26 (2.1-fold, 5.2-fold) and NIB50 (9.0-fold, 7.5-fold) cells exposed to UC-CM and BM-CM, respectively.

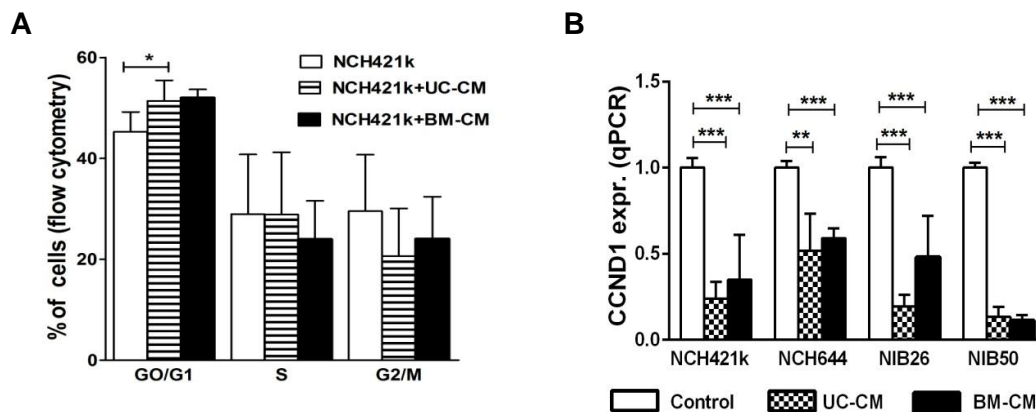


Figure 31: GSLCs cell cycle analysis in presence of UC-CM and BM-CM. (A) FACS cell cycle analysis of NCH421k cells after 72 h treatment with both types of MSC-CM. (B) *CyclinD1* (*CCND1*) expression (qRT-PCR) was decreased in all GSLCs lines after 72 h treatment with UC-CM and BM-CM. The mean \pm SD of three independent experiments are provided. * $p<0.05$, ** $p<0.01$, *** $p<0.001$.

Moreover, upon presence of CM of both types the GSLCs spheroid morphology was strongly affected (Fig. 32). In NCH421k and NIB26 cells an indicative size reduction and loosened structure was observed upon 72 h exposure to UC-CM and BM-CM. Likewise, the NCH644 and NIB50 spheroid morphology was affected upon presence of both types of MSC-CM, yet besides loosened structure the change from spheroid to adherent growth of cells was noticed.

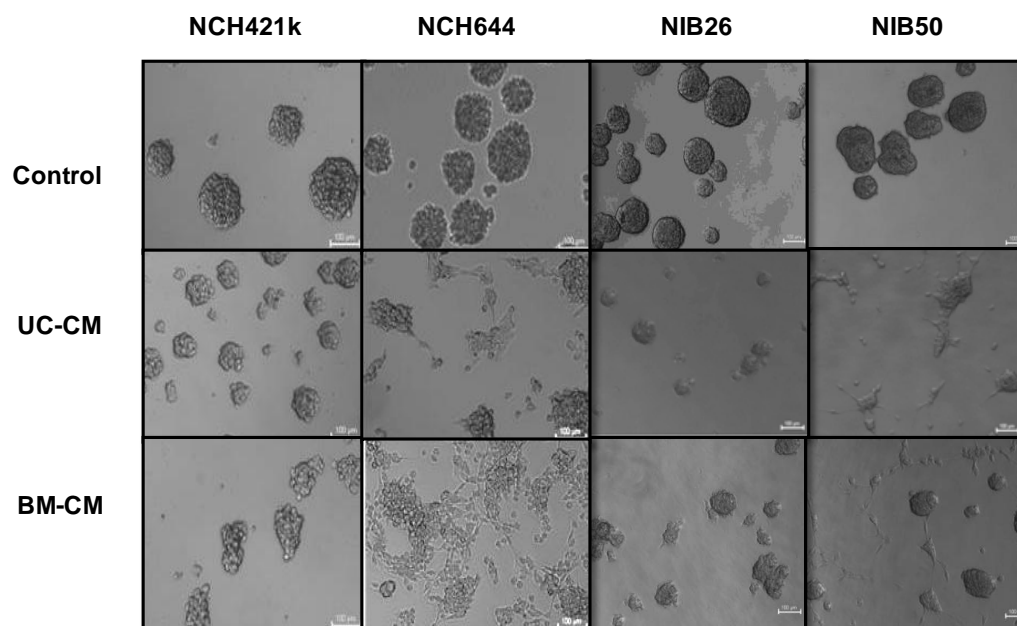


Figure 32: Morphology of GSLCs cells in presence of UC-CM and BM-CM. Scale bar 100 μ m.

4.3.5. MSC-CM impact on induction of apoptosis in GSLCs

The induction of apoptosis in NCH421k cells grown in MSC-CM of both origins for 72 h was first investigated by mitochondrial membrane potential assay (MMP). A significant decrease of MMP upon exposure to UC-CM (23 %) and BM-CM (31 %) was observed (Fig. 33A). To further confirm the onset of apoptosis in GSLCs cells exposed to MSC-CM of either type *Bax* and *Bcl-2* gene expression were analyzed in the NCH421k, NCH644, NIB26 and NIB50 cells grown in UC-CM and BM-CM for 72 h. Yet, the analysis of the *Bax/Bcl-2* gene ratio failed to prove any significant change to occur in the CM cultured GSLCs, compared to control (NBE) ones (Fig. 33B)

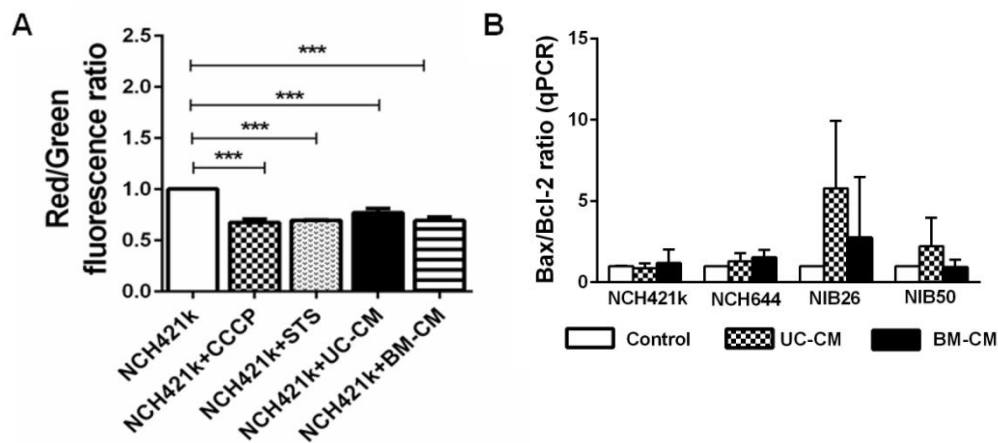


Figure 33: MSC-CM influence on activation of apoptosis in GSLCs lines. (A) Mitochondrial membrane potential (MMP) loss was ascertained by JC-1 staining after exposure of NCH421k cells to UC-CM and BM-CM for 72 h. To induce loss of MMP the CCCP and STS were used as positive controls. (B) *Bax* and *Bcl-2* gene expression analysis (qRT-PCR) was performed in NCH421k, NCH644, NIB26 and NIB50 cells exposed for 72 h to both types of MSC-CM. The ratio between the *Bax* and *Bcl-2* was unaffected. Data shown are mean \pm SD of three independent experiments. *** $p < 0.001$. CCCP-carbonylcyanide-chlorophenyl-hydrazone, STS-staurosporin.

To finally exclude the onset of apoptosis in NCH421k cells upon exposure to UC-CM and BM-CM we performed the Annexin-V staining. The test failed to detect the increased number of apoptotic cells in NCH421k culture exposed to both types of MSC-CM (Table 8). To conclude, our results showed that paracrine factors present in UC-CM or BM-CM cannot induce the onset of apoptosis in GSLCs.

Table 8: Examination of apoptosis in NCH421k cells by AnnexinV/PI measurements.

	Live	Early apoptosis	Late apoptosis	Dead
NCH421k	93.34 ±4.20	4.83±2.63	1.06±1.70	0.76±0.69
NCH421k+STS	42.98 ±12.73*	45.26±13.87*	5.66±0.56	0.80±1.02
NCH421k + UC-CM	91.06±2.54	7.01±2.33	1.24±1.41	0.56±0.55
NCH421k + BM-CM	88.82±6.51	7.69±2.45	2.82±4.32	0.67±0.68

The NCH421k cells were exposed to UC-CM and BM-CM for 72 h and the fraction of apoptotic cells was determined by AnnexinV/PI measurements using FACS. Live cells were negatively stained for both dyes, early apoptotic were stained only with Annexin when late apoptotic were double stained with Annexin and PI. Dead cells were PI stained. STS, an inducing intrinsic apoptotic pathway was used as positive control. The data of three independent experiments are expressed as the mean ± standard deviation (SD) and *p value below 0.05 was considered significant.

4.3.6. MSC-CM influence on activation of senescence in GSLCs

As MSC-CM did influence cell cycle of GSLC, but the induction of apoptosis was not proved, the senescence induction was investigated. The senescence assay employing β -galactosidase activity (SA- β -gal) revealed a significant increase in the number of β -galactosidase positive NCH421k (17 % and 33 %), NCH644 (33 % and 39 %), NIB26 (20 % and 25 %) and NIB50 (30 % and 31 %) cells, exposed to of UC-CM and BM-CM respectively for 72 h, when compared to control NBE (Fig. 34). In GSLCs exposed only to NBE percentage of senescent cells was 10.7 % in NCH421k, 6.6 % in NCH644, 3.3 % in NIB26 and 8.2 % in NIB50 cells.

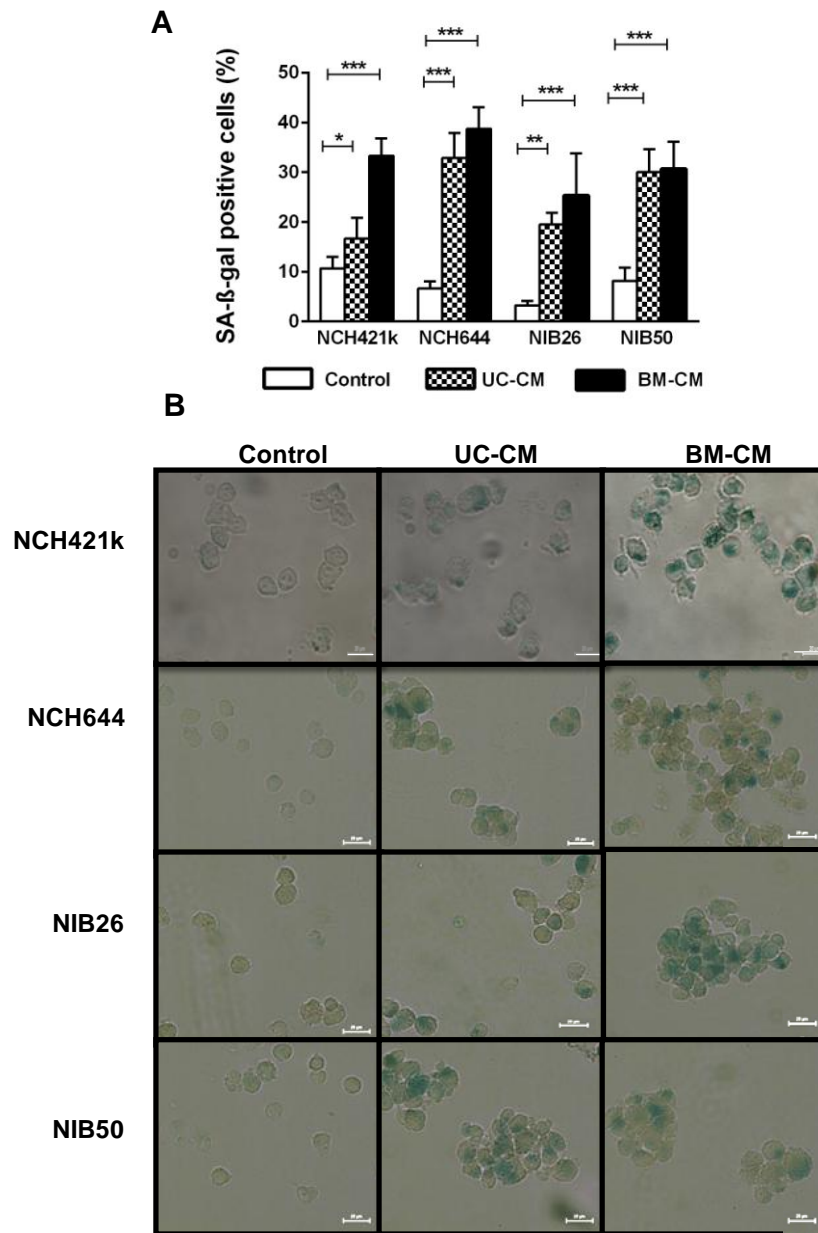


Figure 34: Induction of senescence in GSLCs in presence of MSC-CM. (A) Senescence-associated β -galactosidase staining (SA- β -gal) was employed to detect induction of senescence in NCH421k, NCH644, NIB26 and NIB50 cells after presence of UC-CM and BM-CM for 72 h. Data shown are mean \pm SD of three independent experiments. * $p < 0.05$, ** $p < 0.01$, *** $p < 0.001$. (B) Spheroids of NCH421k, NCH644, NIB26 and NIB50 were cultured in presence of UC-CM and BM-CM for 72 h, dissociated to single cells and fixed. The SA- β -gal activity of cells at suboptimal pH 6 was used to detect senescent cells. Representative pictures of three independent experiments are given. Scale bar: 20 μ m.

To reveal the background of senescence signaling in NCH421k cells exposed to both types of MSC-CM a qRT-PCR analysis using Senescence RT² Profiler PCR Array was performed. The PCR arrays revealed changed expression of 13 genes involved in senescence (*ATM*, *CDKN1A*, *CDKN2A*), cell adhesion (*CD44*, *COL1A1*), oxidative stress (*PRKCD*, *NOX4*), IGF related pathway (*IGFBP3*, *IGFBP5*), p53/pRb signaling (*MORC3*, *CITED2*) and cytoskeleton formation (*FNI*, *SERPINE1*) (Table 9). Those genes were consistently up- and downregulated in exposed NCH421k cells at least 2.1 fold.

Table 9: List of de-regulated genes in NCH421k cells exposed to either UC-CM or BM-CM relative to NBE exposed NCH421k cells. Fold increase in mRNA levels are calculated as described in Material and methods. The mean ± SD of three independent experiments are provided. *p<0.05. Fc, fold change.

Gene Symbol	NCH421k+UC-CM		NCH421k+BM-CM		pathway/process
	Fc	p-value	Fc	p-value	
<i>ATM</i>	2.6	0.032*	-1.2	0.406	senescence
<i>CD44</i>	2.7	0.022*	1.4	0.241	cell adhesion
<i>COL1A1</i>	7.5	0.043*	1.5	0.210	cell adhesion
<i>MORC3</i>	2.1	0.046*	-1.1	0.606	p53/pRb signaling
<i>NOX4</i>	2.1	0.045*	1.8	0.163	oxidative stress
<i>CDKN1A</i>	3.0	0.054*	6.9	0.001*	senescence
<i>IGFBP5</i>	1.5	0.343	30.1	0.017*	IGF related
<i>SERPINE1</i>	4.1	0.172	3.8	0.010*	cytoskeleton
<i>IGFBP3</i>	-2.1	0.009*	2.0	0.048*	IGF related
<i>CDKN2A</i>	1.3	0.311	-2.1	0.022*	senescence
<i>CITED2</i>	-1.4	0.101	-2.8	0.034*	p53/pRb signaling
<i>FNI</i>	2.1	0.082	-2.4	0.012*	cytoskeleton
<i>PRKCD</i>	-1.4	0.294	-2.2	0.016*	oxidative stress

Pathway analysis in GO and KEGG pathway identified the involvement of five genes, *SERPINE1*, *CDKN1A*, *IGFBP3*, *CDKN2A* and *ATM* in the p53 pathway (Table 10) and induced in senescence.

Table 10: KEGG pathway analysis of de-regulated genes in NCH421k cells as detected with Senescence RT² Profiler PCR Array. Differentially expressed genes in NCH421k cells exposed to of both types MSC-CM (Table 10) were subjected to ontology enrichment analysis in KEGG to detect their involvement in cellular pathways. Biomolecular identification number (Biomolecule Ids) corresponds to ENSEMBL gene description (<http://www.ensembl.org>); *p*-value (<0.01); *p*-FDR (false discovery rate, <0.01).

KEGG term	<i>p</i> -value	<i>p</i> -FDR	Biomolecule Ids	Gene name
p53 signaling pathway	1.17E-11	4.34E-10	ENSG00000106366	<i>SERPINE1</i>
			ENSG00000124762	<i>CDKN1A</i>
			ENSG00000146674	<i>IGFBP3</i>
			ENSG00000147889	<i>CDKN2A</i>
			ENSG00000149311	<i>ATM</i>

To validate the PCR Array data, a qRT-PCR analysis on independently gathered NCH421k cells' mRNA samples assessing *CDKN1A* expression confirmed a significant increase of *CDKN1A* gene expression in NCH421k cells grown in UC-CM (1.4-fold) and BM-CM (6.7-fold) (Fig. 35A). Likewise, the *CDKN1A* expression increased in NCH644 (3.2-fold) and NIB50 cells (5.0-fold) exposed to BM-CM (Fig. 35A). The expression of *CDKN2A* gene was decreased for 1.7 fold in NCH421k cells exposed to BM-CM (Fig. 35B). On contrary, an increased expression of *CDKN2A* was observed in NCH644 (3.4-fold) and NIB50 (1.9-fold) exposed to BM-CM (Fig. 4C), whereas in NIB26 cells an increased expression of *CDKN2A* was detected upon exposure to both types of CM's, UC-CM (7.7-fold) and BM-CM (5.7-fold) (Fig. 35B).

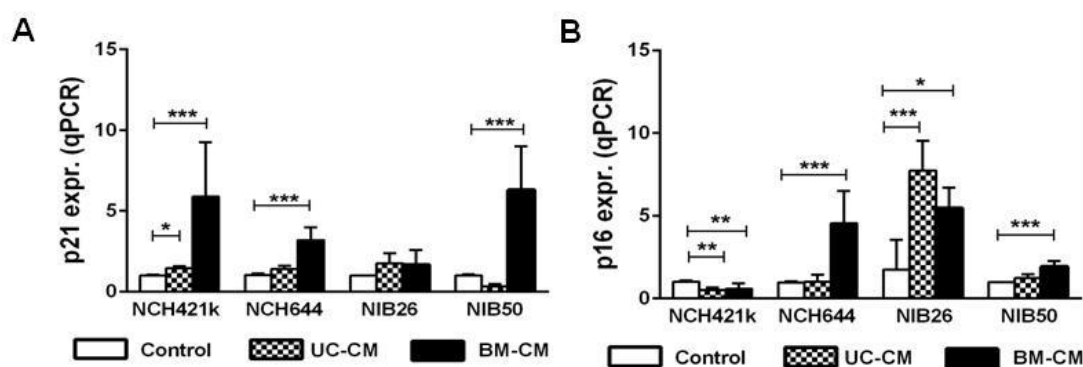


Figure 35: *p21* and *p16* gene expression in GSLCs exposed to MSC-CM. qRT-PCR analysis of (A) *p21* expression and (B) *p16* expression after 72 h treatment with both types of MSC-CM in NCH421k, NCH644, NIB26 and NIB50 cells. Data shown are mean \pm SD of three independent experiments. **p*<0.05, ***p*<0.01, ****p*<0.001.

Alltogether, the results of increased expression of *CDKN1A* and *CDKN2A* in GSLCs are consistent with the observed β -galactosidase staining (Fig. 34), implying on the ability of the MSC paracrine factors to induce GSLC growth arrest and senescence.

4.3.7. MSC-CM influence on stemness and differentiation marker expression in GSLCs

To evaluate the impact of MSC-CM on the stemness of GSLCs, the expression of indicative GSLC marker CD133/prominin was examined by qRT-PCR. An increased *CD133* gene expression was observed in NCH421k cells (1.8-fold and 2.5 fold) and NIB26 cells (3.0-fold), whereas in NCH644 cells a decreased *CD133* gene expression (2.3-fold and 3.9-fold) was noticed after 72 h of exposure to UC-CM and BM-CM, respectively (Fig. 36A). FACS analysis of CD133 glycosylated epitope (CD133/2) revealed a decrease in NCH644 cells exposed to UC-CM (59.5 %) and to BM-CM (61.3 %) for 72 h (Fig. 36B). On contrary, in NCH421k cells exposed to both types of MSC-CM for 72 h, FACS analysis failed to demonstrate changes in CD133 antigen expression. Also, a prolonged culture of NCH421k cells in MSC-CM for 7 days had no impact on their CD133 antigen expression (Fig. 36B).

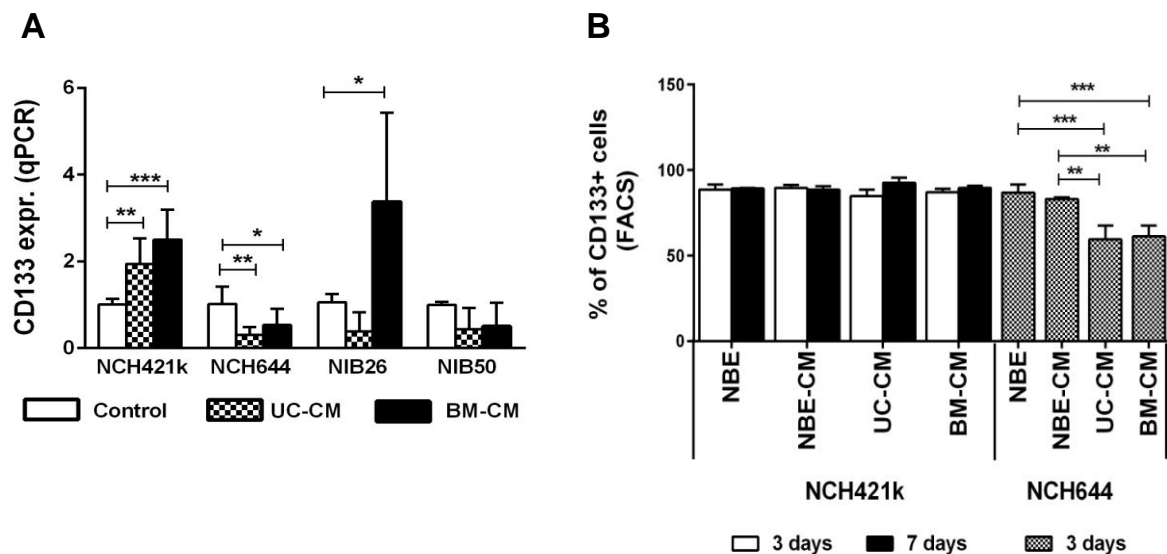


Figure 36: MSC-CM influence on CD133 expression in GSLCs. (A) Analysis of *CD133* expression by qRT-PCR after 72 h treatment with both types of MSC-CM was evaluated in all GSLCs. (B) Determination of CD133 protein expression by FACS after exposure to UC-CM and BM-CM in NCH421k for 3 and 7 days and in NCH644 for 3 days. The mean \pm SD of three independent experiments are provided. * $p < 0.05$, ** $p < 0.01$, *** $p < 0.001$.

Beside CD133 expression, we investigated also the MSC-CM impact on the expression of other markers associated with stemness of GSLCs, such as *Sox-2*, *Notch-1* and *Nestin*. The qRT-PCR analyses revealed decreased expression of *Sox-2* in NCH421k (1.5-fold, 1.8-fold), NCH644 (2.0-fold, 1.1-fold), NIB26 (6.3-fold, 4.3-fold) and NIB50 cells (5.1-fold, 5.2-fold) exposed to UC-CM and BM-CM, respectively (Fig. 37A). Likewise, a decreased expression of *Notch-1* was noted in NCH644 (1.7-fold, 1.1-fold), NIB26 (3.9-fold, 2.9-fold) and NIB50 cells (2.3-fold, 1.7-fold) when exposed to UC-CM and BM-CM, respectively (Fig. 37B). Yet, no change in *Notch-1* expression was observed in NCH421k cells exposed to either type of MSC-CM (Fig. 37B). Also *Nestin* expression did not change in NCH421k cells exposed to any MSC-CM, whereas it increased in NCH644 cells exposed to BM-CM (2.9-fold). Contrarily, *Nestin* decreased in NIB26 (3.0-fold and 3.3-fold) and NIB50 cells (7.2-fold and 7.6-fold) exposed to UC-CM and BM-CM, respectively (Fig. 37C).

Interestingly, the expression of the differentiation markers was severely affected in GSLCs upon exposure to both types of MSC-CM. Namely, the expression of glial cell markers the *vimentin* and *GFAP* increased in MSC-CM cultured GSLCs. The neuronal marker *beta III tubulin* decreased in NCH421k cells (1.6-fold and 2.5-fold) exposed to UC-CM and BM-CM, respectively and in NIB26 cells (2.2-fold) exposed to UC-CM only, whereas it increased in NCH644 cells exposed to UC-CM (2.6-fold) and BM-CM (5.2-fold) (Fig. 37D). *Vimentin* expression increased in NCH421k cells (1.4-fold, 1.6-fold), NCH644 cells (2.0-fold, 2.6-fold) and NIB50 cells (10.2-fold, 9.5-fold), when exposed to UC-CM and BM-CM, respectively (Fig. 37E). The *GFAP* expression increased in NCH421k cells (36-fold, 164-fold), NCH644 cells (2265-fold, 6909-fold) and NIB50 cells (14-fold, 416-fold), when exposed to UC-CM and BM-CM, respectively (Fig. 37F), whereas in NIB26 cells the *GFAP* gene expression was under detection level.

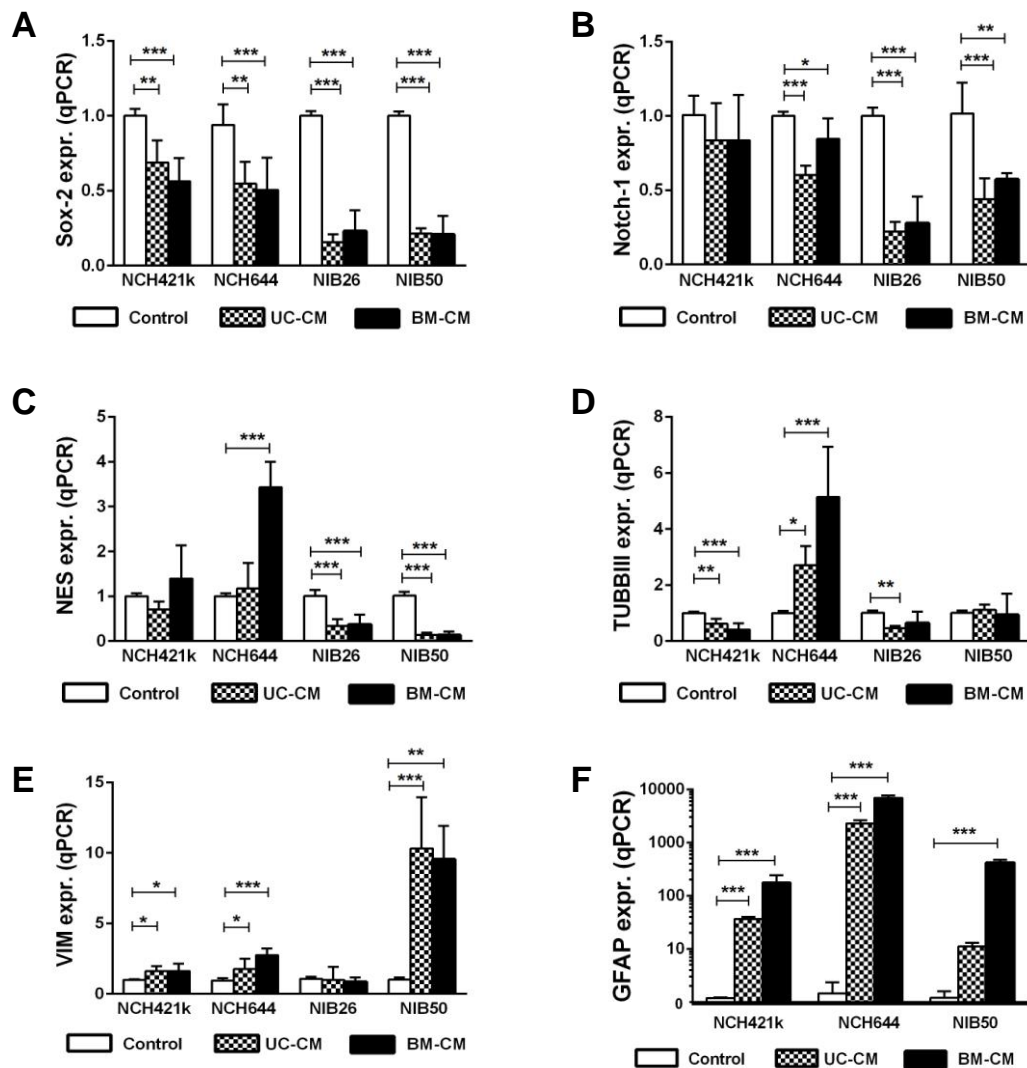


Figure 37: MSC-CM influence on stemness and glial differentiation markers expression. NCH421k, NCH644, NIB26 and NIB50 cells exposed to both types of MSC-CM for 72 h were analyzed using qRT-PCR for GSLCs markers expression (A) *Sox-2*, (B) *Notch-1*, (C) *Nestin*, marker of differentiated neural cells (D) *beta III tubulin*, markers of glial astrocyte cells (E) *vimentin* and (F) *GFAP*. The mean \pm SD of three independent experiments are provided. * $p < 0.05$, ** $p < 0.01$, *** $p < 0.001$.

This data implies on the shift in differentiation potential of GSLCs towards the glial phenotype possibly induced by the MSC's conditioned media.

4.3.8. MSC-CM impact on chemoresistance of NCH421k and NCH644 cells

GSLCs are known for their high resistance towards chemotherapeutics compared to more differentiated tumor cells (Liu et al., 2006). Based on the observed inhibitory effect of MSC-CM on GSLC's cell cycle and their tendency to differentiate, we hypothesized on MSC-CM impairing the resistance of GSLCs. Therefore, the NCH421k and NCH644 cells were exposed to chemotherapeutic agents TMZ and 5-FU in presence of MSC-CM.

Indeed, the viability of NCH421k and NCH644 cells simultaneously treated for 48 h with TMZ and both types of MSC-CM decreased compared to NCH421k or NCH644 cells exposed only to TMZ. For the NCH421k cells we observed a significant decrease upon joint exposure of 2.5 μ M TMZ and UC-CM (20.3 %), as also upon joint exposure of either 2.5. or 1 mM TMZ with BM-CM (10.6 % and 10.4 %, respectively) (Fig. 38A). The viability of NCH644 cells decreased after simultaneous treatment with either 500 μ M or 1 mM TMZ and UC-CM (10.7 % and 18.6 % respectively). Moreover, a 17.7 % decrease of NCH644 cells viability was detected after simultaneous treatment with 1 mM TMZ and BM-CM (Fig. 38A), when compared to TMZ treated cells only.

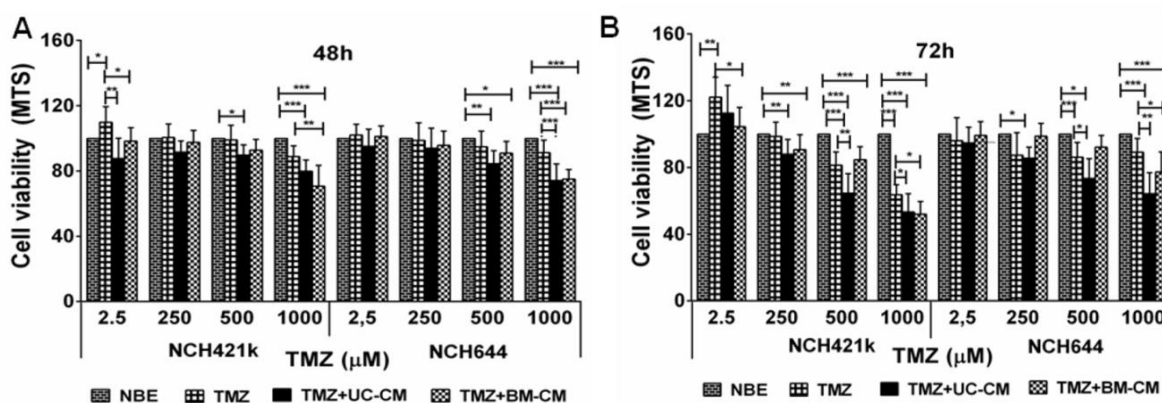


Figure 38: MSC-CM influence on NCH421k and NCH644 resistance upon exposure to TMZ. Viability of NCH421k and NCH644 cells incubated in TMZ and both types of MSC-CM for (A) 48 h and (B) 72 h was determined by MTS assay. The mean \pm SD of three independent experiments are provided. *p<0.05, **p<0.01, *** p<0.001.

The viability of NCH421k cells after simultaneous exposure to 1mM TMZ and MSC-CM for 72 h resulted in their decreased viability in UC-CM and BM-CM presence (16.2 % and 18.2 % respectively) compared to TMZ treated cells only (Fig. 38B). Likewise, the decreased viability of NCH644 cells was observed upon joint exposure to 1 mM TMZ and MSC-CM, with 27.9 % and 18.5 % decrease for UC-CM and BM-CM, respectively (Fig. 38B).

A simultaneous treatment of NCH421k and NCH644 with 5-FU (1 μ M, 50 μ M, 150 μ M) and BM-CM for 48 h, resulted in mean 10.0 % (NCH421k) and 18.4 % (NCH644) decreased viability, compared to 5-FU treated cells only (Fig. 39A). Moreover, a decreased viability of NCH644 cells was detected after simultaneous exposure to BM-CM with 1 μ M (9.5 %) and 150 μ M (15.4 %) 5-FU, compared to 5-FU treated cells only (Fig. 39A).

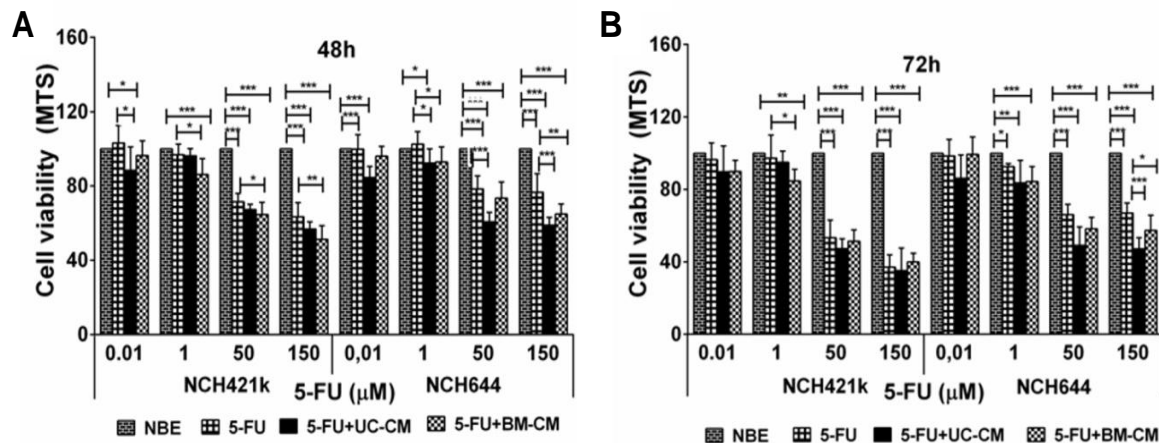


Figure 39: MSC-CM influence on NCH421k and NCH644 resistance upon exposure to 5-FU. Influence of 5-FU and MSC-CM of both types on viability of NCH421k and NCH644 cells was evaluated using MTS assay after incubation for (A) 48 h and (B) 72 h. The mean \pm SD of three independent experiments are provided. *p<0.05, **p<0.01, *** p<0.001.

A 72 h simultaneous treatment of NCH421k cells with 1 μ M 5-FU and BM-CM revealed a decrease of their viability for 13.1 %, when compared to only 5-FU exposed cells (Fig. 39B). The NCH644 cell survival after 72 h was reduced after simultaneous exposure of 150 μ M 5-FU with UC-CM and BM-CM (27.9 % and 14.5 % respectively) (Fig. 6D), when compared to TMZ treated cells only (Fig. 39B).

To conclude, these results imply on the ability of MSC paracrine signals to reduce the GSLCs chemoresistance, to two very different DNA damaging agents, the TMZ and 5-FU.

4.4. INDIRECT CO-CULTURES OF NCH421k CELLS WITH BM-MSCs AND UC-MSCs

Investigation of the MSC conditioned media one-way paracrine signalling revealed an anti-tumor effect on GSLC lines resulting in the onset of senescence, reduced stemness profile and lower cytostatic resistance threshold. In light of these results, we also evaluated MSC paracrine effect on GSLCs upon two-way paracrine signalling, in indirect co-culture system.

4.4.1. MSC influence on proliferation of NCH421k cells

Proliferation of the NCH421k cells indirectly co-cultured with UC-MSCs and BM-MSCs for 72 h was determined with immunostaining of Ki67 protein. It revealed a 19.3 % proliferation index decrease in NCH421k cells when indirectly co-cultured with UC-MSCs (Fig. 40A). This was further confirmed with 1.7-fold decrease of *CCND1* expression of NCH421k cell's upon indirect contact with UC-MSCs (Fig. 40B).

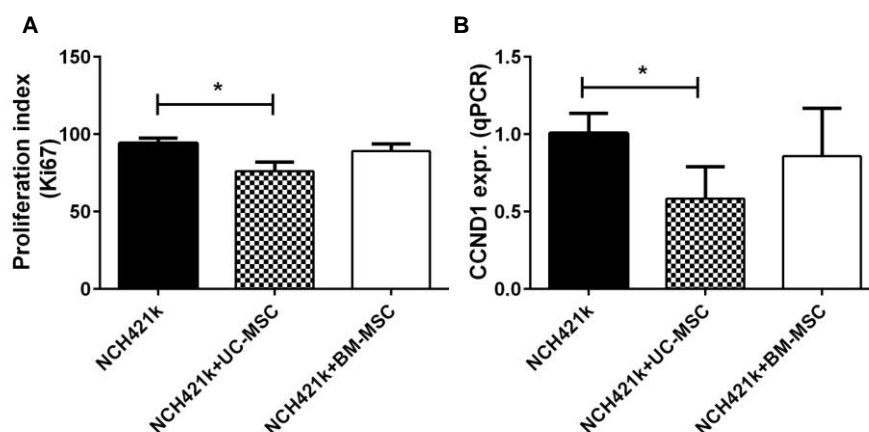


Figure 40: Proliferation of NCH421k cells co-cultured with MSCs. NCH421k cells were indirectly co-cultured with UC-MSC and BM-MSC for 72 h. (A) Proliferation potential of NCH421k cells assessed with Ki-67 immunostaining decreased in co-culture with UC-MSCs. (B) *CyclinD1* (*CCND1*) expression (qRT-PCR) was decreased in presence of UC-MSCs. The mean \pm SD of three independent experiments are provided. * $p < 0.05$.

4.4.2. MSC influence on activation of senescence in NCH421k cells

Based on findings of senescence onset in the GSLCs exposed to MSC-CM we investigated whether the same effect can be confirmed upon indirect co-culturing of NCH421k and both types of MSCs for 72 h. qRT-PCR analysis of *p21* expression revealed a 10.6-fold and 11.0-fold increase in NCH421k cells co-cultured with UC-MSCs and BM-MSCs, respectively (Fig. 41A). On contrary, *p16* expression was found unaffected in the same culture conditions (Fig. 41B).

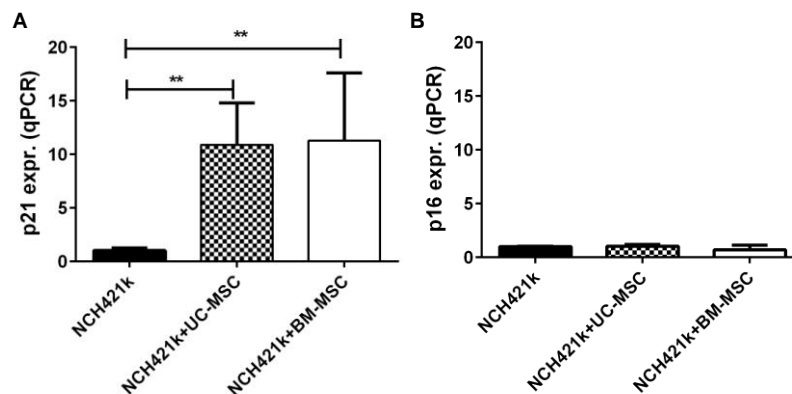


Figure 41: Analysis of genes associated with senescence in NCH421k cells indirectly co-cultured with UC-MSCs and BM-MSCs. NCH421k and both types of MSCs were co-cultured for 72 h, respectively. QRT-PCR analysis revealed upregulation of *p21* gene expression (A) while *p16* gene expression was found unaffected (B). The mean \pm SD of three independent experiments are provided. ** $p < 0.01$.

This result's implies on the same mode of paracrine action of MSCs on GSLCs as similar observations in *p21* expression in NCH421k cells was detected after exposure to MSC-CM or upon indirect co-culturing with UC-MSCs and BM-MSCs.

4.4.3. MSC influence on onset of apoptosis in NCH421k cells

Although MSC conditioned medium failed to activate the process of apoptosis in NCH421k cells we decided to test whether the MSCs can trigger apoptosis in these cells upon indirect co-culture. Again a qRT-PCR analysis showed that the ratio of *bax/bcl-2* gene expression was found unaffected, indicating on failure of apoptosis onset in NCH421k cells upon indirect co-culture with UC-MSCs or BM-MSCs for 72 h, respectively (Fig. 42).

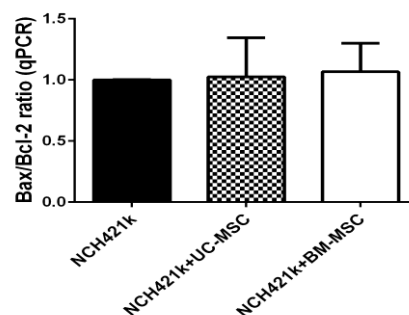


Figure 42: Apoptosis in NCH421k cells indirectly co-cultured with UC-MSCs and BM-MSCs. NCH421k cells were co-cultured with both types of MSCs for 72 h. QRT-PCR analysis of *bax* and *bcl-2* gene expression was performed. The ratio of *bax/bcl-2* was unaffected. The mean \pm SD of three independent experiments are provided.

4.4.4. Influence of MSCs on stemness and differentiation markers expression in NCH421k cells

Regarding the fact that MSC conditioned media affected the GSLCs stemness marker expression, pointing of initiation of differentiation of GSLCs, we decided to investigate NCH421k stemness marker expression upon indirect co-culturing with both types of MSCs for 72 h. Interestingly, a 3.4-fold decrease of *CD133* gene expression was detected when NCH421k cells were co-cultured in presence of UC-MSCs (Fig. 43A). Yet, FACS analysis failed to confirm any change in CD133 expression in NCH421k indirectly co-cultured with either type of MSCs (Fig. 43B).

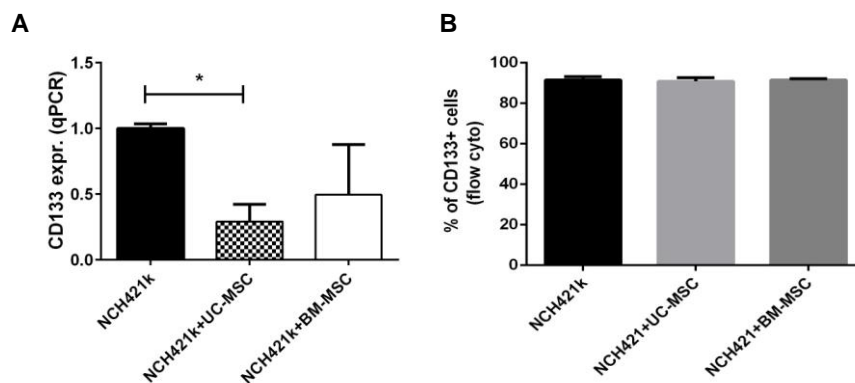


Figure 43: Analysis of CD133 expression of NCH421k cells indirectly co-cultured with UC-MSCs and BM-MSCs. NCH421k cells were co-cultured with both types of MSCs for 72 h. (A) *CD133* expression (qRT-PCR) was decreased in presence of UC-MSCs. (B) FACS analysis failed to prove any change in *CD133* expression upon indirect co-culturing. The mean \pm SD of three independent experiments are provided. * $p < 0.05$.

Further on we investigated the expression of *Sox-2*, *Notch-1* and *nestin* stemness markers in GSLCs upon co-cultivation with UC-MSCs and BM-MSCs. Indeed, the qRT-PCR analysis revealed a 1.6-fold and 1.2-fold decreased expression of *Sox-2* in GSLCs co-cultured with UC-MSC and BM-MSC, respectively (Fig. 44A). On contrary, expression of *nestin* was increased in GSLCs exposed to UC-MSC (0.6-fold) and BM-MSC (0.5-fold) (Fig. 44B). MSCs of either source failed to affect *Notch-1* expression when indirectly co-cultured with NCH421k (Fig. 44C).

However, the expression of differentiation markers, *β III tubulin*, *vimentin* and *GFAP* in NCH421k increased upon co-culturing with both types of MSCs. In detail, expression of *β III tubulin* increased 0.8-fold and 0.7-fold (Fig. 44D), *vimentin* increased 2.8-fold and 2.1-fold (Fig. 44E) and *GFAP* increased 26.1-fold and 28.1-fold (Fig. 44F) in NCH421k co-cultured with UC-MSCs and BM-MSCs, respectively.

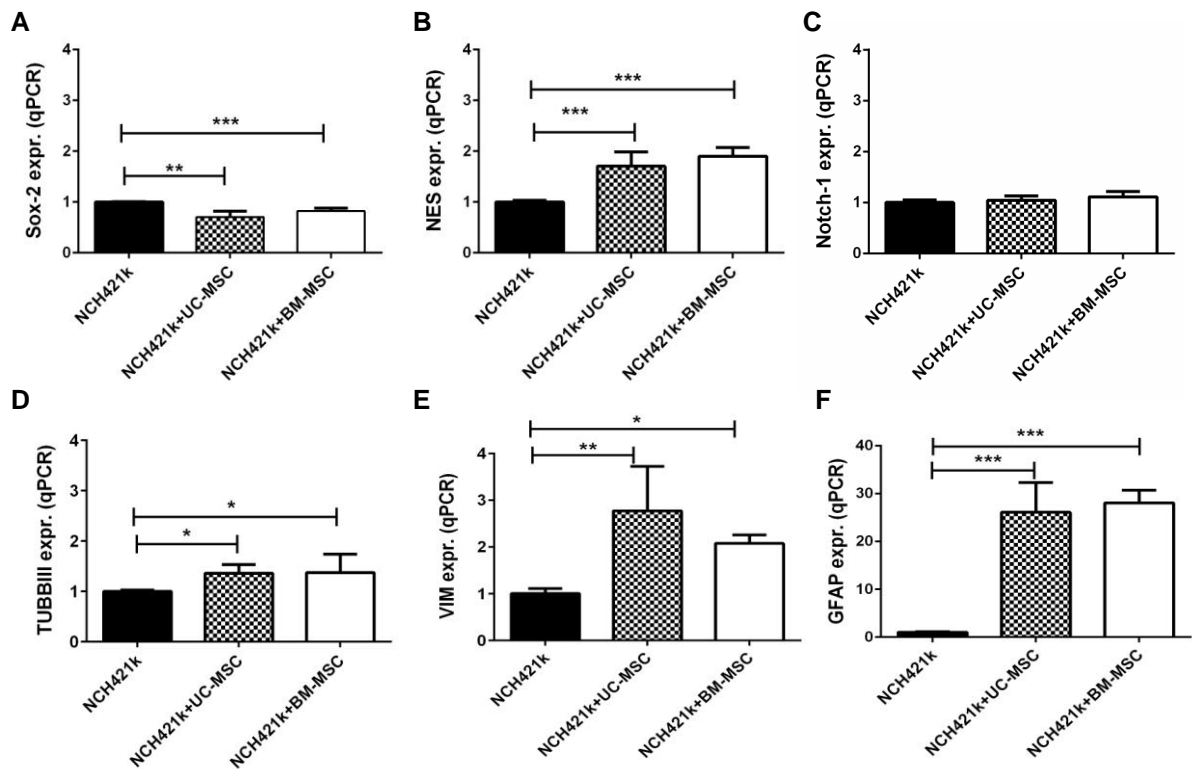


Figure 44: Analysis of stemness markers in NCH421k cells indirectly co-cultured with UC-MSCs and BM-MSCs. The qRT-PCR analysis after 72 h co-culturing of with both types of MSCs and NCH421k cells for GSLCs markers expression (A) *Sox-2*, (B) *Nestin*, (C) *Notch-1*, marker of differentiated neural cells (D) *beta III tubulin*, markers of glial astrocyte cells (E) *vimentin* and (F) *GFAP*. The mean \pm SD of three independent experiments are provided. * $p < 0.05$, ** $p < 0.01$, *** $p < 0.001$.

To conclude, *via* two-way paracrine signaling of UC-MSCs and BM-MSCs with NCH421k cells we observed the shift of GSLCs to more differentiated phenotype similar to observed upon one-way paracrine signaling upon exposure of NCH421k cells to UC-MSCs and BM-MSCs conditioned medium.

5. DISCUSSION AND CONCLUSIONS

5.1. DISCUSSION

5.1.1. Influence of adipose tissue harvesting-site on characteristics of isolated MSCs

MSCs have emerged as a promising therapeutic tool for cell-based therapies of various diseases (Heatman et al., 2015). In general, strategies for therapeutic application of MSCs can be divided into tissue engineering approaches using differentiated MSCs, and regenerative medicine approaches based on the paracrine effects of undifferentiated cells or direct cell-to-cell interactions (Caplan et al., 2007). Various adult and foetal tissues that contain MSCs have been identified (Hass et al., 2011). Among these, adipose tissue has been recognized as a valuable source for MSC isolation, due to its relatively good accessibility over a lifespan and the lower ethical burden (Wegmeyer et al., 2013). AT-MSCs can be isolated very efficiently from lipoaspirates or from small pieces of adipose biopsies (Zuk et al., 2001; Buschmann et al., 2013). As several anatomical locations have been identified as sources of AT-MSCs, here we investigated the influence of the anatomical location of the tissue-harvesting site on AT-MSC quality for clinical applications, which were characterised as cell proliferation, replicative senescence and differentiation. The first objective of this dissertation was to compare the three most-common sites of adipose tissue harvesting to offer surgeons and clinicians more informative protocols on AT-MSCs source for particular applications.

The most commonly used techniques to obtain adipose tissue for AT-MSC isolation are liposuction and tissue biopsies (Dubois et al., 2008). The yield of the AT-MSCs was found to be comparable between these two harvesting techniques (Buschmann et al., 2013, Iyyanki et al., 2015). Our data demonstrate that sufficient AT-MSCs can be isolated from relatively small amounts of adipose tissue i.e. 2 ml biopsies.

Three anatomical harvest sites for AT-MSC extraction were selected here: thighs, hips and abdomen. With regard to the adipose tissue-harvesting site, the highest number of AT-MSCs was obtained from the thigh adipose pads, compared to the hip and abdomen adipose pads, although only seven donors were included in the study. In contrast, the anatomical location of the harvesting site has been reported to have no influence on AT-MSC yields by Buschmann et al., (2013) and Choudhery et al. (2015). Thus, our observation on the highest number of AT-MSCs from the thighs needs to be upgraded with a higher number of AT-MSC samples.

The isolated AT-MSCs were highly proliferative and, their cumulative population doubling levels were comparable across all of the anatomical harvesting sites. This is in agreement with previously published data by Jurgens et al. (2008) on similar growth kinetics from the

abdomen and hip/thigh adipose tissues derived AT-MSCs. Similar observations were reported by Schipper et al. (2008) and Choudhery et al. (2015), when they tested AT-MSCs from different anatomical locations for maximal population doublings.

However, we did note an increased number of senescent cells among the AT-MSCs harvested from the different anatomical locations. There were increased numbers of senescent cells at early (passage 6) and middle (passage 12) passages for AT-MSCs derived from hips, compared to AT-MSCs derived from thighs and abdomen. Our data thus imply on different growth characteristics of these AT-MSCs in terms of the anatomical location of the harvest site. In general, *in-vitro* cultured MSCs have a limited lifespan, and they enter into replicative senescence after a certain number of cell divisions (Wagner et al., 2008). A comparison of *in-vitro* proliferation of MSCs from different tissues before undergoing senescence revealed that UC-MSCs can be cultured for the longest time, followed by AT-MSCs and BM-MSCs (Kern et al., 2006). The susceptibility of MSC lines to early senescence should be carefully monitored before any clinical applications, as the therapeutic potential of the MSCs can be significantly impaired due to their decreased migration potential and immunoregulatory functions, as demonstrated by Sepulveda et al. (2014). Moreover, senescent UC-MSCs seem to alter their characteristic effects when in co-cultures with other cells, as these were shown to promote proliferation and migration of cancer breast cells *in-vitro* and also in a mouse xenograft model (Di et al., 2014). Hence, as senescent cells produce various cytokines, chemokines and growth factors, known as the senescence-associated secretory phenotype (Sabin and Anderson, 2011), senescent MSCs can lose the therapeutic efficiency of MSCs. Indeed, the secretome analysis of senescent BM-MSCs revealed that a subset of proteins that are involved in extracellular matrix remodelling and the IGF signalling pathway are differentially expressed compared to non-senescent cells (Severino et al., 2013). Thus, our observations here are of the outmost importance, as they suggest that cell proliferation data should be supplemented with the information on the disposition towards senescence of AT-MSCs, as a parameter of the cell quality.

The differentiation of isolated AT-MSCs into adipocytes, osteocytes and chondrocytes was dependent on their harvesting site as the thigh-derived AT-MSCs showed more osteogenic and chondrogenic differentiation, but not adipogenic differentiation, compared to the hip and abdomen AT-MSCs. On the contrary, Choudhery et al. (2015) reported comparable differentiation into osteocytes and chondrocytes of AT-MSCs extracted from various anatomical locations. The observed discrepancy might result from applying different adipose tissue removal techniques and AT-MSC isolation techniques, or from the low number of samples included in the present study.

Although previous studies have shown a decrease in MSC quality with donor age (Schipper et al., 2008, Choudhery et al., 2014), our data show no differences in cell proliferation and differentiation of the AT-MSCs in spite of the wide age range of the donors (12-71 years). This is in agreement with some previous studies reporting on the absence of effect of donor age on proliferation and differentiation of AT-MSCs (Ding et al., 2014, Buschmann et al., 2013). The discrepancies that can be observed might result from different isolation techniques, culture media and cell culture techniques. However, for more detailed conclusions, this needs to be confirmed in larger AT-MSC populations from these different anatomical locations, due to the low number of donors ($n = 7$) involved in this study.

In conclusion, with respect to the first objective of possible correlations between the harvest sites and the AT-MSC characteristics, we conclude that there are no relationships between AT-MSC harvesting site and proliferation rate in cultured AT-MSCs, and that this was also independent of the donor age, which was a relatively surprising observation. In contrast to this, the onset of replicative senescence was significantly earlier during cultivation of hip-derived AT-MSCs, which would thus not be recommended if these cells are to be expanded *in vitro* over several passages before their application. This observation is of particular importance, as it suggests that the proliferation data should be supplemented with the information on the disposition towards senescence of AT-MSCs to indicate the cell quality. Moreover, a preference towards osteogenic and chondrogenic differentiation was seen for thigh-derived AT-MSCs, although we suggest larger population studies to confirm this.

5.1.2. Expansion of AT-MSCs microcarrier-based spinner system

5.1.2.1. Optimization of AT-MSC seeding efficiency on microcarriers

For particular and successful applications, MSCs need to be propagated *in vitro* to provide sufficient cell numbers that retain their proliferative and differentiation potential. This is a challenging task, as the classical MSC expansion using culture flasks (T-flasks) is limited in terms of cell growth rate during long cultivation, i.e., over multiple passages, where the cells can be exposed to infection and contamination, and might also lose their quality. The number of *in-vitro* passages is limited and although MSCs have many of the stemness characteristics, they undergo replicative senescence (Wagner et al., 2008). Microcarrier-based spinner systems offer the opportunity to expand MSCs in a rapid, controllable, and cost-effective manner (Frauensuh et al., 2007; Schop et al., 2010). The expansion of MSCs on microcarriers in a spinner system is challenging, as the optimal MSC attachment and culture conditions need to be well defined to obtain large quantities of good quality MSCs. Optimising such conditions was the second objective in the present dissertation.

Bioreactor systems have emerged as a promising technology for cell expansion using microcarriers to immobilise and cultivate these adherent cells under stirring conditions. The basic requirement for cell proliferation on microcarriers is a homogenous cell distribution over the microcarrier surface (Chen et al., 2013). The microscopy observations of the cell attachment to these microcarriers suggests that at least 4 h are enough to ensure maximal attachment, although the cells then need at least 1 day to adapt to these new culture conditions, to grow and divide (Hewitt et al., 2011). In our hands, approximately 50 % of the AT-MSCs adhered after 24 h on Cytodex-1 and Cytodex-3 microcarriers, which is in agreement with some previous studies (Schop et al., 2010, Hupfeld et al., 2014). The cell growth conditions are also an important issue to discuss. Although Schop (2010) also reported inhibiting effects of higher serum concentrations on initial seeding rates, we could not confirm this. Moreover, Frauenschuh (2007) reported 80 % and 50 % adherence of porcine BM-MSCs after 3 h of incubation with Cytodex-1 and Cytodex-3 microcarriers, respectively. Similarly, nearly complete seeding efficiencies of human foetal MSCs were reported for only 1 day of incubation on Cytodex-3 microcarriers (Goh et al., 2013).

The second parameter that influenced the initial cell attachment was the stirring rate, and we found higher AT-MSC seeding efficiencies upon intermittent agitation, compared to under static conditions. This can be attributed to a greater availability of microcarriers surface for cell attachment. Similar was observed by Hewitt et al. (2011), who reported on non-uniformly attached MSCs on microcarriers and the abundant presence of unpopulated microcarriers when static conditions were used. Moreover, we also believe that this is related to the ability of MSCs derived from various tissue sources to secrete various different endogenous extracellular matrices, which results in different actin organisation, thus affecting MSC adhesion and expansion on different types of microcarriers (Sart et al., 2013).

5.1.2.2. Optimization of AT-MSC expansion on microcarriers in spinner flasks

After we defined the initial AT-MSC seeding conditions, we optimised the parameters that can influence the growth of AT-MSCs on these microcarriers. Interestingly, although pre-incubation of both Cytodex-1 and Cytodex-3 with various serum concentrations (i.e., 20 %, 100 %) had no influence on the initial seeding efficiencies, it affected the final AT-MSC numbers after 10 days of cultivation. Namely, pre-coating of either of these types of microcarriers with pure serum resulted in lower AT-MSC densities at the end of the culture process. This might be due to the presence of various proteins in serum that can change the surface characteristics of the microcarriers that led to inhibition of AT-MSC proliferation. However, despite initially lower numbers of attached AT-MSCs under static conditions in the first 24 h of culturing, compared to an intermittent agitation regime, no differences in AT-MSC density were observed later than the third day. Interestingly, the high cell seeding

efficiency was reported to have either a deleterious or neutral effect on MSC expansion on microcarriers (Hewitt et al., 2011). Taken together the number of adhered cells was thus sufficient for further AT-MSC growth on Cytodex-1 and Cytodex-3, and high numbers of attached MSCs on microcarriers does not necessarily lead to more successful expansion of these MSCs.

For successful AT-MSC expansion on microcarriers, a suitable feeding regime must be provided to ensure optimal sufficient nutrient supply and removal of growth inhibitory metabolic products. Our results show that a 50 % medium change every 2 days can support the optimal AT-MSC growth on Cytodex-1 and Cytodex-3, which is in agreement with observations made by others (Chen et al., 2015). To fully exploit the advantages of cell cultivation on microcarriers, the optimal bead concentration must be used, to gain the highest MSC yield possible per volume of culture medium. Once the MSCs overgrow the microcarrier surface area, they will search for any place left for attachment, which will result in the formation of cell-microcarrier aggregates. However, this can be avoided by addition of fresh microcarriers during the culture process (Ferrari et al., 2012). Our data reveal that the addition of solely fresh microcarriers in the early stages of AT-MSC cultivation (i.e., day 3) can prevent aggregation of Cytodex-3, but not of Cytodex-1 microcarriers. Similarly, human foetal MSCs (Goh et al., 2013) preferred growth on Cytodex-3 over Cytodex-1, as shown by the avoidance of cell-microcarrier aggregate formation and higher cell yields.

5.1.2.3. Differentiation of AT-MSCs after expansion on MCs in spinner flasks

To use the MSCs expanded on microcarriers for any further clinical applications, their differentiation into mesodermal cell types, as adipocytes, chondrocytes and osteocytes, must be retained. In our hands, AT-MSC cultivation on microcarriers caused no changes in their surface marker expression. On the contrary, analysis of AT-MSC differentiation upon cultivation on microcarriers revealed increased AT-MSC osteogenic potential. Similar observations have already been shown for several other types of MSCs, including BM-MSCs (Sun et al., 2010) and foetal-derived MSCs (Goh et al., 2013). Sart et al. (2009) also reported on spontaneous osteogenic differentiation of rat ear MSCs upon cultivation on microcarriers. While the exact mechanism of MSCs increased osteogenic potential upon cultivation on microcarriers is so far unknown, it can be speculated that several factors might have an influence, such as: shear stress in spinner flasks (Sart et al., 2009), gelatine and collagen surfaces of microcarriers (Sart et al., 2009), and the three-dimensional environment, to allow more efficient cell-to-cell communication (Goh et al., 2013).

In conclusion for the second objective, we optimised the culture parameters for initial AT-MSC adhesion and growth on Cytodex-1 and Cytodex-3 microcarriers. The pre-incubation of microcarriers in pure serum failed to improve AT-MSC adhesion, and even resulted in lower

AT-MSC numbers at the end of the culture process. Conversely, despite better initial AT-MSC adhesion to microcarriers upon intermittent agitation, the final AT-MSC numbers achieved were comparable among both the intermittent and static regimes. During expansion of the AT-MSCs on microcarriers, media change every 2 days was found to be optimal for cell growth. Although similar final AT-MSC numbers on both types of microcarriers were achieved, our data show superior suitability of Cytodex-3 over Cytodex-1 for AT-MSCs expansion in spinner flasks, due to reduced formation of cell–microcarrier aggregates upon addition of fresh microcarriers during the cultivation process. Of note, the total cell yields obtained at the end of the culture process were at the higher end of the yields reported in the literature (Chen et al., 2013). Moreover, the differentiation of AT-MSCs upon growth on microcarriers was not affected. In contrast, we observed improved osteogenic differentiation of AT-MSCs expanded on microcarriers. To our knowledge, this is the first report of successful AT-MSC expansion on Cytodex-1 and Cytodex-3 microcarriers.

5.1.3. Paracrine effect of UC-MSCs and BM-MSCs on GSLCs

5.1.3.1. Antiproliferative effects of MSC paracrine signaling

GBM is an incurable disease due to impossible or incomplete tumor resection, and resistance to conventional therapeutic regimes (Krakstad and Chekenya, 2010). Nearly inevitable GBM recurrence also results from the presence of the highly tumorigenic subpopulation of glioma initiating and propagating cells, also known as GSLCs (Visvader et al., 2010). These show the stemness characteristics of normal NSCs in addition to oncogenic properties, such as high resistance to cytotoxic drugs and to radiation (Eyler and Rich, 2008; Liu et al., 2006). Thus these cells represent the key target for the improvement of GBM treatment.

Cell therapy is being revisited with the view of using MSCs for cancer treatments, and the growing evidence shows that MSCs home onto sites of tumorigenesis, where they can inhibit tumor cell growth (Hong et al., 2014). The evident MSC tropism towards GBM (Bago et al., 2013, Bexell et al., 2009) can also be exploited to enhance the antitumor effects of naïve MSCs by modification of the MSCs to carry therapeutic genes, and different approaches have shown promising results. In the study of Martinez-Quintanilla et al. (2013), MSCs engineered to coexpress a prodrug converting enzyme, *Herpes simplex* virus thymidine kinase, and TNF apoptosis-inducing ligand (S-TRAIL) significantly decreased tumor growth of highly aggressive GBM and prolonged survival of mice bearing GBM tumors. Similarly, MSCs loaded with oncolytic *Herpes simplex* virus reduced tumor volumes and prolonged survival of mice (Duebgen et al., 2014). Moreover, MSCs engineered to express the antiangiogenesis

factor endostatin and a pro-drug to activate the enzyme carboxylesterase 2 suppressed tumor initiation and even reduced nestin-positive GSLC populations in tumors (Yin et al., 2011).

Numerous studies have demonstrated the *in vitro* ability of human MSCs to impair the growth of various GBM cell lines (Kleinschmidt et al., 2011; Liang et al., 2014; Motaln et al., 2012; Motaln et al., 2015; Yang et al., 2014). As previous data from our group demonstrated that BM-MSCs can impair the growth of co-cultured GBM cell lines through release of various cytokines (Motaln et al., 2012; reviewed in Tajnšek et al., 2013), the third objective of the dissertation was to investigate the UC-MSC and BM-MSC paracrine effects on GSLCs, in terms of both exposure to the MSC conditioned media, and in indirect co-cultures *in vitro*.

However, to our knowledge there are no data so far that have addressed the influence of MSCs on isolated GSLC cultures. Herein, we used the medium conditioned by UC-MSCs and BM-MSCs, and observed the phenotype changes in the CD133-positive GSLC lines NCH421k, NCH644, NIB50 and NIB26, cultured in defined medium, as described by Capper et al. (2009). These GSLCs expressed the CD133 (Prominin 1) protein and were characterised for the features of GSLCs, as described in Campos et al. (2011) and Capper et al. (2009).

We showed that the exposure of NCH421k cells to UC-MSC and BM-MSC conditioned media resulted in the inhibition of the cell cycle in G0/G1 phase *via* decreased expression of *cyclin D1* in all four of these tested GSLC lines, NCH421k, NCH644, NIB26 and NIB50 cells (Kološa et al., 2015). Similarly, induction of cell-cycle arrest in the G0/G1 phase by the UC-MSC conditioned medium has been shown *in vitro* in the U251 cell line (Yang et al., 2014), as well as in *in-vivo* studies where injected UCB-MSCs were shown to decrease cyclin D1 expression in C6-xenograft-bearing mice (Jiao et al. 2011). We also observed decreased proliferation and decreased expression of the *cyclinD1* gene in NCH421k cells; however, this only occurred with co-cultures with UC-MSCs, and not with BM-MSCs. However, BM-MSCs can decrease cell proliferation of three GBM cell lines (i.e., U87, U251, U373 cells) in indirect co-cultures (Motaln et al., 2012). Similarly, indirectly co-cultured UCB-MSCs reduced the survival of U87 cells (Kang et al., 2008). One explanation for this might be the more rapid growth of UC-MSCs compared to BM-MSCs in the co-cultures with GSCLs, which would result in greater amounts of paracrine factors produced within the defined time.

Several studies have shown the MSC potential to induce apoptosis in glioma cells and xenografts upon indirect interactions and direct cell-to-cell contact (Dasari et al., 2010; Gondi et al., 2010; Jiao et al., 2011), as also by exposure of glioma cells to MSC conditioned medium (Yang et al., 2014). However, here we failed to show that MSC conditioned medium can trigger apoptotic processes in GSLCs, as assayed by AnnexinV/PI staining and *bax/bcl-2* gene expression (Kološa et al., 2015). This might be due to the reportedly higher resistance

of CD133-positive GSLCs to apoptosis, compared to differentiated cancer cells, as they express higher levels of the anti-apoptotic genes that express Bcl-2, Bcl-XL, Flip and IAPs than differentiated CD133-negative GBM cells (Capper et al., 2009; Liu et al., 2006). It is thus likely, that MSC conditioned medium failed to induce apoptosis as these cells did not secrete the pro-apoptotic factors needed to trigger apoptosis in GSLCs, which would possibly require higher concentrations, due to their reportedly higher resistance to apoptosis (Capper et al., 2009; Liu et al., 2006). Moreover, we did not observe onset of apoptosis in NCH421k cells with indirect co-cultures, similar to when the conditioned media were used. As well as the considerations discussed above, it appears that cell-cell interactions are needed for such an event to occur as a result of GSLC-MSC crosstalk, as suggested by Gondi et al. (2010). They demonstrated apoptotic responses in GBM cells only upon direct co-culture with UCB-MSCs. The same was reported by Akimoto et al. (2013) and Dasari et al. (2010), who showed that UCB-MSCs induced apoptosis when co-cultured with U87 and primary GBM cells. However, apoptotic responses were observed in GBM cells co-cultured with AT-MSC and UC-MSC conditioned media (Yang et al., 2014), and therefore this subject remains controversial. As we observed increased senescence of GSLCs upon exposure to MSC conditioned medium (discussed further below), we can explain this in the light of the recent observations that the cell senescence and apoptosis pathways are simultaneously engaged in stress responses to environmental stimuli, and that each cell type ‘decides’ which outcome will occur, as senescence or apoptosis (Childs et al., 2014).

To the best of our knowledge, the data presented here are the first to show an induction of senescence as a ‘preferred’ response of GSLCs to BM-MSC and UC-MSC paracrine effects (Kološa et al., 2015). All of the tested GSLC lines exposed to either of these MSC conditioned media changed morphology, and showed senescence-associated β -galactosidase activity and increased expression of two common senescence-associated genes, the cell-cycle inhibitor and tumor-suppressor genes for p21 and/or p16. In NCH421k cells indirectly co-cultured with UC-MSCs and BM-MSCs, the p21 mRNA levels were also up-regulated. We confirmed the involvement of p21 and p16 in the activation of senescence in NCH421k cells exposed to UC-MSC and BM-MSC conditioned media using Senescence PCR Arrays. The analysis of 84 key genes associated with senescence revealed up-regulation of the *ATM*, *CD44*, *COL1A1* (collagen, type I, alpha 1), *MORC3* (MORC family CW-type zinc finger 3), *NOX4* (NADPH oxidase 4), *CDKN1A* (p21; cyclin-dependent kinase inhibitor 1A), *IGFBP5* (insulin-like growth factor binding protein 5), and *SERPINE1* (serpin peptidase inhibitor, clade E) genes, and down-regulation of the *IGFBP3* (insulin-like growth factor binding protein 3), *CDKN2A* (p16; cyclin-dependent kinase inhibitor 2A), *CITED2* (Cbp/p300-interacting transactivator, with Glu/Asp-rich carboxyterminal domain, 2), *FNI* (fibronectin 1), and *PRKCD* (protein kinase C, delta) genes. To elaborate on the underlying mechanisms, we performed ontology-enrichment analysis in KEGG, and identified the p53 signalling pathway

as the key trigger of senescence induction (Ben-Porath et al., 2006) in NCH421k cells. We further indicated the involvement of the p53 signalling pathway in NCH421k cell senescence activation by MSC conditioned media as the *ATM* and *NOX-4* genes were significantly expressed. ATM most likely induced the p53 signalling pathway, as is known to have a key role in the activation of the DNA damage response programme, which can act via p53, in turn, to up-regulate p21 (*CDKN1A*) (Sabin et al., 2011), and which we showed was up-regulated in GSLCs exposed to MSC conditioned media. Moreover, NOX-4 is known to be involved in the generation of ROS (Weyemi et al., 2012), which has been shown to be triggered by the DNA damage response, and consequently to result in the activation of p21 (Passos et al., 2010). We demonstrated the loss of NCH421k cell mitochondrial membrane potential, which might have resulted from NOX-4-mediated ROS generation that further activated the senescence process. The involvement of ROS production in activation of senescence was also shown by Moiseeva et al. (2006), who reported on sustained exposure of fibroblasts to interferon-(IFN)- β , which resulted in increased ROS production and activation of the DNA damage signalling pathway via ATM kinase, and activation of the p53 pathway. Additional evidence for the p53-dependent senescence pathway in GSLCs is seen with the up-regulation of the *MORC3* gene, which in human osteosarcoma cells was shown to regulate p53 activation and consequently to induce premature senescence (Takahashi et al., 2007). Up-regulation of the *SERPINE1* gene revealed by the qPCR arrays here has also been reported to be a critical downstream target of p53 in the induction of senescence in mouse embryonic fibroblasts (Kortlever et al., 2006), where SERPINE1 was shown to partially protect IGFBP5 from proteolysis (Nam et al., 1997). Similar to that seen for NCH421k cells treated with MSC conditioned media, IGFBP5 was shown to be up-regulated in senescent fibroblasts and endothelial cells (Kim et al., 2007). The mechanisms of the induction of senescence with MSC conditioned media in the other three GSLC lines was not studied in detail, although we confirmed that these cells also express wild-type p53, which implies the same mechanism as that described above.

Taken together, we confirmed the activation of senescence pathways in GSLCs, and speculate that these are possibly induced by MSC secreted factors that can act in a paracrine manner. We observed *cyclin D1* downregulation in all of the GSLC lines. *Cyclin D1* expression represents a critical feature, and preclinical data have shown that an antisense-mediated decrease in cyclin D1 inhibited tumor growth and increased its chemosensitivity (Shapiro et al., 2006). As well as *cyclin D1*, the decrease in the GSLCs observed was associated with alterations to cell-cycle inhibitors (i.e., *p21*) in NCH421k cells, and also *p16* up-regulation in the other three GSLC lines (i.e., NCH644, NIB26, NIB50 cells), which were all p53 positive. These two tumor suppressor genes, *p21* and *p16*, have different roles during the senescence process. The p21 regulates the initial phases of the cell-cycle arrest, and its expression decreases after senescence is achieved (Childs et al., 2014). Conversely, the

expression of p16 is crucial for stabilisation of the senescence process, as this result in permanent cell-cycle arrest in G0/G1 phase in the already senescent cells (Childs et al., 2014). However, these can both activate pRB independently (Childs et al., 2014; Sabin et al., 2011). Thus, we propose the activation of intertwined p53–p21–pRB and p16–pRB tumor suppressor signalling pathways, with prominent roles for the cyclin-dependent kinase inhibitors (CDKIs), p21 and p16 (Kuilman et al., 2010; Sabin et al., 2011), in the mechanism of senescence induction in GSLCs.

5.1.3.2. Paracrine effects of UC-MSCs and BM-MSCs change stemness profile of GSLCs

CD133-positive GSLCs have been associated to increased chemoresistance (Campos et al., 2010; Eyler and Rich et al., 2008; Liu et al., 2006; Ulasov et al., 2011) and linked with high GBM recurrence and poor patient prognosis (Ardebili et al., 2011; Han et al., 2015; Wu et al., 2015). Thus, an alternative avenue for more effective GBM treatment proposes the induction of a more differentiated state of GSLCs, to lead them towards lower resistant to chemotherapy and radiotherapy, although still as malignant GBM cells (Campos et al., 2011).

Here, we examined first the effects of MSC conditioned media on the expression of several GSLC stemness markers including CD133/prominin1 in the cell plasma membrane in GSLCs ((Kološa et al., 2015), as this represent the most used, although not exclusive, GSLC marker (Campos et al., 2010; Denysenko et al., 2010). The data here showed different effects of MSC conditioned media on CD133 expression in GSLCs. In the NCH644 cells, we noted decreased CD133 mRNA and protein expression, in contrast to the NCH421k cell line. In the NIB26 and NIB50 GSLCs, there was also no change in the CD133 mRNA levels. Similar to the exposure to MSC conditioned medium, in the NCH421k cells the expression level of the CD133 protein was not affected in indirect co-cultures with UC-MSCs and BM-MSCs. These differences can be explained by the complexity of CD133 expression, as translation of *CD133* can be initiated from five tissue-restricted promoters that yield several alternatively spliced transcripts, and as the CD133 proteins have eight possible glycosylation sites, which represent a hurdle for the detection of CD133 for the total CD133 protein and mRNA levels, although the heterogeneous origin of these GSLCs might also contribute (Campos et al. 2010; Campos et al. 2011). Other known GSLC stemness markers, such as the *Sox-2* and *Notch-1* genes in GSLCs, were also down-regulated by MSC paracrine activity. SOX-2 is known to be highly expressed in GSLCs, to maintain self-renewal and cellular proliferation (Gangemi et al., 2009), and to sustain the undifferentiated state of GSLCs (Balbous et al., 2014), as well as being a prognostic marker for survival for patients with GBM (Miconi et al., 2015). Notch signalling is also involved in the maintenance of stemness in GSLCs and in the promotion of their proliferation (Alonso et al., 2011; Gangemi et al., 2009; Saito et al., 2013). As inhibition of the Notch pathway results in decreased proliferation and self-renewal of GSLCs (Saito et

al., 2013), and their reduced radio-resistance (Wang et al., 2010), we can speculate that the MSCs affected all of these GSLC characteristics in a paracrine manner also in our tested cell lines. A decrease in *nestin* gene expression was only found in NIB26 and NIB50 GSLCs exposed to both types of MSC conditioned media. These results are not surprising, as Nestin is also present in neural stem/progenitor cells, and presumably GSLC progenitors, and is highly abundant in GBM tumors (Denysenko et al., 2010). High levels of *nestin* expression are associated with poor patient prognosis (Strojnik et al., 2007; Wan et al., 2011). The observed decrease in the GSLC stemness markers upon exposure to MSC conditioned medium was further accompanied by a massive up-regulation of the glial marker vimentin and of the astrocyte marker GFAP. Our study also revealed loosened spheroid structure, spheroid size reduction, and most importantly, a change from spheroid to adherent type of growth, which represents an additional cue towards possible transition to a more differentiated GSLC phenotype.

As with MSC conditioned medium exposure, there was also decreased Sox-2 mRNA expression in NCH421k cells in indirect co-cultures with UC-MSCs and BM-MSCs. The *Notch-1* expression in NCH421k cells was not affected by the co-culturing with both of these types of MSCs, as for their exposure to MSC conditioned media. The only difference in the bilateral paracrine effect was the increased *Nestin* gene expression. However, increased expression of the neuronal marker β -III-tubulin and the markers of astrocyte differentiation GFAP and vimentin were observed, indicating differentiation and reduced stemness of GSLCs.

Taken together, these data suggest that MSC secreted factors can initiate a differentiation process in GSLCs by influencing their processes of stemness maintenance and further shifting the GSLCs towards more differentiated states; i.e., the astrocytic cell lineage.

5.1.3.3. Decreased resistance of GSLCs in presence of MSCs conditioned media

Based on the detected changes in stemness profile of GSLCs induced by MSC conditioned media, we deduced on the reduced chemoresistance of GSLCs in the presence of MSC conditioned media. Indeed, we confirmed that the MSC conditioned media decreased the resistance of the NCH421k and NCH644 cells to TMZ (Kološa et al., 2015), the first-choice chemotherapeutic in the standard therapy for patients with GBM (Carlsson et al., 2014). TMZ is a DNA-alkylating agent that causes DNA damage predominantly by methylating the O6 position of guanine, which eventually induces cell death (Köritzer et al., 2013). However, with GSLCs, TMZ failed to show cytotoxic effects through DNA nicks, due to their active MGMT (Liu et al., 2006), and therefore TMZ can only improve the overall survival of patients with GBM that lacks MGMT expression (Köritzer et al., 2013). Numerous studies

have confirmed this higher resistance of GSLCs compared to GBM cells (Liu et al., 2006; Ulasov et al., 2011). It has been suggested, that cytokines, such as IL-24 (Sart et al., 2014; Yeh et al., 2014), are responsible for sensitising GSLCs, as MSCs indeed commonly secrete this cytokine, which has also been shown to act synergistically with TMZ to override the resistance in melanoma cells (Zheng et al., 2008).

To further examine the influence of MSC conditioned media on the resistance of GSLCs to other chemotherapeutics, we exposed them to 5-fluoro-uracil (5-FU) simultaneously with MSC conditioned media, and noted decreased survival of both NCH421k and NCH644 cells, compared to treatment with 5-FU alone (Kološa et al., 2015). The 5-FU exerts its anticancer effects after being metabolised to an inhibitor of thymidylate synthase, which leads to increased levels of deoxyuridine triphosphate and an imbalance in deoxynucleotide levels, which results in severe DNA damage and prevention of DNA synthesis (Longley et al., 2003).

Interestingly, applying either TMZ or 5-FU alone or simultaneously with MSC conditioned media decreased the survival of NCH421k cells more than of NCH644 cells. Again, this might be due to the reported heterogeneity and/or plasticity of GSLCs (Deheeger et al., 2014; Fessler et al., 2013; Motaln et al., 2015; Podergajs et al., 2013). In addition, GSLCs have also been shown to overexpress multidrug resistance proteins, including ABC transporter homologues that protect them against the effects of cytotoxic drugs (Martin et al., 2013). It is possible that MSC conditioned media have paracrine effects on the synthesis of these transporters. Alternatively, decreased chemoresistance of GSLCs is due to decreased GSLCs stemness, as reflected in the expression of the described stemness markers. Namely, Jeon et al. (2011) showed that SOX2 increased the GSLCs chemoresistance by inducing ABC transporters. Similarly, Notch-1 inhibition sensitised GSLCs to radiation treatment (Wang et al., 2010), and as demonstrated by Ulasov et al. (2011), doubled the toxicity of TMZ for CD133-positive GSLCs. Taken together, we speculate that MSC secreted cytokines are responsible for the increased TMZ and 5-FU sensitivity of GSLCs, where the underlying mechanisms are yet to be revealed.

In conclusion to the third objective of this study, MSC conditioned media were shown to affect the NCH421k, NCH644, NIB26 and NIB50 GSLC cell-cycle regulation, which results in an induction of senescence, possibly via two powerful tumor-suppressor signalling pathways, as the p53–p21–pRB and p16–pRB links. Apoptosis in these GSLC was not induced in a paracrine manner by the UC-MSCs and BM-MSCs. We also confirmed that paracrine effects of MSCs on GSLCs influence the expression of the GSLC stemness markers, possibly shifting them towards a more differentiated phenotype. Additionally, reduced chemoresistance of NCH421k and NCH644 cells to TMZ in the presence of MSC conditioned media was observed. Moreover, these data also show that paracrine effects upon

exposure to MSC conditioned media and in co-cultured cells were similar. However, these data should be further supplemented with larger panels of GSLC cells and further ‘-omics’ data to reveal the mechanisms of the MSC influence on GSLCs.

5.2. CONCLUSIONS

In conclusion all of the hypotheses proposed in this dissertation were confirmed. In the first part of the doctoral dissertation, AT-MSCs were isolated from eight tissue samples from various anatomical locations, including thigh, hips and abdomen. All of the AT-MSC lines expressed specific MSC surface markers and differentiated to cells of mesodermal lineage (i.e., adipocytes, osteocytes, chondrocytes). The investigation into the correlation between adipose harvest site and AT-MSC characteristics revealed an earlier onset of replicative senescence in the hip-derived AT-MSCs compared to the thigh and abdomen AT-MSCs. Conversely, the data showed comparable proliferation rate across all of these anatomical harvesting sites. Therefore, the obtained data indicate the importance of examination of the disposition of AT-MSCs for senescence together with the proliferation data to obtain reliable data of the cell quality. Moreover, we observed increased osteogenic and chondrogenic differentiation of the thigh-derived AT-MSCs compared to the hip and abdomen AT-MSCs. Additionally, our data indicate an absence of correlation between AT-MSC characteristics and the age of the donors. Further studies on larger populations are needed to validate these findings of tissue-harvesting-site effects on AT-MSC onset of replicative senescence and on the indications to certain type of differentiation.

In the second part of the dissertation, the data for the optimisation of the culture parameters for adhesion and expansion of AT-MSCs on microcarriers in spinner flasks gave rise to the following conclusions. The pre-coating of microcarriers with low and high serum concentrations had no influence on the initial AT-MSC adhesion to Cytodex-1 and Cytodex-3 microcarriers, although this did surprisingly affect the total AT-MSC yields, as lower AT-MSC numbers were detected on microcarriers pre-coated with pure serum. In the process of AT-MSC adhesion to microcarriers, intermittent agitation of the cultures compared to static conditions resulted in higher initial AT-MSC attachment to the microcarriers, although the final AT-MSC yields were comparable with both of these tested regimes, which indicates that higher seeding efficiency is not necessary for the successful expansion of these cells. Furthermore, for successful expansion of AT-MSCs on microcarriers, changing of the culture media every 2 days provides greater final AT-MSC numbers achieved, compared to media changing every 3 days. The addition of fresh microcarriers during the culturing process led to increases in the total AT-MSC yield, and even more importantly, prevented the formation of AT-MSCs–microcarrier aggregation of Cytodex-3, but not also of Cytodex-1, indicating the superior applicability of Cytodex-3 over Cytodex-1 microcarriers for AT-MSC expansion.

With regard to the third part of the dissertation, MSC conditioned media from UC-MSCs and BM-MSCs were shown to influence the GSLC lines (i.e., NCH421k, NCH644, NIB26, NIB50 cells) in terms of their cell-cycle regulation and induction of senescence. This appears

to be through the involvement of the p53–p21–pRB and p16–pRB tumor suppressor signalling pathways. Paracrine effects of UC-MSCs and BM-MSCs failed to activate apoptosis in these GSLCs. On the other hand, MSC paracrine factors altered the stemness of the GSLCs and shifted them towards a more differentiated phenotype, as shown by the down-regulation of *Sox-2* and *Notch-1* and the up-regulation of the *GFAP* and *vimentin* genes. Moreover, the MSC conditioned media and TMZ acted synergistically to reduce the chemoresistance of the NCH421k and NCH644 cells.

In conclusion, we have managed to identify correlations between the adipose tissue harvesting site and characteristics of the isolated AT-MSCs. We have also developed a protocol for the expansion of AT-MSCs in a microcarrier-based spinner system. Our findings will contribute to the further exploitation of AT-MSCs in research and in the clinic. We also showed that the paracrine effects of MSCs can affect key GSLCs characteristics, to shift them towards more differentiated and less resistant phenotypes. In summary, these data provide new insight into the paracrine effects of MSCs on GSLCs, and they pave the way towards successful eradication of GSLCs in GBM treatment.

6. SUMMARY (POVZETEK)

6.1. SUMMARY

Mesenchymal stem cells (MSCs) are recognized as a promising therapeutic tool in the field of cell-based therapies and regenerative medicine. Several tissue sources have been identified, and among these, MSCs derived from bone marrow, adipose tissue, and umbilical cord have been most intensively studied. Adipose tissue was recognized as the preferable source, due to its accessibility and the ease of isolation of adipose tissue MSCs (AT-MSCs), plus the several anatomical locations that can serve as a source for AT-MSC isolation. As the anatomical harvest site can have an impact on AT-MSC proliferation, life-span and differentiation, these parameters should be carefully examined to identify the anatomical location that will harbour the best quality AT-MSCs.

In this doctoral dissertation, we investigated three aspects of MSCs:

First, the most appropriate anatomical location for MSC extraction was investigated. We isolated AT-MSCs from adipose tissue that had been surgically removed from thigh, hips and abdomen. This study showed no relationships between AT-MSC proliferation and donor age, and a possible dependence on AT-MSC harvesting site. With respect to AT-MSC differentiation, a preference towards osteogenic differentiation was observed for thigh-derived AT-MSCs. Most importantly, the hip-derived AT-MSCs showed earlier onset of replicative senescence than the AT-MSCs isolated from thighs and abdomen. Further studies on larger AT-MSC populations are needed to validate these data.

Second, for clinical applications, large numbers of good quality MSCs are required, and which are difficult to obtain solely by expansion of MSCs in classic culture flasks. Microcarrier-based bioreactor systems represent good alternatives through the provision of large surface areas for MSC expansion in relatively small culture volumes in a more controlled manner. However, to take advantage of microcarrier cultivation technologies for MSC expansion, the culture parameters should be optimised. Therefore, our study also focused on optimisation of the culture parameters, which enabled successful adhesion and growth of AT-MSCs on Cytodex-1 and Cytodex-3 microcarriers in spinner flasks. We observed no effects of microcarrier pre-coating with various concentrations of serum in the first 24 h of cultivation on AT-MSC adherence to Cytodex-1 and Cytodex-3 microcarriers. Furthermore, an intermittent agitation regime led to higher numbers of attached AT-MSCs to microcarriers, compared to a static regime. By applying a 2-day feeding regime and addition of fresh microcarriers during culturing, we managed to obtain high cells densities of 8.5×10^5 cells/ml on Cytodex-1 microcarriers, and 8.3×10^5 cells/ml on Cytodex-3 microcarriers.

Although comparable cell densities were observed on these microcarriers, the Cytodex-3 microcarriers were shown to be more suitable for expansion of AT-MSCs, due to absence of cell–microcarrier aggregate formation, which was observed with Cytodex-1.

Finally, the potential of MSCs as antitumor cellular agents in glioblastoma (GBM) was considered. GBM is the most frequent and lethal type of brain tumor, which originates from astrocytes. Previous hierarchical models of cancer development predicted that small populations of cancer stem cells appear after tumor initiation and that these maintain the tumor mass. Today, the fluid model of cancer development predicts that glioma stem-like cells (GSLCs) are the main driving force in GBM progression. These GSLCs are characterised by high plasticity, as different differentiation states of the cancer cells in a tumor are observed, which results in several sub-clones of GSLCs within the same tumor. Many studies have confirmed the pivotal role of GSLCs in GBM progression, resistance to therapy, and tumor recurrence. Therefore, the developments of new treatment approaches that target the GSLCs are urgently needed. However, very few studies have investigated the effects of MSCs on GSLCs. In this third part of the dissertation, we investigated the effects of secreted factors (i.e., conditioned media) from UC-MSCs and BM-MSCs on several GSLC lines (i.e., NCH421k, NCH644, NIB26, NIB-50 cells). The paracrine factors present in conditioned media from both types of MSCs impaired GSLCs cell-cycle progression in the G0/G1 phase, as shown by down-regulation of *cyclin D1*. Importantly, although the paracrine factors of UC-MSCs and BM-MSCs failed to induce apoptosis in the GSLCs, they triggered the onset of senescence via cell-cycle inhibitors, mostly through p21 and p16. PCR analysis of senescence-associated genes identified significant dysregulation of 13 genes. Based on these data, pathway analysis in GO and KEGG implied the involvement of the p53 signalling pathway. Hence, our data point to the involvement of the p53–p21–pRB and p16–pRB tumor suppressor signalling pathways in this activation of senescence in GSLCs caused by the MSC paracrine effects. Moreover, the MSC conditioned media altered the stemness of the GSLCs by shifting them towards a more differentiated phenotype, as shown by the down-regulation of *Sox-2* and *Notch-1*, and the up-regulation of the astrocyte markers *vimentin* and *GFAP*. Finally, an increased sensitivity towards temozolomide, the most used chemotherapeutic for patients with GBM was promoted in the presence of MSC conditioned media. Similar to what was observed above, indirect co-culturing of UC-MSCs and BM-MSCs with the NCH421k GSLC line led to their impaired proliferation and reduced stemness, as shown by down-regulation of *Sox-2* and up-regulation of *vimentin* and *GFAP*.

Altogether, our findings support the concept that MSCs have the intrinsic ability to influence key GSLC properties, possibly leading to more efficient GBM treatment through the targeting of GSLCs.

6.2. POVZETEK

Mezenhimske matične celice (MMC) je mogoče izolirati iz različnih tkiv odraslega človeka, kot sta kostni mozeg in maščobno tkivo. Vir so tudi fetalna tkiva, pri čemer je bilo največ raziskav izvedenih na MMC izoliranih iz popkovnice in popkovnične krvi. Izolirane MMC imajo sposobnost pritrditve na plastično podlago gojitvenih posod, izražajo značilne površinske označevalce CD13, CD29, CD44, CD73, CD90, CD105 in ne izražajo hematopoetskih površinskih označevalcev CD14, CD34, CD45 ter HLA-DR. Poleg tega je za MMC značilna sposobnost diferenciacije v celice mezodermalnega zarodnega sloja, kot so maščobne, kostne in hrustančne celice. Predvsem pa so se MMC izkazale kot obetavno terapevtsko orodje v regenerativni medicini in pri zdravljenju različnih bolezni, od avtoimunskih, nevrodegenerativnih, vnetnih bolezni pa do rakavih obolenj.

Maščobno tkivo se je pokazalo kot posebno primeren vir MMC, saj je enostavno dostopno, tudi v večjih količinah, obenem pa je izolacija MMC iz maščevja enostavna. Možnost odvzema maščobnega tkiva na več telesnih predelih poraja vprašanje, kakšen je vpliv anatomske lokacije maščevja na nekatere pomembne lastnosti izoliranih MMC, kot so proliferacija, dolgoživost in diferenciacija. Poznavanje vpliva telesnega predela na kvaliteto prisotnih MMC bi tako vodilo v hitro pridobivanje kvalitetnih MMC iz maščevja (AT-MMC; iz ang. adipose tissue) v terapevtske namene. Obetajoči rezultati preliminarnih študij in kliničnih raziskav osvetljujejo tudi prihodnje izzive pri uporabi MMC v terapevtske namene. Eden večjih izzivov tako predstavlja zagotavljanje zadostnega števila kvalitetnih MMC. Čeprav je glede na dostopnost maščobnega tkiva možno izolirati visoko število AT-MMC to še vedno ne zadostuje za direktno uporabo v terapevtske namene. Sedanji način pridobivanja velikega števila MMC temelji na namnoževanju celic v gojitvenih posodah (iz ang. culture flasks), kar pa je zahtevna naloga, saj je potrebna količina MMC pri terapevtski uporabi najmanj 1-2 milijona celic na kilogram telesne teže bolnika. Obenem je tak način namnoževanja celic delovno zelo intenziven, cenovno neugoden in zaradi pogostega presajanja celic tudi podvržen okužbam.

V doktorskem delu smo obravnavali tri aspekte, ki lahko vodijo k boljši klinični uporabi MMC.

V prvem delu teze smo se najprej osredotočili na izolacijo in karakterizacijo lastnosti AT-MMC iz maščevja stegna, bokov in trebuha.

AT-MMC smo izolirali iz maščevja, ki je bilo pridobljeno s kirurškim izrezom, količina maščevja pa je bila zelo majhna, od 1 do 3.7 ml. Vse pridobljene AT-MMC, ne glede na mesto odvzema maščevja, so izražale površinske označevalce značilne za MMC in bile

sposobne diferenciacije v maščobne, kostne in hrustančne celice. Primerjava števila izoliranih celic glede na telesni predel odvzema maščevja je pokazala največjo prisotnost AT-MMC v maščevju stegna. Obenem so stegenske AT-MMC bolj diferencirale v kostne in hrustančne celice v primerjavi z AT-MMC izoliranimi iz bokov in trebuha. Proliferacijska sposobnost AT-MMC je bila neodvisna od starosti darovalcev v razponu med 12 in 71 let. Prav tako nismo opazili razlik v proliferaciji AT-MMC glede na telesni predel odvzema maščevja. Izračun kumulativne podvojitve populacije je pokazal, da se po 200 dnevih gojenja celična rast pri vseh AT-MMC linijah ustavi, v tem času pa pride od 22 do 56 podvojitve populacije pri posameznih AT-MMC linijah. Nasprotno, telesni predel odvzema maščevja je vplival na hitrost procesa oz. pojavnost replikativne senescence v celičnih kulturah AT-MMC pri *in vitro* gojenju. Primerjava deleža senescentnih celic določenega z barvanjem betagalaktozidazne aktivnosti pri suboptimalni vrednosti pH 6 je pokazalo značilno povečan delež senescentnih celic pri AT-MMC pridobljenih iz maščevja bokov na nizki (pasaža 6) in srednji (pasaža 12) pasaži v primerjavi z AT-MMC izoliranih iz maščevja stegna in trebuha.

Naši rezultati kažejo, da so AT-MMC pridobljene iz telesnega predela bokov manj kvalitetne od AT-MMC izoliranih iz maščevja stegna in trebuha. Čeprav izkazujejo vse značilnosti MMC so zaradi hitrejšega nastopa replikativne senescence v *in vitro* celični kulturi manj kvalitetne v smislu dolgotrajnejšega namnoževanja in je zato njihova uporabnost zmanjšana. Vsekakor pa je potrebno poudariti, da je potrebno pridobljene rezultate potrditi na večjem številu AT-MMC izoliranih iz telesnih predelov stegna, bokov in trebuha.

V drugem delu teze smo raziskali pogoje za optimizacijo gojenja AT-MMC na mikronosilcih v mešalnih steklenkah.

Gojenje celic na mikronosilcih v bioreaktorju omogoča pridobivanje velikega števila celic, saj omogoča gojenje adherentnih celic v suspenziji, pri čemer se močno poveča površina za rast MMC glede na volumen gojitvene suspenzije. Obenem je tak način gojenja mnogo bolj nadzorovan, saj so celice izpostavljene enakim okoljskim pogojem (koncentracija O₂, pH, prisotnost metabolnih produktov, itd.), katere je možno enostavno spremljati. V primerjavi s klasičnim gojenjem celic v gojitvenih posodah se gojenje celic na mikronosilcih odraža tudi v zmanjšani heterogenosti celične kulture. Dodatno prednost gojenja celic na mikronosilcih predstavlja dejstvo, da lahko celice ob doseženi konfluenci same preidejo na novo dodane mikronosilce, kar omogoča pridobitev večjega števila celic, brez uporabe proteolitičnih encimov in presajanja celic, s čimer se zmanjša tudi možnost okužb pri precepljanju celic. Kljub vsem naštetim prednostim gojenja celic na mikronosilcih predstavlja velik izziv izbira primernih mikronosilcev za uspešno pritrnitev in določitev optimalnih pogojev za rast celic. Pri gojenju MMC na mikronosilcih je poleg pridobivanja velikega števila MMC pomembno tudi, da MMC po gojenju na mikronosilcih ohranijo svoje značilne lastnosti, kot so izražanje

površinskih označevalcev značilnih za MMC in sposobnost diferenciacije v celice mezodermalnega sloja.

V tem delu smo se osredotočili na optimizacijo pogojev gojenja, ki bi omogočali namnoževanje AT-MMC na mikronosilcih v mešalnih steklenkah. Pri tem smo uporabili dve vrsti mikronosilcev, Cytodex-1 in Cytodex-3. Cytodex-1 mikronosilci so narejeni iz mrežno povezanega dekstrana, njihova površina pa je prekrita s pozitivno nabitimi N,N-dimetilamino skupinami. Cytodex-3 mikronosilci so prav tako narejeni na osnovi mrežno povezanega dekstrana in prekriti s tanko plastjo kolagena.

V začetnih poskusih smo raziskali kateri parametri vplivajo na pritrjevanje AT-MMC na mikronosilce. Tako smo preverili vpliv predinkubacije Cytodex-1 in Cytodex-3 mikronosilcev v gojitvenem mediju ali čistem FBS (serum govejega zarodka, iz. ang. foetal bovine serum) na pritrjevanje AT-MMC v statičnih pogojih, vendar razlik v pritrjevanju AT-MMC med obema vrstama mikronosilcev nismo opazili. Ponovljen poskus v mešalnih steklenkah je potrdil, da predinkubacija mikronosilcev bodisi z gojitvenem mediju ali FBS ne vpliva na pritrjevanje AT-MMC, tako na Cytodex-1 kot na Cytodex-3 mikronosilce. V nadaljnjih poskusih smo tako predinkubacijo Cytodex-1 in Cytodex-3 mikronosilcev izvedli samo v gojitvenem mediju. Preverili smo še pritrjevanje AT-MMC na obe vrsti mikronosilcev v prvih 24 urah pri različnih pogojih mešanja, in sicer smo primerjali mešanje s premorom (zaporedni intervali s 5 minutnim mešanjem pri 40 rpm in 30 minutnim premorom brez mešanja) ter brez mešanja mikronosilcev. Izkazalo se je, da se večji delež AT-MMC pritrdi pri režimu mešanja s premorom, kar je nekako pričakovano, saj je celicam s tem na voljo večja površina mikronosilcev. Razlik v pritrjevanju AT-MMC med testiranima vrstama mikronosilcev nismo opazili.

Nadalje smo se osredotočili na optimizacijo pogojev gojenja AT-MMC na Cytodex-1 in Cytodex-3 mikronosilcih v mešalnih steklenkah, ki bi omogočali produkcijo večjega števila celic za uporabo v terapevtske namene. Rezultati so pokazali, da čeprav predinkubacija mikronosilcev ne vpliva na samo pritrjevanje AT-MMC, vpliva na končno število pridobljenih celic. Na obeh vrstah mikronosilcev smo namreč opazili manjše končno število AT-MMC pri predinkubaciji s FBS, čemur bi lahko botrovala zasičenost površine mikronosilcev z makromolekulami prisotnimi v FBS, kar bi lahko onemogočalo širjenje AT-MMC po površini mikronosilcev. Izbira režima mešanja suspenzije mikronosilcev v prvih 24 urah gojenja ni vplivala na končno število pridobljenih AT-MMC, kljub temu, da smo opazili večji delež pritrjenih celic po 24 pri mešanju s premorom. Iz tega sklepamo, da visok delež pritrjenih AT-MMC ni pogoj za njihovo uspešno rast na mikronosilcih. Testiranje režima menjave gojitvenega medija vsake 2 ali 3 dni je pričakovano pokazalo, da pri pogostejši menjavi medija zagotovimo optimalnejši vnos hranil, kar se odraža v večjem končnem številu

pridobljenih AT-MMC na obeh vrstah mikronosilcev. Opazili smo, da po šestem dnevu gojenja AT-MMC na mikronosilcih prihaja do tvorbe skupkov tako pri uporabi Cytodex-1 kot Cytodex-3, kar vodi v večjo heterogenost celične kulture AT-MMC. V izogib temu smo tretji dan gojenja dodali nove mikronosilce v gojilno suspenzijo. Izkazalo se je, da je tak način preprečevanja tvorbe skupkov uspešen samo v primeru gojenja AT-MMC na Cytodex-3, ne pa tudi na Cytodex-1 mikronosilcih. Opažene razlike so najverjetneje posledica različnih površinskih lastnosti Cytodex-1 kot Cytodex-3 mikronosilcev. Pričakovano je dodajanje novih mikronosilcev tekom procesa gojenja AT-MMC zaradi povečane površine za rast celic vodilo tudi večjega končnega števila celic v primerjavi s prej testiranimi pogoji na obeh vrstah mikronosilcev. Ob opaženi odsotnosti tvorbe skupkov so se tako kot primernejši mikronosilci za gojenje AT-MMC pokazali Cytodex-3, čeprav je bilo končno število pridobljenih AT-MMC na obeh vrstah mikronosilcev primerljivo. Tako optimiziran postopek je dosegel visoko število AT-MMC po gojenju na Cytodex-3 mikronosilcih, in sicer 48 milijonov AT-MMC (830.000 celic/ ml celične suspenzije) po desetih dneh gojenja.

Da bi preverili vpliv gojenja AT-MMC na mikronosilcih v mešalnih steklenkah na njihovo matičnost smo preverili izražanje površinskih označevalcev značilnih za MMC in diferenciacijo v celice mezodermalnega zarodnega sloja. Analiza izražanja površinskih označevalcev značilnih za MMC je pokazala njihovo nespremenjeno izražanje po gojenju AT-MMC na mikronosilcih in sposobnost diferenciacije v maščobne, kostne in hrustančne celice. Sposobnost diferenciacije AT-MMC v kostne celice se je po gojenju na mikronosilcih celo povečala, saj smo opazili povečano prisotnost kalcijevih depozitov.

Naši rezultati kažejo, da preinkubacija Cytodex-1 in Cytodex-3 mikronosilcev v gojitvenem mediju omogoča pritrnitev zadostnega števila AT-MMC za uspešno nadaljno rast na mikronosilcih ob dvo-dnevni menjavi gojitvenega medija. Dodajanje novih mikronosilcev tekom procesa gojenja AT-MMC vodi do zmanjšanja tvorbe skupkov v primeru Cytodex-3 mikronosilcev in v povečanje končnega števila pridobljenih AT-MMC z ohranjeno matičnostjo.

V tretjem delu teze smo se osredotočili na uporabo MMC v klinični praksi, konkretnije v onkologiji. Raziskali smo vpliv protitumorskega delovanja MMC iz Whartonove žolice popkovnice (UC-MMC, UC; iz ang. umbilical cord) in kostnega mozga (BM-MMC, BM; iz ang. bone marrow) na gliomske matičnim celicam podobne celice (GMC) *in vitro*.

Med novejši pristope zdravljenja raka sodi celična terapija. MMC v telesu izkazuje usmerjeno gibanje proti tumorjem in izločajo različne citokine, kemokine in druge topne molekule, ki vplivajo na delovanje tumorskih celic. V tem smislu že vrsto let potekajo intenzivne raziskave prav na možganskih tumorjih, kot so maligne oblike glioma. Glioblastom

multiforme (GBM) spada med najpogostejšo vrsto tumorjev centralnega živčnega sistema. Obenem sodi med najbolj smrtno oblike raka, saj je preživetje bolnikov po diagnozi zelo kratko, v povprečju med 12 in 15 mesecev. Kljub napredku na področju kirurških metod, kemoterapije in obsevanja je ponovitev bolezni neizogibna, vzrok temu pa naj bi bila prisotnost rakavih matičnih celic. Hierarhični model nastanka raka predvideva, da se maligni GBM razvije iz maloštevilne populacije rakavih matičnih celic. Slednje so tako sposobne tvoriti nov tumor, saj imajo sposobnost samoobnavljanja in neomejenega podvojevanja, ter diferenciacije v različne bolj zrele celične tipe, ki tvorijo tumorsko maso. V zadnjem času se vse bolj uveljavlja t.i. dinamičen model rakavih matičnih celic, kateri predvideva, da na rakave matične celice močno vpliva tumorsko mikrookolje in lahko povzroči tudi dediferenciacijo diferenciranih celičnih tipov v bolj matičnim celicam podobne celice. GMC posedujejo tudi določene lastnosti nevrlnih matičnih celic, kot je izražanje površinskih označevalcev, npr. nestin, SOX-2 in Musashi-1. Med najpogosteje uporabljane označevalce GMC sicer sodi transmembranski glikoprotein CD133. Poleg specifičnih kazalcev je za GMC značilna visoka stopnja odpornosti na kemoterapevtike in obsevanje, kar neizogibno povzroči povrnitev bolezni oz. recidiv. Zaradi teh lastnosti predstavljajo GMC ključno tarčo pri razvoju novih terapevtskih pristopov k zdravljenju GBM.

Študije v *in vitro* in *in vivo* modelih so pokazale protitumorsko delovanje MMC pridobljenih iz različnih virov na GBM celice, kot so ustavitev celičnega cikla, sprožitev apoptoze ali senescence. Vnos MMC v miši s humanimi GBM tumorji je tako zmanjšala velikost tumorja, medtem ko so pri sočasnem vnosu MMC in GBM celic opazili zmanjšano število novo nastalih tumorjev. Kljub temu pa ostaja neodgovorjeno vprašanje, kakšen vpliv imajo MMC na same GMC celice, kjer sta bili po našem vedenju izvedeni le dve študiji. Ugotovljeno je bilo, da se MMC v *in vivo* modelu prednostno umestijo k CD133 pozitivnim gliomskim celicam. Obenem je bilo dokazano, da MMC tudi zmanjšajo delež CD133 pozitivnih celic prisotnih v GBM tkivu.

Glede na vlogo, ki jo imajo GMC v odpornosti pri zdravljenju GBM in glede na rezultate študij, ki so pokazale protitumorsko delovanje MMC, smo se v tretjem delu teze osredotočili na raziskavo vpliva UC-MMC in BM-MMC na čisto populacijo GMC v *in vitro* pogojih. Ugotavljali smo, kako topni faktorji, ki jih sproščajo MMC, vplivajo na celične linije GMC (NCH421k, NCH644, NIB26 in NIB50) po 72 urah izpostavitve. Protitumorsko delovanje topnih faktorjev prisotnih v kondicioniranem mediju UC-MMC in BM-MMC smo najprej preverili z izpostavitvijo NCH421k celic in zaznali zaustavitev celičnega cikla v G0/G1 fazi. Nadalje smo ustavitev celičnega cikla v G0/G1 fazi po izpostavitvi kondicioniranemu mediju obeh vrst MMC potrdili pri vseh celičnih linijah GMC: NCH421k, NCH644, NIB26 in NIB50 preko znižanega izražanja gena *ciklina D1*.

Apoptoza in senescenca predstavljata dva možna programirana celična odziva na neugodne vplive iz okolja, zato smo najprej preverili ali kondicioniran medij MMC sproži apoptozo v GMC. Ugotovili smo, da kondicioniran medij UC-MMC in BM-MMC zniža mitohondrijski membranski potencial v NCH421k celicah. Dodatni testi spremljanja apoptoze, in sicer merjenje spremembe asimetrije celične membrane in razmerje izražanja pro-apoptotskega gena *bax* in anti-apoptotskega gena *bcl-2* niso potrdili sprožitve apoptoze v GMC po izpostavitvi izločenim faktorjem MMC. Sklepamo, da je njihova prisotnost v kondicioniranemu mediju MMC povzročila stresni odziv v GMC s spremembo mitohondrijskega membranskega potenciala, a ta ni bil zadosten, da bi sprožil apoptozo v GMC, saj je znano, da so GMC na apoptotske signale bolj odporne.

Nadalje smo ugotovili, da kondicioniran medij UC-MMC in BM-MMC sproži senescenco v vseh štirih linijah GMC, kar smo določili z barvanjem betagalaktozidazne aktivnosti pri suboptimalni vrednosti pH 6.0. Da bi lahko razumeli sprožitev senescence v GMC smo NCH421k celice izpostavili kondicioniranemu mediju obeh vrst MMC, ter izvedli analizo izražanja genov povezanih s senescenco. S testom Cellular Senescence RT-Prolifer PCR Array smo prikazali številne statistično značilno spremenjene gene. Tako je prišlo do povišanega izražanja gena *ATM* (ATM kinaza, iz ang. ataxia telangiectasia mutated), *CD44*, *COL1A1* (kolagen, tip I, alfa 1), *MORC3* (ang. MORC family CW-type zinc finger 3), *NOX4* (NADPH oksidaza 4), *CDKN1A* (p21; inhibitor od ciklina odvisne kinaze 1A), *IGFBP5* (inzulinu podobni rastni faktor vezni protein 5), *SERPINE1* (serpin peptidazni inhibitor, skupine E) in znižanega izražanja gena *IGFBP3* (inzulinu podobni rastni faktor vezni protein 3) *CDKN2A* (p16; inhibitor od ciklina odvisne kinaze 2A), *CITED2* (Cbp/p300-povezujoč transaktivator, z Glu/Asp-bogato karboksi-terminalno domeno), *FNI* (fibronektin 1), *PRKCD* (protein kinaza C, delta). Z vnosom spremenjeno izraženih genov v podatkovno zbirko genske ontologije KEGG smo ugotovili, da je pri nastopu senescence v NCH421k celicah ob prisotnosti parakrinih faktorjev MMC vključena tudi p53 signalna pot. Preverili smo izražanje dveh ključnih genov povezanih s senescenco, in sicer *p21* in *p16*. Pri NCH421k, NCH644, NIB26 in NIB50 celicah, ki smo jih izpostavili kondicioniranemu mediju UC-MMC in BM-MMC, smo ugotovili, da pri NCH421k celicah pride do povišanega izražanja gena *p21* in znižanega izražanja gena *p16*, medtem ko pri preostalih GMC linijah pride od povišanega izražanja obeh genov. *p21* je vključen v regulacijo ustavitve celičnega cikla v začetni fazi in se njegovo izražanje zniža ob nastopu senescence. Vloga *p16* je stabilizacija procesa senescence z vzdrževanjem ustavitve celičnega cikla v fazi G0/G1. Tako *p21* in *p16* pa lahko sprožita aktivacijo pRB. Kondicioniran medij obeh vrst MMC je v vseh celičnih linijah GMC vodil do znižanega izražanja ciklina D1. V vseh štirih linijah GMC smo tudi potrdili izražanje gena *p53*. Na podlagi teh dejstev sklepamo, da parakrini faktorji, ki jih MMC izločajo v medij sprožijo senescenco v GMC, po dveh različnih poteh odvisno od podvrste GMC, ki se med

seboj prepletata, in sicer bodisi preko aktivacije p53-p21-pRB ali p16-pRB tumor-supresorske signalne poti.

Preverili smo tudi kakšen vpliv ima kondicioniran medij UC-MMC in BM-MMC na kazalce matičnosti v GMC. Ugotovili smo, da ima kondicioniran medij obeh vrst MMC različen vpliv na izražanje gena *CD133* v GMC, saj smo pri NCH421k celicah ugotovili povišanje, pri NCH644 pa njegovo znižanje. Ko smo preverili izražanje proteina CD133 s pretočno citometrijo pri NCH421k celicah nismo zaznali sprememb, medtem ko smo pri NCH644 celicah potrdili njegovo znižanje ob prisotnosti kondicioniranega medija obeh vrst MMC. Vzroke za nedoslednost v izražanju CD133 bi lahko pripisali heterogeni naravi GMC in njihovemu odzivu na kondicioniran medij MMC. Drugo možnost predstavlja ugotovljena različna regulacija izražanja gena CD133, saj se lahko translacija *CD133* začne na petih različnih promotorjih, kar vodi v nastanek večih alternativno spojitvenih transkriptov, obenem pa ima CD133 osem možnih glikolizacijskih mest, kar posledično vodi do težav pri določitvi CD133 na genskem kot tudi proteinskem nivoju.

Vendar pa naši rezultati kažejo, da kondicionirana medija UC-MMC in BM-MMC znižata izražanje genov *Sox-2* in *Notch-1* v linijah GMC. Ker sta tako SOX-2 in Notch-1 vključena v vzdrževanje matičnosti in proliferacijo GMC, lahko sklepamo, da parakrini faktorji prisotni v kondicioniranemu mediju MMC znižajo matičnost GMC. V prid temu kaže tudi povišano izražanje vimentina in GFAP pri GMC izpostavljenih kondicioniranemu mediju MMC, ki nakazuje diferenciacijo GMC v astrocitno smer. Obenem se je po izpostavitvi kondicioniranemu mediju MMC močno spremenila morfolologija GMC. Pri NCH421k in NIB26 celicah smo opazili zmanjšanje velikosti sferoidov, ki so postali nepravilnih oblik, medtem ko smo pri NCH644 in NIB50 celicah poleg nepravilne oblike sferoidov opazili tudi spremembo načina rasti, saj so se sferoidi, ki so prej plavali v suspenziji pritrdili na površino in so se celice sferoida začele razraščati po podlagi. Tako spremenjen način rasti GMC po gojenju v prisotnosti kondicioniranega medija MMC iz značilne sferoidne rasti v pritrjen način rasti dodatno potrjuje, da gre za izgubo oz. zmanjšanje matičnosti.

Ena pglavitnih, sicer neželenih lastnosti GMC, ki vpliva na zdravljenje GBM, je njihova odpornost na citostatike. Preverili smo, ali kondicioniran medij UC-MMC in BM-MMC lahko vpliva na odpornost NCH421k in NCH644 celic na temozolomid, ki je najpogosteje uporabljan citostatik pri zdravljenju GBM. Pokazalo se je, da hkratna izpostavitvev NCH421k in NCH644 celic 1000 μM temozolomidu in kondicioniranemu mediju UC-MMC ali BM-MMC za 72 ur zniža njihovo odpornost na ta citostatik. Pri izpostavitvi NCH421k in NCH644 celic 150 μM 5-fluorouracilu skupaj s kondicioniranim medijem UC-MMC ali BM-MMC za 72 ur smo opazili znižano odpornost samo pri NCH644 celicah. Sklepamo torej, da MMC izločajo faktorje, ki povečajo dovzetnost GMC na delovanje citostatikov ali pa je povečana

dovzetnost na delovanje citostatikov posledica zmanjšane matičnosti GMC ob prisotnosti kondicioniranega medija MMC.

Če povzamemo, prikazani rezultati kažejo, da parakrini faktorji prisotni v kondicioniranem mediju UC-MMC in BM-MMC sprožijo senescenco, znižajo matičnost in odpornost na citostatike v NCH421k, NCH644, NIB26 in NIB50 GMC. Da bi preverili ali MMC izkazujejo podoben učinek na GMC tudi ob posredni izmenjavi parakrinih faktorjev smo UC-MMC in BM-MMC 72 ur gojili v indirektni kokulturi z NCH421k celicami. Uporabili smo Boydenove kamrice, ki fizično ločijo obe vrsti celic, a obenem omogočijo medsebojno izmenjavo izločenih topnih faktorjev. Spremljanje izražanja genov *bax* in *bcl-2* je pokazalo, da tudi ob posredni intreakciji NCH421k in MMC ne pride do sprožitve apoptoze v NCH421k celicah. Smo pa potrdili povišano izražanje gena *p21* gena ne pa tudi gena *p16*, kar sovpada z opaženim učinkom kondicioniranega medija MMC na NCH421k celice in nakazuje na enako pot aktivacije senescence. Spremljanje izražanja markerjev matičnosti je pokazalo, da pride pri NCH421k celicah gojenih v indirektni kokulturi z UC-MMC in BM-MMC do znižanega izražanja gena *Sox-2* in povišanega izražanja gena za *vimentin* in *GFAP*. Spremembo izražanja CD133 nismo zaznali na genskem kot tudi ne na proteinskem nivoju, enako kot pri izpostavitvi NCH421k kondicioniranemu mediju UC-MMC ali BM-MMC. Zaključimo lahko na zelo podoben parakrini vpliv MMC, torej tudi ob povratnem odgovoru GMC na faktorje, ki jih izločajo MMC.

Iz dobljenih rezultatov lahko zaključimo, da imajo UC-MMC in BM-MMC sposobnost sprožitve senescence in diferenciacije, ter znižanja odpornosti na citostatike v GMC. S tem so zmanjšane ključne lastnosti GMC, ki so odgovorne za vzdževanje in recidiv bolezni.

7. REFERENCES

- Abdallah B.M., Kassem M. 2008. Human mesenchymal stem cells: from basic biology to clinical applications. *Gene Therapy*, 15, 2: 109-116
- Aleynik A., Gernavage K.M., Mourad Y.Sh., Sherman L.S., Liu K., Gubenko Y.A., Rameshwar P. 2014. Stem cell delivery of therapies for brain disorders. *Clinical and Translational Medicine*, 19, 3: 24-34
- Alonso M.M., Diez-Valle R., Manterola L., Rubio A., Liu D., Cortes-Santiago N., Urquiza L., Jauregi P., Lopez de Munain A., Sampron N., Aramburu A., Tejada-Solís S., Vicente C., Otero M.D., Bandrés E., García-Foncillas J., Idoate M.A., Lang F.F., Fueyo J., Gomez-Manzano C. 2011. Genetic and epigenetic modifications of sox2 contribute to the invasive phenotype of malignant gliomas. *PLoS One*, 6, 11: e26740, doi: 10.1371/journal.pone.0026740: 11 p.
- Amorin B., Alegretti A.P., Valim V., Pezzi A., Laureano A.M., da Silva M.A., Wieck A., Silla L. 2014. Mesenchymal stem cell therapy and acute graft-versus-host disease: a review. *Human Cell*, 27, 4: 137-150
- Arango-Rodriguez M. L. 2015. Could cancer and infection be adverse effects of mesenchymal stromal cell therapy? *World Journal of Stem Cells*, 7, 2: 408–417
- Ardebili S.Y., Zajc I., Gole B., Campos B., Herold-Mende C., Drmota S., Lah T.T. 2011. CD133/prominin1 is prognostic for GBM patient's survival, but inversely correlated with cysteine cathepsins' expression in glioblastoma derived spheroids. *Radiology and Oncology*, 45: 102-115
- Bago J. R., Alieva M., Soler C., Rubio N., Blanco J. 2013. Endothelial differentiation of adipose tissue-derived mesenchymal stromal cells in glioma tumors: Implications for cell-based therapy. *Molecular Therapy*, 21, 9: 1758–1766
- Balbous A., Cortes U., Guilloteau K., Villalva C., Flamant S., Gaillard A., Milin S., Wager M., Sorel N., Banfi A., Muraglia A., Dozin B., Mastrogiacomo M., Cancedda R., Quarto R. 2000. Proliferation kinetics and differentiation potential of ex vivo expanded human bone marrow stromal cells: Implications for their use in cell therapy. *Experimental Hematology*, 28, 6: 707–715

- Bao S., Wu Q., McLendon R.E., Hao Y., Shi Q., Hjelmeland A.B., Dewhirst M.W., Binger D.D., Rich J.N., 2006. Glioma stem cells promote radioresistance by preferential activation of the DNA damage response. *Nature*, 444, 7120: 756-760
- Beltrami A.P., Cesselli D., Beltrami C.A. 2011. At the stem of youth and health. *Pharmacology and Therapeutics*, 129, 1: 3–20
- Ben-Porath I., Weinberg R.A. 2005. The signals and pathways activating cellular senescence. *International Journal of Biochemistry and Cell Biology*, 37, 5: 961–976
- Bexell D., Gunnarsson S., Tormin A., Darabi A., Gisselsson D., Roybon L., Scheduling S., Bengzon J. 2009. Bone marrow multipotent mesenchymal stroma cells act as pericyte-like migratory vehicles in experimental gliomas. *Molecular Therapy*, 17, 1: 183–190
- Birnbaum T., Roider J., Schankin C.J., Padovan C.S., Schichor C., Goldbrunner R., Straube A. 2007. Malignant gliomas actively recruit bone marrow stromal cells by secreting angiogenic cytokines. *Journal of Neuro-oncology*, 83, 3: 241–247
- Bjerkvig R., Tysnes B.B., Aboody K.S., Najbauer J., Terzis A.J. 2005. Opinion: the origin of the cancer stem cell: current controversies and new insights. *Nature Reviews Cancer*, 5, 11: 899-904
- Bleau A.M., Hambardzumyan D., Ozawa T., Fomchenko E.I., Huse J.T., Brennan C.W., Holland E.C. 2009. PTEN/PI3K/Akt pathway regulates the side population phenotype and ABCG2 activity in glioma tumor stem-like cells. *Cell Stem Cell*, 6, 4: 226-235
- Boomsma R.A., Geenen D.L. 2012. Mesenchymal stem cells secrete multiple cytokines that promote angiogenesis and have contrasting effects on chemotaxis and apoptosis. *PLoS One*, 7, 4: e35685, doi: 10.1371/journal.pone.0035685: 8 p.
- Brooke G., Tong H., Levesque J.P., Atkinso, K. 2008. Molecular trafficking mechanisms of multipotent mesenchymal stem cells derived from human bone marrow and placenta. *Stem Cells and Development*, 17, 5: 929–940
- Bruder S.P., Jaiswal N., Haynesworth S.E. 1997. Growth kinetics, self-renewal, and the osteogenic potential of purified human mesenchymal stem cells during extensive subcultivation and following cryopreservation. *Journal of Cellular Biochemistry*, 64, 2: 278–294

- Buschmann J., Gao S., Härter L., Hemmi S., Welti M., Werner C. M., Calcagni M., Cinelli P., Wanner G. A. 2013. Yield and proliferation rate of adipose-derived stromal cells as a function of age, body mass index and harvest site - increasing the yield by use of adherent and supernatant fractions? *Cytotherapy*, 15, 9: 1098–1105
- Campos B., Herold-Mende C.C. 2011. Insight into the complex regulation of CD133 in glioma. *International Journal of Cancer*, 128, 3: 501–510
- Campos B., Wan F., Farhad, M., Ernst A., Zeppernick F., Taherer K.E., Ahmadi R., Lohr J., Dictus C., Gdynia G., Combs S.E., Goidts V., Helmke B.M., Eckstein V., Roth W., Beckhove P., Lichter P., Unterberg A., Radlwimmer B., Herold-Mende C. 2010. Differentiation therapy exerts antitumor effects on stem-like glioma cells. *Clinical Cancer Research*, 16, 10: 2715-2728
- Campos B., Zeng L., Daotrong P. H., Eckstein V., Unterberg A., Mairbäurl H., Herold-Mende C. 2011. Expression and regulation of AC133 and CD133 in glioblastoma. *Glia*, 59, 12: 1974–1986
- Caplan A.I. 1991. Mesenchymal stem cells. *Journal of Orthopaedic Research*, 9, 5: 641–650
- Caplan A.I. 2007. Adult mesenchymal stem cells for tissue engineering versus regenerative medicine. *Cell Physiology*, 213, 2: 341–347
- Capper D., Gaiser T., Hartmann C., Habel A., Mueller W., Herold-Mende C. 2009. Stem-cell-like glioma cells are resistant to TRAIL/Apo2L and exhibit downregulation of caspase-8 by promoter methylation. *Acta Neuropathologica*, 117, 4: 445–56
- Carlsson S.K., Brothers S.P., Wahlestedt C. 2014. Emerging treatment strategies for glioblastoma multiforme. *EMBO Molecular Medicine*, 6, 11: 1359-1370
- Castro-Manreza M.E., Montesinos J. J. 2015. Immunoregulation by mesenchymal stem cells: biological aspects and clinical applications. *Journal of Immunology Research*, 2015: 394917, doi: 10.1155/2015/394917: 20 p.
- Chamberlain G., Fox J., Ashton B., Middleton J. 2007. Mesenchymal stem cells: their phenotype, differentiation capacity, immunological features, and potential for homing. *Stem Cells*, 25, 11: 2739–2749

- Chen A., Reuveny S., Oh S. K. 2013. Application of human mesenchymal and pluripotent stem cell microcarrier cultures in cellular therapy: achievements and future direction. *Biotechnology Advance*, 31, 7: 1032-1046
- Chen A.K., Chew Y.K., Tan H.Y., Reuveny S., Weng Oh S.K.I. 2015. Increasing efficiency of human mesenchymal stromal cell culture by optimization of microcarrier concentration and design of medium feed. *Cytotherapy*, 17, 2: 163-173
- Chen M., Wang X., Ye Z., Zhang Y., Zhou Y., Tan W.S. 2011. A modular approach to the engineering of a centimeter-sized bone tissue construct with human amniotic mesenchymal stem cells-laden microcarriers. *Biomaterials*, 32: 7532-7542
- Childs B. G., Baker D. J., Kirkland J. L., Campisi J., van Deursen J. M. 2014. Senescence and apoptosis: Duelling or complementary cell fates? *EMBO Reports*, 15, 11: 1139–1153
- Chomczynski P., Sacchi N. 1987. Single-step method of RNA isolation by acid guanidinium thiocyanate-phenol-chloroform extraction. *Analytical Biochemistry*, 162, 1: 156-159
- Choudhery M.S., Badowski M., Muise A., Harris D.T. 2013. Comparison of human mesenchymal stem cells derived from adipose and cord tissue. *Cytotherapy*, 15, 3: 330-343
- Choudhery M.S., Badowski M., Muise A., Pierce J., Harris D.T. 2015. Subcutaneous adipose tissue-derived stem cell utility is independent of anatomical harvest site. *BioResearch Open Access*, 4, 1: 131-145
- Choudhery M.S., Badowski M., Muise A., Pierce J., Harris D.T. 2014. Donor age negatively impacts adipose tissue-derived mesenchymal stem cell expansion and differentiation. *Journal of Translational Medicine*, 12: 8, doi: 10.1186/1479-5876-12-8: 14 p.
- Christodoulou I., Kolisis F.N., Papaevangelidou D., Zoumpourlis V. 2013. Comparative evaluation of human mesenchymal stem cells of fetal (Wharton's Jelly) and adult (adipose tissue) origin during prolonged *in vitro* expansion: Considerations for cytotherapy. *Stem Cells International*, 2013: 246134, doi: 10.1155/2013/246134: 12 p.
- Clavreul A., Guette C., Faguer R., Tétaud C., Boissard A., Lemaire L., Rousseau A., Avril T., Henry C., Coqueret O., Menei P. 2014. Glioblastoma-associated stromal cells (GASCs) from histologically normal surgical margins have a myofibroblast phenotype and angiogenic properties. *Journal of Pathology*, 233, 1: 74-88

- Cristofalo V.J., Allen R.G., Pignolo R.J., Martin B.G., Beck J.C. 1998. Relationship between donor age and the replicative lifespan of human cells in culture: a reevaluation. *Proceedings of the National Academy of Sciences of the United States of America*, 95, 18: 10614-10619
- da Silva Meirelles L., Maistro Malta T., de Deus Wagatsuma V.M., Palma P.V., Araújo A.G., Ribeiro Malmegrim K.C., Morato de Oliveira F., Panepucci R.A., Silva W.A. Jr., Kashima Haddad S., Covas D.T. 2015. Cultured human adipose tissue pericytes and mesenchymal stromal cells display a very similar gene expression profile. *Stem Cells and Development*, ahead of print, doi:10.1089/scd.2015.0153: 10 p.
- Dasari V.R., Velpula K.K., Kaur K., Fassett D., Klopfenstein J.D., Dinh D.H., Gujrati M., Rao J.S., 2010. Cord blood stem cell-mediated induction of apoptosis in glioma downregulates X-linked inhibitor of apoptosis protein (XIAP). *PLoS ONE*, 5, 7: e11813, doi: 10.1371/journal.pone.0011813: 13 p.
- Deheeger M., Lesniak M.S., Ahmed A.U. 2014. Cellular plasticity regulated cancer stem cell niche: a possible new mechanism of chemoresistance. *Cancer Cell and Microenvironment*, 1, 5: 1-10
- Dell'Albani P. 2008. Stem cell markers in gliomas. *Neurochemical Research*, 33, 12: 2407-2415
- Denysenko T., Gennero L., Roos M., Melcarne A., Juenemann C., Faccani G., Morra I., Cavallo G., Reguzzi S., Pescarmona G., Ponzetto A. 2010. Glioblastoma cancer stem cells: heterogeneity, microenvironment and related therapeutic strategies. *Cell Biochemistry and Function*, 28, 5: 343–351
- Di G.H., Liu Y., Lu Y., Liu J., Wu C., Duan H.F. 2014. IL-6 secreted from senescent mesenchymal stem cells promotes proliferation and migration of breast cancer cells. *PLoS One*, 9, 11: e113572, doi: 10.1371/journal.pone.0113572: 15 p.
- Dimri G.P., Lee X., Basile G. 1995. A biomarker that identifies senescent human cells in culture and in aging skin in vivo. *Proceedings of the National Academy of Sciences of the United States of America*, 92, 20: 9363–9367
- Ding D.C., Chang Y.H., Shyu W.C., Lin S.Z. 2015. Human umbilical cord mesenchymal stem cells: a new era for stem cell therapy. *Cell Transplantation*, 24, 3: 339-347

- Ding D-C., Chou H-L., Hung W-T., Liu H-W., Tang-Yuan Chu T-Y. 2013. Human adipose-derived stem cells cultured in keratinocyte serum free medium: Donor's age does not affect the proliferation and differentiation capacities. *Journal of Biomedical Science*, 20: 59, doi: 10.1186/1423-0127-20-59: 11 p.
- Dominici M., Le Blanc K., Mueller I., Slaper-Cortenbach I., Marini F., Krause D., Deans R., Keating A., Prockop D.J., Horwitz E. 2006. Minimal criteria for defining multipotent mesenchymal stromal cells. The International Society for Cellular Therapy position statement. *Cytotherapy*, 8, 4: 315-317
- Dong L.H., Jiang Y.Y., Liu Y.J., Cui S., Xia C.C., Qu C., Jiang X., Qu Y.Q., Chang P.Y., Liu F. 2015. The anti-fibrotic effects of mesenchymal stem cells on irradiated lungs via stimulating endogenous secretion of HGF and PGE2. *Scientific Reports*, 5: 8713, doi: 10.1038/srep08713: 10 p.
- Doorn J., Moll G., Le Blanc K., van Blitterswijk C., de Boer J. 2012. Therapeutic applications of mesenchymal stromal cells: paracrine effects and potential improvements. *Tissue Engineering Part B*, 18, 2: 101-115
- Droujinine I.A., Eckert M.A., Zhao W. 2013. To grab the stroma by the horns: From biology to cancer therapy with mesenchymal stem cells. *Oncotarget*, 4, 5: 651-664
- D'souza N., Rossignoli F., Golinelli G., Grisendi G., Spano C., Candini O., Osturu S., Catani F., Paolucci P., Horwitz E.M., Dominici M. 2015. Mesenchymal stem/stromal cells as a delivery platform in cell and gene therapies. *BMC Medicine*, 13: 186, doi: 10.1038/srep08713: 15 p.
- Dubois S.G., Floyd E.Z., Zvonic S., Kilroy G., Wu X., Carling S., Halvorsen Y.D., Ravussin E., Gimble J.M. 2008. Isolation of human adipose-derived stem cells from biopsies and liposuction specimens. *Methods in Molecular Biology*, 449: 69-79.
- Duebgen M., Martinez-Quintanilla J., Tamura K., Hingtgen S., Redjal N., Wakimoto H., Shah K. 2014. Stem cells loaded with multimechanistic oncolytic herpes simplex virus variants for brain tumor therapy. *Journal of the National Cancer Institute*, 106, 6: dju090, doi: 10.1093/jnci/dju090: 9 p.

- Dvorak HF. 1986. Tumors: wounds that do not heal. Similarities between tumor stroma generation and wound healing. *The New England Journal of Medicine*, 315, 26: 1650-1659
- Elemi U., Lagente-Chevallier O., Boufraquech M., Prenois F., Courtin F., Caillou B., Talbot M., Dardalhon M., Al Ghuzlan A., Bidart J.M., Schlumberger M., Dupuy C. 2012. ROS-generating NADPH oxidase NOX4 is a critical mediator in oncogenic H-Ras-induced DNA damage and subsequent senescence. *Oncogene*, 31, 9: 1117–1129
- Eyler C.E., Rich J.N. 2008. Survival of the Fittest: Cancer stem cells in therapeutic resistance and angiogenesis. *Journal of Clinical Oncology*, 26, 17: 2839–2845
- Fan X., Khaki L., Zhu T.S., Soules M.E., Talsma C.E., Gul N., Koh C., Zhang J., Li Y.M., Maciaczyk J., Nikkhah G., Dimeco F., Piccirillo S., Vescovi A.L., Eberhart C.G. 2010. NOTCH pathway blockade depletes CD133-positive glioblastoma cells and inhibits growth of tumor neurospheres and xenografts. *Stem Cells*, 28, 1: 5-16
- Fernandes A.M., Marinho P.A.N., Sartore R.C., Paulsen B.S., Mariante R.M., Castilho L.R., Rehen S.K. 2009. Successful scale-up of human embryonic stem cell production in a stirred microcarrier culture system. *Brazilian Journal of Medical and Biological Research*, 42: 515-522
- Ferrari C., Balandras F., Guedon E., Olmos E., Chevalot I., Marc A. 2012. Limiting cell aggregation during mesenchymal stem cell expansion on microcarriers. *Biotechnology Progress*, 28, 3: 780-787
- Fessler E., Borovski T., Medema J.P. 2015. Endothelial cells induce cancer stem cell features in differentiated glioblastoma cells via bFGF. *Molecular Cancer*, 14: 157, doi: 10.1186/s12943-015-0420-3: 12 p.
- Fessler E., Dijkgraaf F.E., De Sousa E Melo F., Medema J.F. 2013. Cancer stem cell dynamics in tumor progression and metastasis: Is the microenvironment to blame? *Cancer Letters*, 341, 1: 97-104
- Frauenschuh S., Reichmann E., Ibold Y., Goetz P. M., Sittlinger M., Ringe J. 2007. A microcarrier-based cultivation system for expansion of primary mesenchymal stem cells. *Biotechnology Progress*, 23: 187-193

- Friedenstein A.J., Gorskaja J.F., Kulagina N.N. 1976. Fibroblast precursors in normal and irradiated mouse hematopoietic organs. *Experimental Hematology*, 4, 5: 267–274
- Gangemi R.M., Griffero F., Marubbi D., Perera M., Capra M.C., Malatesta P., Ravetti G.L., Zona G.L., Daga A., Corte G. 2009. *GSOX2* silencing in glioblastoma tumor-initiating cells causes stop of proliferation and loss of tumorigenicity. *Stem Cells*, 27, 1: 40-48
- Gauthaman K., Yee C.F., Cheyyatraivendran S., Biswas A., Choolani M., Bongso A. 2012. Human umbilical cord Wharton's Jelly stem cell (hWJSC) extracts inhibit cancer cell growth in vitro. *Journal of Cellular Biochemistry*, 113, 6: 2027–2039
- Glenn J.D., Whartenby K.A. 2014. Mesenchymal stem cells: Emerging mechanisms of immunomodulation and therapy. *World Journal of Stem Cells*, 6, 5: 526-539
- Goffart N., Kroonen J., Rogister B. 2013. Glioblastoma-initiating cells: Relationship with neural stem cells and the micro-environment. *Cancers*, 14, 5: 1049-1071
- Goh T. K-P., Zhang Z-Y., Chen A. K-L., Reuveny S., Choolani M., Chan J. K. Y. 2013. Microcarrier culture for efficient expansion and osteogenic differentiation of human fetal mesenchymal stem cells. *BioResearch*, 2, 2: 84-97
- Golebiewska A., Bougnaud S., Stieber D., Brons N.H., Vallar L., Hertel F., Klink B., Schröck E., Bjerkvig R., Niclou S.P. 2013. Side population in human glioblastoma is non-tumorigenic and characterizes brain endothelial cells. *Brain*, 136, 5: 1462-1475
- Gondi C.S., Gogineni V.R., Chetty C., Dasari R.V., Gorantla B., Gujrati M., Dinh D.H., Rao J.S., 2010. Induction of apoptosis in glioma cells requires cell-to-cell contact with human umbilical cord blood stem cells. *International Journal of Oncology*, 36, 5: 1165–1173
- Guilhot J., Bennaceur-Griscelli A., Turhan A., Chomel J. C., Karayan-Tapon L. 2014. A mesenchymal glioma stem cell profile is related to clinical outcome. *Oncogenesis* 17, 3: 2157–2166
- Günther H.S., Schmidt N.O., Phillips H.S., Kemming D., Kharbanda S., Soriano R., Modrusan Z., Meissner H., Westphal M., Lamszus K. 2008. Glioblastoma-derived stem cell-enriched cultures form distinct subgroups according to molecular and phenotypic criteria. *Oncogene*, 27, 20: 2897-2909

- Gupta P.B., Chaffer C.L., Weinberg R.A. 2009. Cancer stem cells: mirage or reality? *Nature Medicine*, 15, 9: 1010-1012
- Hall B., Andreeff M., Marini F. 2007. The participation of mesenchymal stem cells in tumor stroma formation and their application as targeted-gene delivery vehicles. *Handbook of Experimental Pharmacology*, 180, 263–283
- Han M., Guo L., Zhang Y., Huang B., Chen A., Chen W., Liu X., Sun S., Wang K., Liu A., Li X. 2015. Clinicopathological and prognostic significance of cd133 in glioma patients: a meta-analysis. *Molecular Neurobiology*, DOI 10.1007/s12035-014-9018-9: 8 p.
- Hass R., Kasper C., Böhm S., Jacobs S.R. 2011. Different populations and sources of human mesenchymal stem cells (MSC): A comparison of adult and neonatal tissue-derived MSC. *Cell Communication and Signaling*, 9: 12, doi: 10.1186/1478-811X-9-12: 14 p.
- Heathman T.R., Nienow A.W., McCall M.J., Coopman K., Kara B., Hewitt C.J. 2015. The translation of cell-based therapies: clinical landscape and manufacturing challenges. *Regenerative Medicine*, 10, 1: 49-64
- Henning R.J., Dennis S., Sawmiller D., Hunter L., Sanberg P., Miller L. 2012. Human umbilical cord blood mononuclear cells activate the survival protein Akt in cardiac myocytes and endothelial cells that limits apoptosis and necrosis during hypoxia. *Translational Research*, 159, 6: 497-506
- Hewitt C.J., Lee K., Nienow A.W., Thomas R.J., Smith M., Thomas C.R. 2011. Expansion of human mesenchymal stem cells on microcarriers. *Biotechnology Letters*, 33, 11: 2325-2335
- Hong I.S., Lee H.Y., Kang K.S. 2014. Mesenchymal stem cells and cancer: Friends or enemies? *Mutation Research*, 768, 98-106
- Huang S., Wu Y., Gao D., Fu X. 2015. Paracrine action of mesenchymal stromal cells delivered by microspheres contributes to cutaneous healing and prevents scar formation in mice. *Cytherapy*, 17, 7: 922-931
- Hupfeld J., Gorr I.H., Schwald C., Beaucamp N., Wiechmann K., Kuentzer K., Huss R., Rieger B., Neubauer M., Wegmeyer H. 2014. Modulation of mesenchymal stromal cell characteristics by microcarrier culture in bioreactors. *Biotechnology and bioengineering*, 111, 11: 2290-2302

- Hwang E.S. 2014. Senescence suppressors: their practical importance in replicative lifespan extension in stem cells. *Cellular and Molecular Life Sciences*, 71, 21: 4207-4219
- Iyyanki T., Hubenak J., Liu J., Chang E.I., Beahm E.K., Zhang Q. 2015. Harvesting technique affects adipose-derived stem cell yield. *Aesthetic Surgery Journal*, 35, 4: 467-476
- Jackson M., Hassiotou F., Nowak A. 2015. Glioblastoma stem-like cells: at the root of tumor recurrence and a therapeutic target. *Carcinogenesis*, 36, 2: 177-185
- Jeon H.M., Sohn Y.W., Oh S.Y., Kim S.H., Beck S., Kim S., Kim H. 2011. ID4 imparts chemoresistance and cancer stemness to glioma cells by derepressing mir-9*-mediated suppression of SOX2. *Cancer Research*, 71, 9: 3410-3421
- Jiao H, Yang B, Guan F, Li J, Shan H, Song L, Hu X, Liang S, Du Y, Jiang C. 2011a. The mixed human umbilical cord blood-derived mesenchymal stem cells show higher antitumor effect against C6 cells than the single in vitro. *Neurology Research*, 33, 4: 405-415
- Jiao H., Gua F., Yang B., Li J., Song L., Hu X., Du Y. 2011b. Human amniotic membrane derived-mesenchymal stem cells induce C6 glioma apoptosis in vivo through the Bcl-2/caspase pathways. *Molecular Biology Reports*, 39, 1: 467-473
- Jiao H., Guan F., Yang B., Li J., Song L., Hu X., Du Y. 2011c. Human umbilical cord blood-derived mesenchymal stem cells inhibit C6 glioma via downregulation of cyclin D1. *Neurology India*, 59, 2: 241-248
- Johal K.S., Lees V.C., Reid A.J. 2015. Adipose-derived stem cells: selecting for translational success. *Regenerative Medicine*, 10, 1: 79-96
- Jurgens W.J., Oedayrajsingh-Varma M.J., Helder M.N., Zandiehoulabi B., Schouten T.E., Kuik D.J., Ritt M.J., van Milligen F.J. 2008. Effect of tissue-harvesting site on yield of stem cells derived from adipose tissue: implications for cell-based therapies. *Cell Tissue Research*, 332, 3: 415-426
- Kang S-G., Jeun S.S., Lim J. Y., Kim S.M., Yang Y.S., Oh W.I., Huh P-W., Park C.K., 2008. Cytotoxicity of human umbilical cord blood-derived mesenchymal stem cells against human malignant glioma cells. *Child's Nervous System*, 24, 3: 293-302

- Karnoub A.E., Dash A.B., Vo A.P., Sullivan A., Brooks M.W., Bell G.W., Richardson A.L., Polyak K., Tubo R., Weinberg R.A. 2007. Mesenchymal stem cells within tumour stroma promote breast cancer metastasis. *Nature*, 449, 7162: 557–563
- Karnoub A.E., Dash A.B., Vo A.P., Sullivan A., Brooks M.W., Bell G.W., Richardson A.L., Polyak K., Tubo R., Weinberg R. a. 2007. Mesenchymal stem cells within tumour stroma promote breast cancer metastasis. *Nature*, 449, 7162: 557–563
- Kern S., Eichler H., Stoeve J., Klüter H., Bieback K. 2006. Comparative analysis of mesenchymal stem cells from bone marrow, umbilical cord blood, or adipose tissue. *Stem Cells*, 24, 5: 1294-1301
- Kim K.S., Seu Y.B., Baek S.H., Kim M.J., Kim K.J., Kim J.H., Kim J.R. 2007. Induction of cellular senescence by insulin-like growth factor binding protein-5 through a p53-dependent mechanism. *Molecular Biology of the Cell*, 18, 11: 4543-4552
- Kim M.D., Kim S.S., Cha H.Y., Jang S.H., Chang D.Y., Kim W., Suh-Kim H., Lee J.H. 2014. Therapeutic effect of hepatocyte growth factor-secreting mesenchymal stem cells in a rat model of liver fibrosis. *Experimental Molecular Medicine*, 46: e110, doi: 10.1038/emm.2014.49: 10 p.
- Kinnaird T., Stabile E., Burnett M.S., Lee C.W., Barr S., Fuchs S., Epstein S.E. 2004. Marrow-derived stromal cells express genes encoding a broad spectrum of arteriogenic cytokines and promote in vitro and in vivo arteriogenesis through paracrine mechanisms. *Circulation Research*, 94, 5: 678-685
- Kleinschmidt K., Klinge P.M., Stopa E., Wallrapp C., Glage S., Geigle P., Brinker T. 2011. Alginate encapsulated human mesenchymal stem cells suppress syngeneic glioma growth in the immunocompetent rat. *Journal of Microencapsulation*, 28, 7: 621–628
- Kološa K., Motaln H., Herold-Mende C., Koršič M., Lah Turnšek T. 2015. Paracrine effects of mesenchymal stem cells induce senescence and differentiation of glioblastoma stem-like cells. *Cell transplantation*, 24, 4: 631-644
- Köritzer J., Boxhammer V., Schäfer A., Shimizu T., Klämpfl T. G., Li Y.-F., Welz C. 2013. Restoration of Sensitivity in Chemo - Resistant Glioma Cells by Cold Atmospheric Plasma. *PloS One*, 8, 5: e64498, doi: 10.1371/journal.pone.0064498: 10 p.

- Kortlever R. M., Higgins P. J., Bernards R. 2006. Plasminogen activator inhibitor-1 is a critical downstream target of p53 in the induction of replicative senescence. *Nature Cell Biology*, 8, 8: 877–884
- Kosaka H., Ichikawa T., Kurozumi K., Kambara H., Inoue S., Maruo T., Nakamura K., Hamada H., Date I. 2012. Therapeutic effect of suicide gene transferred mesenchymal stem cells in a rat model of glioma. *Cancer Gene Therapy*, 19, 8: 572-578
- Krakstad C., Chekenya M. 2010. Survival signalling and apoptosis resistance in glioblastomas: opportunities for targeted therapeutics. *Molecular Cancer*, 9, 135-149
- Kucerova L., Matuskova M., Hlubinova K., Altanero V., Altaner C. 2010. Tumor cell behaviour modulation by mesenchymal stromal cells. *Molecular Cancer*, 9, 129-144
- Kuilman T., Michaloglou C., Mooi W.J., Peeper D.S. 2010. The essence of senescence. *Genes and Development*, 24, 22: 2463-2479
- Li H., Fu X. 2012. Mechanisms of action of mesenchymal stem cells in cutaneous wound repair and regeneration. *Cell Tissue Research*, 348, 3: 371-377
- Li R., Li H., Yan W., Yang P., Bao Z., Zhang C., Jiang T., You Y. 2015. Genetic and clinical characteristics of primary and secondary glioblastoma is associated with differential molecular subtype distribution. *Oncotarget*, 6, 9: 7318-7324
- Liang X., Ding Y., Zhang Y., Tse H.F., Lian Q. 2014 Paracrine mechanisms of mesenchymal stem cell-based therapy: current status and perspectives. *Cell Transplantation*, 23, 9: 1045-1059
- Lin S.P., Chiu F.Y., Wang Y., Yen M.L., Kao S.Y., Hung S.C. 2014. RB maintains quiescence and prevents premature senescence through upregulation of DNMT1 in mesenchymal stromal cells. *Stem Cell Reports*, 3, 6: 975-986
- Liu G., Yuan X., Zeng Z., Tunici P., Ng H., Abdulkadir I.R., Lu L., Irvin D., Black K.L., Yu J.S. 2006. Analysis of gene expression and chemoresistance of CD133+ cancer stem cells in glioblastoma. *Molecular Cancer*, 5, 67-79
- Longley D.B., Harkin D.P., Johnston P.G. 2003. 5-fluorouracil: mechanisms of action and clinical strategies. *Nature Reviews Cancer*, 3, 5: 330-338

- Mahmoudifar N., Doran P.M. 2010. Chondrogenic differentiation of human adipose-derived stem cells in polyglycolic acid mesh scaffolds under dynamic culture conditions. *Biomaterials*, 31, 14: 3858-3867
- Maijenburg M.W., Noort W.A., Kleijer M., Kompier C.J., Weijer K., van Buul J.D., van der Schoot C.E., Voermans C. 2010. Cell cycle and tissue of origin contribute to the migratory behaviour of human fetal and adult mesenchymal stromal cells. *British Journal of Haematology*, 148, 3: 428–440
- Marinho P.A., Vareschini D.T., Gomes I.C., Paulsen B.da S., Furtado D.R., Castilho L.dos R., Rehen S.K. 2013. Xeno-free production of human embryonic stem cells in stirred microcarrier systems using a novel animal/human-component-free medium. *Tissue Engineering Part C*, 19, 2: 146-155
- Mariotti V., Greco S.J., Mohan R.D., Nahas G.R., Rameshwar P. 2014. Stem cell in alternative treatments for brain tumors: potential for gene delivery. *Molecular Cancer Therapeutics*, 2: 24, doi: 10.1186/2052-8426-2-24: 10 p.
- Markvicheva E., Grandfils Ch. 2004. Microcarriers for animal cell culture. V: Fundamentals of Cell Immobilisation Biotechnology, Series Focus on Biotechnology. Willaert R., Nedovich V. (eds). Dordrecht-Boston-London, Kluwer Academic Publishers: 441-461
- Martin I., Wendt D., Heberer M. 2004. The role of bioreactors in tissue engineering. *TRENDS in Biotechnology*, 22, 2: 80-86
- Martín V., Sanchez-Sanchez A.M., Herrera F., Gomez-Manzano C., Fueyo J., Alvarez-Vega M.A., Antolín I., Rodriguez C. 2013. Melatonin-induced methylation of the ABCG2/BCRP promoter as a novel mechanism to overcome multidrug resistance in brain tumour stem cells. *British Journal of Cancer*, 108, 10: 2005-2012
- Martinez-Quintanilla J., Bhere D., Heidari P., He D., Mahmood U., Shah K. 2013. Therapeutic efficacy and fate of bimodal engineered stem cells in malignant brain tumors. *Stem Cells*, 31, 8: 1706-1714
- Matuskova M., Hlubinova K., Pastorakova A., Hunakova L., Altanero V., Altaner C., Kucerova L. 2010. HSV-tk expressing mesenchymal stem cells exert bystander effect on human glioblastoma cells. *Cancer Letters*, 290, 1: 58–67

- McGuirk J.P., Smith J.R., Divine C.L., Zuniga M., Weiss M.L. 2015. Wharton's jelly-derived mesenchymal stromal cells as a promising cellular therapeutic strategy for the management of graft-versus-host disease. *Pharmaceuticals*, 8, 2: 196-220
- McNamara M.G., Lwin Z., Jiang H., Chung C., Millar B.A., Sahgal A., Laperriere N., Mason W.P. 2014. Conditional probability of survival and post-progression survival in patients with glioblastoma in the temozolomide treatment era. *Journal of Neurooncology*, 117, 1: 153-160
- Meir E.G. Van, Hadjipanayis C.G., Norden A.D., Shu H., Wen P.Y., Olson J.J. 2010. Exciting new advances in neuro-oncology: The avenue to a cure for malignant glioma. *A Cancer Journal for Clinicians*, 60, 3: 166-193
- Meirelles L.da S, Maistro Malta T., de Deus Wagatsuma V.M., Palma P.V., Araújo A.G., Ribeiro Malmegrim K.C., Morato de Oliveira F., Panepucci R.A., Silva W.A. Jr., Kashima Haddad S., Covas DT. 2015. Cultured Human Adipose Tissue Pericytes and Mesenchymal Stromal Cells Display a Very Similar Gene Expression Profile. *Stem Cells and Development*, ahead of print, doi:10.1089/scd.2015.0153: 12 p.
- Meirelles L.da S., Fontes A.M., Covas D.T., Caplan A.I. 2009. Mechanisms involved in the therapeutic properties of mesenchymal stem cells. *Cytokine and Growth Factors Reviews*, 20, 5-6: 419-427
- Miconi G., Palumbo P., Dehcordi S.R., La Torre C., Lombardi F., Evtoski Z., Cimini A.M., Galzio R., Cifone M.G., Cinque B. 2015. Immunophenotypic characterization of human glioblastoma stem cells: correlation with clinical outcome. *Journal of Cellular Biochemistry*, 116, 5: 864-876
- Moiseeva O., Mallette F.A, Mukhopadhyay U.K., Moores A., Ferbeyre G. 2006. DNA damage signalling and p53-dependent senescence after prolonged-interferon stimulation. *Molecular Biology of the Cell*, 17, 4: 1583-1592
- Mosmann T. 1983. Rapid colorimetric assay for cellular growth and survival: Application to proliferation and cytotoxicity assays. *Journal of Immunology Methods*, 65: 55-63
- Motaln H., Gruden K., Hren M., Schichor C., Primon M., Rotter A., Lah T.T. 2012. Human mesenchymal stem cells exploit the immune response mediating chemokines to impact the phenotype of glioblastoma. *Cell Transplantation*, 21, 7: 1529-1545

- Motaln H., Schichor C., Lah T.T. 2010. Human mesenchymal stem cells and their use in cell-based therapies. *Cancer*, 116, 11: 2519-2530
- Motaln H., Turnsek T.L. 2015. Cytokines play a key role in communication between mesenchymal stem cells and brain cancer cells. *Protein and Peptide Letters*, 22, 4: 322-331
- Murphy M.B., Moncivais K., Caplan A.I. 2013. Mesenchymal stem cells: environmentally responsive therapeutics for regenerative medicine. *Experimental and Molecular Medicine*, 45: e54, doi: 10.1038/emm.2013.94: 16 p.
- Nakamizo A., Marini F., Amano T., Khan A., Studeny M., Gumin J., Chen J., Hentschel S., Vecil G., Dembinski J., Andreeff M., Lang F.F. 2005. Human Bone Marrow – Derived Mesenchymal Stem Cells in the Treatment of Gliomas. *Cancer Research*, 65, 8: 3307–3318
- Nakamura K., Ito Y., Kawano Y., Kurozumi K., Kobune M., Tsuda H., Bizen A., Honmou O., Niitsu Y., Hamada H., 2004. Antitumor effect of genetically engineered mesenchymal stem cells in a rat glioma model. *Gene Therapy*, 11, 14: 1155-1164
- Nakashima H., Kaur B., Chiocca E. 2010. Directing systemic oncolytic viral delivery to tumors via carrier cells. *Cytokine Growth Factor Reviews*, 21, 2-3: 119–126
- Nam T. J., Busby W. Jr., Clemmons D. R. 1997. Insulin-like growth factor binding protein-5 binds to plasminogen activator inhibitor-I. *Endocrinology*, 138, 7: 2972–2978
- Ng Y-C., Berry J. M., Butler M. 1996. Optimization of physical parameters for cell attachment and growth on macroporous microcarriers. *Biotechnology Bioengineering*, 50: 627-635
- Nienow A.W. 2006. Reactor engineering in large scale animal cell culture. *Cytotechnology*, 50: 9-31
- Oedayrajsingh-Varma M.J., Ham S.M. van, Knippenberg M., Helder M.N., Klein-Nulend J., Schouten T.E., Ritt M.J., Milligen F.J. van. 2006. Adipose tissue-derived mesenchymal stem cell yield and growth characteristics are affected by the tissue-harvesting procedure. *Cytotherapy* 8, 2: 166–177

- Ohgaki H., Kleihues P. 2013. The definition of primary and secondary glioblastoma. *Clinical Cancer Research*, 19, 4: 764–772
- Ong W.K., Sugii S. 2013. Adipose-derived stem cells: fatty potentials for therapy. *The International Journal of Biochemistry and Cell Biology*, 45, 6: 1083-1086
- Osmond T.L., Broadley K.W., McConnell M.J. 2010. Glioblastoma cells negative for the anti-CD133 antibody AC133 express a truncated variant of the CD133 protein. *International Journal of Molecular Medicine*, 25, 6: 883-888
- Ostrom Q.T., Bauchet L., Davis F.G., Deltour I., Fisher J.L., Langer C.E., Pekmezci M., Schwartzbaum J.A., Turner M.C., Walsh K.M., Wrensch M.R., Barnholtz-Sloan J.S. 2014. The epidemiology of glioma in adults: a "state of the science" review. *Neuro-Oncology*, 16, 7: 896-913
- Paladino F.V., Peixoto-Cruz J.S., Santacruz-Perez C., Goldberg A.C. 2015. Comparison between isolation protocols highlights intrinsic variability of human umbilical cord mesenchymal cells. *Cell and Tissue Banking*, DOI 10.1007/s10561-015-9525-6: 14 p.
- Passos J.F., Nelson G., Wang C., Richter T., Simillion C., Proctor C.J., Miwa S., Olijslagers S., Hallinan J., Wipat A., Saretzki G., Rudolph K.L., Kirkwood T.B., von Zglinicki T. 2010. Feedback between p21 and reactive oxygen production is necessary for cell senescence. *Molecular Systems Biology*, 6: 347-361
- Podergajs N., Brekka N., Radlwimmer B., Herold-Mende C., Talasila K. M., Tiemann K., Rajcevic U., Lah T. T., Bjerkvig R., Miletic H. 2013. Expansive growth of two glioblastoma stem-like cell lines is mediated by bFGF and not by EGF. *Radiology Oncology*, 47, 4: 330–337
- Raggi C., Berardi A.C. 2012. Mesenchymal stem cells, aging and regenerative medicine. *Muscles Ligaments and Tendons Journal*, 2, 3: 239-242
- Ramdasi S., Sarang S., Viswanathan C. 2015. Potential of mesenchymal stem cell based application in cancer. *International Journal of Hematology-Oncology and Stem Cell Research*, 9, 2: 95-103

- Ren J., Stroncek D.F., Zhao Y., Jin P., Castiello L., Civini S., Wang H., Feng J., Tran K., Kuznetsov S.A., Robey P.G., Sabatino M. 2013. Intra-subject variability in human bone marrow stromal cell (BMSC) replicative senescence: molecular changes associated with BMSC senescence. *Stem Cell Research*, 11, 3: 1060-1073
- Riganti C., Salaroglio I.C., Caldera V., Campia I., Kopecka J., Mellai M., Annovazzi L., Bosia A., Ghigo D., Schiffer D. 2013. Temozolomide downregulates P-glycoprotein expression in glioblastoma stem cells by interfering with the Wnt3a/glycogen synthase-3 kinase/ β -catenin pathway. *Neuro-Oncology*, 15, 11: 1502-1517
- Ringde'n O., Uzunel M., Rasmusson I., Remberger M., Sundberg B., Lönnies H., Marschall H.U., Dlugosz A., Szakos A., Hassan Z., Omazic B., Aschan J., Barkholt L., Le Blanc K. 2006. Mesenchymal stem cells for treatment of therapy-resistant graft-versus-host disease. *Transplantation*, 27, 81: 1390–1397
- Rombouts W. J. C., Ploemacher R. E. 2003. Primary murine MSC show highly efficient homing to the bone marrow but lose homing ability following culture. *Leukemia*, 17, 1: 160–170
- Rowley J., Abraham E., Campbell A., Brandwein H., Oh S. 2012. Meeting lot-size challenges of manufacturing adherent cells for therapy. *BioProcess International*, 10: 16-22
- Russell K.C., Phinney D.G., Lacey M.R., Barrilleaux B.L., Meyertholen K.E., O'Connor K.C. 2010. In vitro high-capacity assay to quantify the clonal heterogeneity in trilineage potential of mesenchymal stem cells reveals a complex hierarchy of lineage commitment. *Stem Cells*, 28, 4: 788-798
- Ryu C., Park S., Park S., Kim S., Lim J., Jeong C., Yoon W., Oh W., Sung Y., Jeun S. 2011. Gene therapy of intracranial glioma using interleukin 12-secreting human umbilical cord blood-derived mesenchymal stem cells. *Human Gene Therapy*, 22, 6: 733–743
- Sabin R.J., Anderson R.M. 2011. Cellular Senescence - its role in cancer and the response to ionizing radiation. *Genome Integrity*, 2: 7-16
- Sachs P.C., Francis M.P., Zhao M., Brumelle J., Rao R.R., Elmore L.W., Holt S.E. 2012. Defining essential stem cell characteristics in adipose-derived stromal cells extracted from distinct anatomical sites. *Cell Tissue Research*, 349, 2: 505-515

- Saito N., Fu J., Zheng S., Yao J., Wang S., Liu D. D., Yuan Y., Sulman E. P., Lang F. F., Colman H., Verhaak R. G., Yung A. W. K., Koul D. 2013. A high Notch pathway activation predicts response to γ -secretase inhibitors in proneural subtype of glioma tumor-initiating cells. *Stem cells*, 32, 1: 301-312
- Sandberg C.J., Altschuler G., Jeong J., Strømme K.K., Stangeland B., Murrell W., Grasmow U.H., Myklebost O., Helseth E., Vik-Mo E.O., Hide W., Langmoen I.A. 2013. Comparison of glioma stem cells to neural stem cells from the adult human brain identifies dysregulated Wnt-signaling and a fingerprint associated with clinical outcome. *Experimental Cell Research*, 319, 14: 2230-2243
- Santos F.d, Andrade P.Z., Abecasis M.M., Gimble J.M., Chase L.G., Campbell A.M., Boucher S., Vemuri M.C., Silva C.L., Cabral J.M. 2011. Toward a clinical-grade expansion of mesenchymal stem cells from human sources: a microcarrier-based culture system under xeno-free conditions. *Tissue engineering Part C, Methods*, 17, 12: 1201-1210
- Sart S., Agathos S.N., Li Y. 2013. Engineering stem cell fate with biochemical and biomechanical properties of microcarriers. *Biotechnology Progress*, 29, 6: 1354-1366
- Sart S., Schneider Y.J., Agathos S.N. 2009. Ear mesenchymal stem cells: An efficient adult multipotent cell population fit for rapid and scalable expansion. *Journal of Biotechnology*, 139, 4: 291-299
- Sasportas L.S., Kasmieh R., Wakimoto H., Hingtgen S., van de Water J.A., Mohapatra G., Figueiredo J.L., Martuza R.L., Weissleder R., Shah K. 2009. Assessment of therapeutic efficacy and fate of engineered human mesenchymal stem cells for cancer therapy. *Proceedings of the National Academy of Sciences of the United States of America*, 106, 12: 4822–4827
- Schioppa T., Uranchimeg B., Saccani A., Biswas S.K., Doni A., Rapisarda A., Bernasconi S., Saccani S., Nebuloni M., Vago L., Mantovani A., Melillo G., Sica A. 2003. Regulation of the chemokine receptor CXCR4 by hypoxia. *Journal of Experimental Medicine*, 198, 9: 1391–1402
- Schipper B. M., Marra K. G., Zhang W., Donnenberg A. D., Rubin J. P. 2008. Regional anatomic and age effects on cell function of human adipose-derived stem cells. *Annals of plastic surgery*, 60, 5: 538-544

- Schop D., van Dijkhuizen-Radersma R., Borgart E., Janssen F. W., Rozemuller H., Prins H. J. 2010. Expansion of human mesenchymal stromal cells on microcarriers: growth and metabolism. *Journal of Tissue Engineering and Regenerative Medicine*, 4: 131-40
- Sepúlveda J.C., Tomé M., Fernández M.E., Delgado M., Campisi J., Bernad A., González M.A. 2014. Cell senescence abrogates the therapeutic potential of human mesenchymal stem cells in the lethal endotoxemia model. *Stem Cells*, 32, 7: 1865-1877
- Severino V., Alessio N., Farina A., Sandomenico A., Cipollaro M., Peluso G., Galderisi U., Chambery A. 2013. Insulin-like growth factor binding proteins 4 and 7 released by senescent cells promote premature senescence in mesenchymal stem cells. *Cell Death and Disease*, 4: e911, doi: 10.1038/cddis.2013.445: 11 p.
- Shi M., Li J., Liao L., Chen B., Li B., Chen L., Jia H., Zhao R.C. 2007. Regulation of CXCR4 expression in human mesenchymal stem cells by cytokine treatment: role in homing efficiency in NOD/SCID mice. *Haematologica*, 92, 7: 897–904
- Signore M., Pelacchi F., di Martino S., Runci D., Biffoni M., Giannetti S., Morgante L., De Majo M., Petricoin E.F., Stancato L., Larocca L.M., De Maria R., Pallini R., Ricci-Vitiani L. 2014. Combined PDK1 and CHK1 inhibition is required to kill glioblastoma stem-like cells in vitro and in vivo. *Cell Death and Disease*, 5: e1223, doi: 10.1038/cddis.2014.188: 12 p.
- Singh S.K., Clarke I.D., Terasaki M., Bonn V.E., Hawkins C., Squire J., Dirks P.B. 2003. Identification of a cancer stem cell in human brain tumors. *Cancer Research*, 63, 18: 5821-5828
- Singh S.K., Hawkins C., Clarke I.D., Squire J.A., Bayani J., Hide T., Henkelman R.M., Cusimano M.D., Dirks P.B. 2004. Identification of human brain tumour initiating cells. *Nature*, 432: 396–401
- Sohni A., Verfaillie C.M. 2013. Mesenchymal stem cells migration homing and tracking. *Stem Cells International*, 2013: 130763, doi: 10.1155/2013/130763: 8 p.
- Sonabend A., Ulasov I., Tyler M., Rivera A., Mathis J., Lesniak M. 2008. Mesenchymal stem cells effectively deliver an oncolytic adenovirus to intracranial glioma. *Stem Cells* 26, 3: 831–841

- Song B., Kim B., Choi S.H., Song K.Y., Chung Y.G., Lee Y.S., Park G. 2014. Mesenchymal stromal cells promote tumor progression in fibrosarcoma and gastric cancer cells. *The Korean Journal of Pathology*, 48, 3: 217-224
- Spaeth E., Klopp A., Dembinski J., Andreeff M., Marini F. 2008. Inflammation and tumor microenvironments: defining the migratory itinerary of mesenchymal stem cells. *Gene Therapy*, 15, 10: 730-738
- Stieber D., Golebiewska A., Evers L., Lenkiewicz E., Brons N.H., Nicot N., Oudin A., Bougnaud S., Hertel F., Bjerkvig R., Vallar L., Barrett M.T., Niclou S.P. 2014. Glioblastomas are composed of genetically divergent clones with distinct tumorigenic potential and variable stem cell-associated phenotypes. *Acta Neuropathologica*, 127, 2: 203-219
- Stopschinski B.E., Beier C.P., Beier D. 2013. Glioblastoma cancer stem cells – From concept to clinical application. *Cancer Letters*, 338, 1: 32-40
- Strojnik T., Røsland G.V., Sakariassen P.O., Kavalar R., Lah T. 2007. Neural stem cell markers, nestin and musashi proteins, in the progression of human glioma: correlation of nestin with prognosis of patient survival. *Surgical Neurology*, 68, 2: 133-143
- Stuckey D.W., Shah K. 2014. Stem cell-based therapies for cancer treatment: separating hope from hype. *Nature Cancer Reviews*, 14, 10: 683-691
- Studený M., Marini F.C., Dembinski J.L., Zompetta C., Cabreira-Hansen M., Bekele B.N., Champlin R.E., Andreeff M. 2004. Mesenchymal Stem Cells: Potential Precursors for Tumor Stroma and Targeted-Delivery Vehicles for Anticancer Agents. *Journal of the National Cancer Institute*, 96, 21: 1593–1603
- Sun L.Y., Hsieh D.K., Syu W.S., Li Y.S., Chiu H.T., Chiou T.W. 2010. Cell proliferation of human bone marrow mesenchymal stem cells on biodegradable microcarriers enhances in vitro differentiation potential. *Cell Proliferation*, 43, 5: 445-456
- Sun Z., Wang S., Zhao R.C. 2014. The roles of mesenchymal stem cells in tumor inflammatory microenvironment. *Journal of Hematology and Oncology*, 7: 14, doi: 10.1186/1756-8722-7-14: 10 p.

- Tajnšek U., Motaln H., Levičar N., Rotter A., Lah T. 2013. The duality of stem cells: Doubleedged sword in tumor evolution and treatment. V: Trends in Stem Cell Proliferation and Cancer Research. Resende R.R., Ulrich H. (eds). Netherlands, Springer: 391–433
- Takahashi K., Yoshida N., Murakami N., Kawata K., Ishizaki H., Tanaka-Okamoto M., Miyoshi J., Zinn A.R., Shime H., Inoue N. 2003. Dynamic regulation of p53 subnuclear localization and senescence by MORC3. *Molecular Biology of the Cell*, 18, 5: 1701–1709
- Tamura K., Aoyagi M., Ando N., Ogishima T., Wakimoto H., Yamamoto M., Ohno K. 2013. Expansion of CD133-positive glioma cells in recurrent de novo glioblastomas after radiotherapy and chemotherapy. *Journal of Neurosurgery*, 119, 5: 1145-1455
- Tanna T., Sachan V. 2014. Mesenchymal stem cells: potential in treatment of neurodegenerative diseases. *Current Stem Cells Research and Therapy*, 9, 6: 513-521
- Thiessen B., Stewart C., Tsao M., Kamel-Reid S., Schaiquevich P., Mason W., Easaw J., Belanger K., Forsyth P., McIntosh L., Eisenhauer E. 2010. A phase I/II trial of GW572016 (lapatinib) in recurrent glioblastoma multiforme: clinical outcomes, pharmacokinetics and molecular correlation. *Cancer Chemotherapy and Pharmacology*, 65, 2: 353-361
- Timmins N. E., Kiel M., Günther M., Heazlewood C., Doran M. R., Brooke G., Atkinson K. 2012. Closed System Isolation and Scalable Expansion of Human Placental Mesenchymal Stem Cells. *Biotechnology and Bioengineering*, 109, 7: 1817-1826
- Ulasov I.V., Nandi S., Dey M., Sonabend A.M., Lesniak M.S. 2011. Inhibition of Sonic Hedgehog and Notch Pathways Enhances Sensitivity of CD133+ Glioma Stem Cells to Temozolomide Therapy. *Molecular Medicine*, 17, 1-2: 103-112
- van Wezel A. L. 1967. Growth of cell-strains and primary cells on microcarriers in homogeneous culture. *Nature*, 216: 64-65
- Visvader J.E., Lindeman G.J. 2008. Cancer stem cells in solid tumours: accumulating evidence and unresolved questions. *Nature Reviews Cancer*, 8, 10: 755-768
- Visvader J.E., Lindeman G.J. 2010. Stem cells and cancer – The promise and puzzles. *Molecular Oncology*, 4, 5: 369-372

- Wagner W., Bork S., Lepperdinger G., Joussen S., Ma N., Strunk D., Koch C. 2010. How to track cellular aging of mesenchymal stromal cells? *Aging*, 2, 4: 224-230
- Wagner W., Horn P., Castoldi M., Diehlmann A., Bork S., Saffrich R., Benes V., Blake J., Pfister S., Eckstein V., Ho A.D. 2008. Replicative senescence of mesenchymal stem cells: a continuous and organized process. *PLoS One*, 3, 5: e2213, doi: 10.1371/journal.pone.0002213: 12 p.
- Wan F., Herold-Mende C., Campos B., Centner F.S., Dictus C, Becker N., Devens F., Mogler C., Felsberg J., Grabe N., Reifenberger G., Lichter P., Unterberg A., Bermejo J.L., Ahmadi R. 2011. Association of stem cell-related markers and survival in astrocytic gliomas. *Biomarkers*, 16, 2: 136-143
- Wan F., Zhang S., Xie R., Gao B., Campos B., Herold-Mende C., Lei T. 2010. The utility and limitations of neurosphere assay, CD133 immunophenotyping and side population assay in glioma stem cell research. *Brain pathology*, 20, 5: 877–89
- Wang J., Sakariassen P.Ø., Tsinkalovsky O., Immervoll H., Bøe S.O., Svendsen A., Prestegarden L., Røsland G., Thorsen F., Stuhr L., Molven A., Bjerkvig R., Enger P.Ø. 2008. CD133 negative glioma cells form tumors in nude rats and give rise to CD133 positive cells. *International Journal of Cancer*, 122, 4: 761-768
- Wang J., Wakeman T. P., Latha J. D., Hjelmeland A. B., Wang X. F., White R. R., Rich J. N., Bruce A., Sullenger B. A. 2010. Notch promotes radioresistance of glioma stem cells. *Stem Cells*, 28, 1: 17–28
- Wang S. P., Wang Z. H., Peng D. Y., Li S. M., Wang H., Wang X. H. 2012. Therapeutic effect of mesenchymal stem cells in rats with intracerebral hemorrhage: Reduced apoptosis and enhanced neuroprotection. *Molecular Medicine Reports*, 6, 4: 848–854
- Wang S.H., Hung C.S., Peng T.S., Huang C.C., Wei M.H., Guo J.Y., Fu S.Y., Lai C.M., Chen C.C. 2004. Mesenchymal stem cells in the Wharton's jelly of the human umbilical cord. *Stem Cells*, 22, 1330–1337
- Wegmeyer H., Bröske A.M., Leddin M., Kuentzer K., Nisslbeck A.K., Hupfeld J., Wiechmann K., Kuhlen J., von Schwerin C., Stein C., Knothe S., Funk J., Huss R., Neubauer M. 2013. Mesenchymal stromal cell characteristics vary depending on their origin. *Stem Cells and Development*, 22, 19: 2606-2618

- Westermarck B. 2012. Glioblastoma-a moving target. *Upsala Journal of Medical Sciences*, 117, 2: 251–256
- Wu B., Sun C., Feng F., Ge M., Xia L. 2015. Do relevant markers of cancer stem cells CD133 and Nestin indicate a poor prognosis in glioma patients? A systematic review and meta-analysis. *Journal of Experimental and Clinical Cancer Research*, 33, 44: 1-12
- Wynn R.F, Hart C. A., Corradi-Perini C., O'Neill L., Evans C.A., Wraith J.E., Fairbairn L.J., Bellantuono I. 2004. A small proportion of mesenchymal stem cells strongly express functionally active CXCR4 receptor capable of promoting migration to bone marrow. *Blood*, 104, 9: 2643–2645
- Xu G., Jiang X.D., Xu Y., Zhang J., Huang F.H., Chen Z.Z., Zhou D.X., Shang J.H., Zou Y.X., Cai Y.Q., Kou S.B., Chen Y.Z., Xu R.X., Zeng Y.J. 2009. Adenoviral-mediated interleukin-18 expression in mesenchymal stem cells effectively suppresses the growth of glioma in rats. *Cell Biology International*, 33, 4: 466-474
- Yang B., Wu X., Mao Y., Bao W., Gao L., Zhou P., Xie R., Zhou L., Zhu J. 2009. Dual-targeted antitumor effects against brain stem glioma by intravenous delivery of tumor necrosis factor-related, apoptosis-inducing, ligand-engineered human mesenchymal stem cells. *Neurosurgery*, 65, 3: 610–624
- Yang C., Lei D., Ouyang W., Ren J., Li H., Hu J., Huang S. 2014. Conditioned media from human adipose tissue-derived mesenchymal stem cells and umbilical cord-derived mesenchymal stem cells efficiently induced the apoptosis and differentiation in human glioma cell lines in vitro. *BioMed Research International*, 2014: 109389, doi: 10.1155/2014/109389: 13 p.
- Yeh H. Y., Liu B. H., Sieber M., Hsu S. H. 2014. Substrate dependent gene regulation of self-assembled human MSC spheroids on chitosan membranes. *BMC Genomics*, 15, 10–24
- Yin J., Kim J.K., Moon J.H., Beck S., Piao D., Jin X., Kim S.H., Lim Y.C., Nam D.H., You S., Kim H., Choi Y.J. 2011. hMSC-mediated concurrent delivery of endostatin and carboxylesterase to mouse xenografts suppresses glioma initiation and recurrence. *Molecular Therapy*, 19, 6: 1161-1169

Zheng M., Bocangel D., Ramesh R., Ekmekcioglu S., Poindexter N., Grimm E.A., Chada S. 2008. IL-24 overcomes TMZ-resistance and enhances cell death by downregulation of MGMT in human melanoma cells. *Molecular Cancer Therapy*, 7, 12: 3842–3851

Zuk P.A., Zhu M., Mizuno H. 2001. Multilineage cells from human adipose tissue: implications for cell-based therapies. *Tissue Engineering*, 7, 2: 211-228

ACKNOWLEDGEMENT (ZAHVALA)

Najprej se zahvaljujem prof. dr. Tamari Lah Turnšek za usmerjanje pri delu in izdelavi doktorske naloge. Nadalje se zahvaljujem dr. Heleni Motaln za nasvete in pomoč pri laboratorijskem delu.

Nacionalnemu inštitutu za biologijo se zahvaljujem, da mi je omogočil izvedbo doktorskega dela.

Special thanks go to my co-advisor prof. dr. Stevens Kastrup Rehen that enabled me to get the knowledge of using microcarriers for cell cultivation. Obrigada!

Posebej se zahvaljujem predsednici Komisije za zagovor prof. dr. Mojci Narat in članoma doc. dr. Miomirju Kneževiću in prof. dr. Marku Kreftu za hiter pregled doktorske naloge in vse pripombe.

Zahvaljujem se dr. Alešu Leskovšku (Simed d.o.o., Ljubljana), ki nam je omogočil dostop do vzorcev maščevja za izolacijo MMC.

I would like to thank prof.dr. Christel Herold-Mende (University of Heidelberg, Germany) for providing us two cell lines of GSLCs.

Zahvala gre tudi vsem nekdanjim in sedanjim sodelavcem Oddelka za genetsko toksikologijo in biologijo raka za pomoč in podporo ter druženje in klepet o tem in onem.

Nazadnje še posebna zahvala mojemu Mitju za vso spodbudo, podporo in potrpežljivost ter sončici Sari za neizmeren vir energije.

Zahvala še staršema za podporo in da sta me naučila vztrajnosti.

Annex A

List of chemicals used in experiments

Chemicals	Manufacturer
βFGF (beta fibroblast growth factor, human)	Gibco, GB
5-FU (5-fluorouracil)	Sigma-Aldrich, DE
Acetic acid	Merck, DE
AgNO ₃	Sigma-Aldrich, DE
Alcian blue 8-GX	Sigma-Aldrich, DE
Alizarin red S	Sigma-Aldrich, DE
B-27 (serum supplement, 50x)	Gibco, GB
BSA (bovine serum albumin)	Sigma-Aldrich, DE
Cetypyridinium chloride	Sigma-Aldrich, DE
Citric acid	Sigma-Aldrich, DE
Collagenase I	Gibco, GB
Crystal violet	Sigma-Aldrich, DE
Dexamethasone	Sigma-Aldrich, DE
DMEM (Dulbecco's Modified Eagle's Medium)	Sigma-Aldrich, DE
EDTA (ethylenediaminetetraacetic acid)	Sigma-Aldrich, DE
EGF (epidermal growth factor, human)	Gibco, GB
FBS (foetal bovine serum)	PAA, AT
Glutaraldehyde solution (25 %)	Sigma-Aldrich, DE
Glycerophosphate	Sigma-Aldrich, DE
Heparin	Sigma-Aldrich, DE
High-Capacity cDNA Archive Kit	Applied Biosystems, USA
Hoechst 33342	Invitrogen, GB
IBMX, 3-isobutyl-1-methyl-xanthine	Sigma-Aldrich, DE
Indomethacine	Sigma-Aldrich, DE
Insulin	Sigma-Aldrich, DE
Isopropanol	Sigma-Aldrich, DE
K ₃ [Fe(CN) ₆] (potassium ferricyanide)	Sigma-Aldrich, DE
K ₄ [Fe(CN) ₆] · 3H ₂ O (potassium ferrocyanide)	Sigma-Aldrich, DE
L-ascorbic acid	Sigma-Aldrich, DE
L-glutamine	Gibco, GB
MgCl ₂	Merck, DE
MTS	Promega, USAA
Na ₂ HPO ₄	Merck, DE
Na ₂ S ₂ O ₃	Sigma-Aldrich, DE
NaCl	Merck, DE
NaHCO ₃	Sigma-Aldrich, DE
Na-pyruvate	Gibco, GB
NBE (Neurobasal medium)	Gibco, Life Technologies, GB
NH ₄ Cl	Sigma-Aldrich, DE
Oil red O	Sigma-Aldrich, DE
Paraformaldehyde	Sigma-Aldrich, DE

continue

Continued

PBS (Dulbecco's Phosphate buffered saline 10x)	PAA, AT
Penicillin/streptomycin	Gibco, GB
PI (propidium iodide)	BD Biosciences, USA
PI/RNase staining buffer	BD Biosciences, USA
PMS (phenazine methosulphate)	Sigma-Aldrich, DE
Pyrogallol	Sigma-Aldrich, DE
SDS (sodium dodecyl sulphate)	Sigma-Aldrich, DE
STS (Staurosporine)	Sigma-Aldrich, DE
TaqMan PCR Master mix	Applied Biosystem, USA
TGF β 3 (transforming growth factor beta 3)	Sigma-Aldrich, DE
TMZ (temozolomide)	Sigma-Aldrich, DE
Triton X-100	Fluka, DE
Trypan Blue	Sigma-Aldrich, DE
Trizol	Gibco, Life Technologies, GB
Trypsin	Sigma-Aldrich, DE
Trypsin-EDTA (0.25 %)	Gibco, Life Technologies, GB
X-gal (5-bromo-4-chloro-3-indolyl- β -D-	Sigma-Aldrich, DE

Annex B

Monoclonal antibodies used in FACS

Antibodies	Manufacturer	Reference number
CD13	BD Biosciences, USA	BD#557454
CD29	BD Biosciences, USA	BD#559883
CD44	BD Biosciences, USA	BD#555479
CD73	BD Biosciences, USA	BD#550257
CD90	BD Biosciences, USA	BD#555596
CD14	BD Biosciences, USA	BD#555397
CD34	BD Biosciences, USA	BD#555821
CD45	BD Biosciences, USA	BD#555482
CD105	Molecular Probes, USA	MHCD10505
HLA-DR	BD Biosciences, USA	BD#340688
FITC-IgG1	BD Biosciences, USA	BD#555748
FITC-IgG2a	BD Biosciences, USA	BD#555573
PE-IgG1	BD Biosciences, USA	BD#555749
PE-IgG2b	BD Biosciences, USA	BD#555743
APC-IgG1	BD Biosciences, USA	BD#555751

Annex C

Taqman gene expression assays used listed in alphabetical order

Gene Assay	Reference number
BAX	Hs99999001_m1
BCL2	Hs0060823_m1
CCND1	Hs00765553_m1
CD133/PROMININ 1	Hs00195682
CDKN1A (p21)	Hs00355782_m1
CDKN2A (p16)	Hs00923894_m1
GAPDH	Hs01076091_m1
NESTIN	Hs00707120_s1
NOTCH1	Hs01062014_m1
SOX2	Hs01053049_s1
TUBB3	Hs00801390_s1
VIMENTIN	Hs00185584_m1